DOCTOR OF PHILOSOPHY

Bioactive carbohydrates: isolation, synthesis and conjugation

Shan, Yulong

Award date:
2011

Awarding institution:
Bangor University

Bioactive carbohydrates

—

Isolation, Synthesis and Conjugation

A thesis in fulfilment

for the

Degree of a

Philosophiae Doctor

in Chemistry

in the

School of Chemistry

by

Yulong Shan

Prifysgol Bangor ● Bangor University

Contents

Abbreviations

AgOTf	silver trifluoromethanesulfonate
BabA	blood group antigen binding adhesin
CPS	capsular polysaccharide
CRD	Carbohydrate recognition domains
CSA	camphorsulfonic acid
DAB	1,4-dideoxy-1,4-imino-D-arabinitol
DCE	1,2-dichloroethane
DCM	dichloromethane
DMDP	2*R*, 5R-dihydroxymethyl-3*R*, 4R-dihydroxypyrrolidine
DNJ	1-deoxynojirimycin
EDA	ethylene diacetamide
ER	endoplasmic reticulum
GlcNAc	*N*-acetyl glucosamine
GNPs	gold nanoparticle
homoDMDP	2,5-dideoxy-2,5-imino-DL-glycero-D-manno-heptitol
LacNAc	*N*-acetyl-lactosamine
LPS	lipopolysaccharide
MHC	major histocompatibility complex
NIS	*N*-iodosuccinimide
PCV	pneumococcal conjugate vaccine
PHAs	Polyhydroxy alkaloids
PMNL	polymorphonuclear leukocyte
PPTS	pyridinium *p*-toluenesulfonate
PPV	Pneumococcal polysaccharide vaccines
TFA	trifluoroacetic acid
THAP	trihydroxy-acetophenone monohydrate
TLR2	toll-like receptor 2
TMSOTf	trimethylsilyl trifluoromethanesulfonate

Acknowledgements

First of all, I would like to deeply thank my supervisor, Dr Martina Lahmann. She has offered me this PhD position; she guided me through my PhD with her profound knowledge and research experience. She not only helps me with my research, but also saved me from some bad situations. She always had time for me, every time I go to her office; she stopped what she was doing and helped me. I will never forget the help she gave me.

Secondly, I would also like to thank Dr Vera Thoss and Professor Mark S. Baird, they helped me with my first year PhD, especially Dr Vera Thoss, she introduced me to her lovely bluebells. I'm also grateful to my research committee, Dr Patrick J. Murphy and Dr Michael A. Beckett. They gave me a lot of great suggestions. I owe special grateful thanks to Professor Stefan Oscarson. I really enjoyed our group meetings every year in Dublin, and I gained a lot of knowledge from it. Also I give my thanks to my collaborators: Dodi Safari, Marco Marradi, Fabrizio Chiodo, Huberta A. Th. Dekker, Roberto Adamo, Ger T. Rijkers, Johannis P. Kamerling, Soledad Penadés and Harm Snippe. I would like thank you to my research group members and staff from Bangor University.

At last, I would like thank my wife, my 11 months old son, my parents, parents-in-law and my sister for their support during my PhD.

Finally, I want to say something to my lovely son: "DuoDuo, I love you and I miss you so much, I'm on the way home!"

老婆，儿子，爸妈，董爸董妈，姐，*谢谢你们的支持，这篇论文一大半功劳是你们的，****永远爱你们！***

Abstract

In this thesis four projects related to bioactive carbohydrates are described. The first project is about the extraction of iminosugars from *Hyacinthoides non-scripta.* This is the first time that extraction from English bluebell seeds has been described. Efficient extraction and isolation methods are reported. Another project discusses the development of a total synthetic carbohydrate conjugate vaccine candidate against *Streptococcus pneumoniae* type 14 using Gold nanoparticles as carrier. The synthetic pathway of the introduction of a linker for conjugation, and the deprotection of the tetrasaccharide corresponding to the repeating unit of the *Streptococcus pneumoniae* type 14 capsular polysaccharide is described. The biological results of the developed vaccine candidate are briefly discussed. In the third project, attempts to synthesise regioselectively sulfated disaccharides to be used in binding studies with FedF adhesin of *E. coli* are described. In this section, an improved high-yielding method based on the Heyns rearrangement for the synthesis of *N*-acetyl lactosamine (LacNAc) is also reported. In the fourth part, conjugation of the Lewis b hexasaccharide to be used for studies of Lewis b blood group antigen binding adhesin is reported.

Abstract Chinese

文章摘要

此论文包含四个课题，其中涉及到具有生物活性的糖类物质.课题一讨论关于从英国风铃花（*Hyacinthoides non-scripta*）种子中萃取亚胺碱。此报告是第一次论述从风铃花种子中萃取亚胺碱，之前研究侧重于风铃花的花朵和茎。其中阐述了有效的萃取和提纯方法. 课题二讨论了关于可对抗肺炎链球杆菌（*Streptococcus pneumoniae* type 14）的以纳米粒子做载体的糖类结合疫苗的合成路径.具体涉及到为和肺炎链球杆菌荚膜多糖相对应的四糖重复单元的轭和反应引入连接基团,以及脱保护反应。并且给出了此改进疫苗的生物测试结果。课题三论述了关于可选择性合成硫化二糖,此糖类化合物用于与大肠杆菌粘附素 FedF 的结合研究.此课题还深入研究了 Heyns 重排合成方法高效合成 N-乙酰-D 乳糖胺 (LacNAc)。课题四是关于 Lewis b 己糖的轭和反应研究，用于

Lewis b 血型抗原结合黏附素的结合研究。

Chapter 1 – General Introduction

1.1 Chemistry of carbohydrates

Carbohydrates are compounds consisting of polyhydroxylated aldehydes or ketones. Most of them can also be described with a simple empirical formula $C_n (H_2O)_n$. The carbon atom number can vary from 3-9. Carbohydrates can be classified into four groups, monosaccharides, disaccharides, oligosaccharides and polysaccharides [1].

Carbohydrate synthesis involves some key reactions, such as the glycosylation reaction (Scheme 1). The glycosylation reaction can be performed by activating the anomeric position of a glycosyl donor, which then is connected to a glycosyl acceptor containing a free hydroxyl group. This is the key reaction to make oligosaccharides [2].

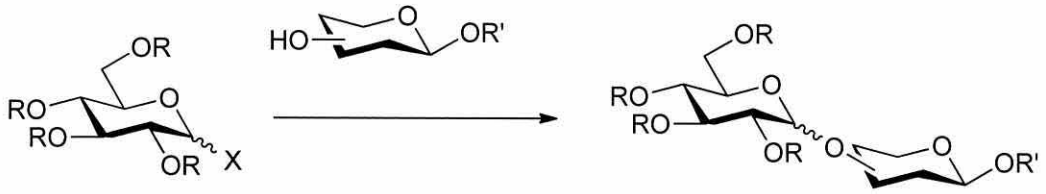

X = leaving group R,R' = protecting groups

Scheme 1: Glycosylation reaction.

There are three types of hydroxyl groups in carbohydrate structures. The first is the primary hydroxyl group which is normally at the C-6 position, the second are the secondary hydroxyl groups which are usually at the C-2, 3, 4 positions, and the third hydroxyl group is at the anomeric centre. The anomeric centre hydroxyl group can react as an alcohol or a hemiacetel hydroxyl group. It can act as an alcohol to form an acetate or a benzyl ether. It can act as an aldehyde to form a glycosidic linkage [1] [2].

Carbohydrate synthesis normally starts with free sugars. In order to increase the solubility of sugar in non-polar organic solvents and get it ready for further regioselective reactions, the majority of the hydroxyl groups need to be protected. The acetylation reaction is one of the most common reactions in carbohydrate synthesis. Free sugars react with acetic anhydride to form stable esters. Several common reaction conditions are used. Bases such as pyridine and sodium acetate or Lewis acids such as $ZnCl_2$ and boron trifluoride (BF_3) are used for this reaction. Sugars can also be protected by different protecting groups, such as acetals, benzyl ethers, trityl ethers, silyl ethers, and other esters and ethers [1] [2] [3].

The glycosidic linkage can be cleaved under acidic conditions (Scheme 2). During an acid hydrolysis a carboxonium ion is formed as an intermediate [2].

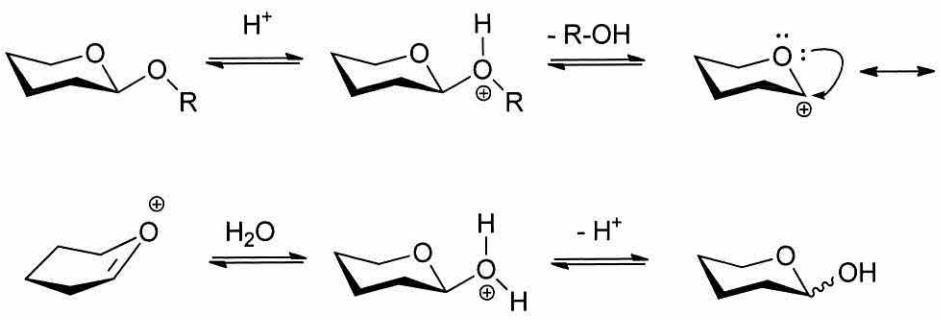

Scheme 2: An oxycarbenium ion intermediate is formed during the cleavage of a glycosidic bond.

1.2 Biology of carbohydrates

Carbohydrates can easily be found in nature. They play an important role in biological systems. They provide, for example, a source of energy and form polysaccharides as building blocks to provide strong structures. Sugars can also be found in glycoproteins and glycolipids. In addition, carbohydrates are used for medical purpose, e.g. carbohydrate based vaccines are used [2] [3].

1.2.1 Glycoproteins

Proteins that have carbohydrates attached to them are called glycoproteins. They can be divided into two types, *O*-linked glycoproteins and *N*-linked glycoproteins. *O*-linked glycoproteins are those proteins where the sugar chains are attached to the hydroxyl oxygen on the side chain of the amino acids serine or threonine. *N*-linked glycoproteins are proteins where the sugar chains are attached to the amide nitrogen atom of the amino acid asparagine [4]. The sugars have different functions in the glycoprotein structures. There is, for example, a type of a glycoprotein named mucin which can be found on internal epithelial surfaces. It protects the epithelium from chemical, physical, and microbial disturbances [5]. Mucins can also be found on the surface of fish skin making them feel slimy [6]. Glycoproteins play an important role for the immune system. Glycoproteins can act as antibodies to react with antigens to protect the body from bacterial and microbial infections. The glycoproteins called Major Histocompatibility Complex I (MHC) and MHC II interact with different T cells during the immune response [3].

1.2.2 Lectins

Lectins are sugar-binding proteins which can recognise specific sugars and sugars on glycoproteins and glycolipids in biological systems. Lectins can contain one or more carbohydrate binding sites, which are called carbohydrate recognition domains (CRD) [2]. Lectins with many CRDs can increase the binding due to multivalent effects between the CRDs and the sugars of glycoproteins or glycolipids [1]. Lectins can be classified into types according to their difference in affinity to different monosaccharides, these monosaccharides are mannose, galactose and *N*-acetyl galactosamine (GalNAc), *N*-acetyl glucoseamine (GlcNAc), L-fucose and *N*-acetylneuraminic acid. Concanavalin A is such a lectin [7]. It can be extracted in large quantities from Jack Beans [8] and binds to mannose [1] [2]. Several references are useful for lectin studies [9] [10] [11].

1.2.3 Glycolipids

Glycolipids are lipids attached to carbohydrate structures. They can be found on the exoplasmic surface of cell membranes. Glycolipids are devided into different types, such as glycosphingolipids, glyceroglycolipids and glycophosphatidylinositols. Glycosphingolipids are membrane glycoproteins acting as recognition markers involved in cell-cell interactions. They have also a role in organising specialised membrane domains. Bacterial glycolipids such as lipopolysaccharides (LPS) are present in the outer membrane of Gram-negative bacteria. LPS is an endotoxin that can be recognised by the immune system [1] [2] [3].

1.3 References

1. Davis, B.G.; Fairbanks, A. J. *Carbohydrate chemistry*, Oxford Science Publication, **2008**, 1-29
2. Lindhorst, T. K., *Essentials of carbohydrate chemistry and biochemistry*, Germany, **2002**, 1-23
3. Taylor, M. E.; and Drickamer, K., *Introduction to Glycobiology*, Oxford University Press, **2003**, 1-12
4. Ruddock, L. W.; Molinari, M. *J Cell Sci*, **2006**, *119*, 4373
5. Marin, F.; Corstjens, P.; De Gaulejac, B.; De Vrind-De Jong, E.; Westbroek, P.; *J. Biol. Chem*, **2000**, *275* (*27*), 20667–20675
6. Ascencio, F.; Martinez-Arias, W.; Romero, M. J.; Wadström, T.; *Fems. Immunol. Med. Mic.* **1998**, *20*, 219
7. Drickamer, K.; Taylor, M.E. *Trends Biochem. Sci.*, **1998**, *23*, 321-324
8. Jones, D. B.; Johns, C. O.; *J. Biol. Chem.* **1916**, *28*, 67
9. Dodd, R.B.; Drickamer, K. *Glycobiology*, **2001,** *11* (5), 71R-79
10. Imberty, A.; Mitchell, E.P.; Wimmerova, M. *Curr. Opin. Struc. Biol*, **2005**, *15* (5), 525-534
11. Singh, T., et al., *Biochem. J.* **2006**, *393*, 331-341.

Chapter 2 – Isolation and Identification of iminosugar from *Hyacinthoides non-scripta* (English Bluebell)

2.1 Introduction

2.1.1 *Hyacinthoides non-scripta* (English Bluebell)

The English bluebell (*Hyacinthoides non-scripta*) is an herb belonging to the Lily family and is widely distributed and common throughout the United Kingdom. There are 11 species in the genus *Hyacinthoides*; *Hyacinthoides non-scripta* is one of them. Other common species include Spanish bluebell (*Hyacinthoides hispanica*) coming from the Iberian Peninsula in Spain and the Italian bluebell (*Hyacinthoides italica*) that is native in the Mediterranean region [1]. The name was given for the blue bell shaped flowers appearing from April to June. It is estimated that 25 to 49 % of the world bluebell population is found in the UK [2]. In previous research, water soluble imino sugars (polyhydroxy alkaloids) have been isolated from bluebell fruits and stalks [3]. This project aims to extract bluebell seeds, which has not been reported earlier, in order to investigate the imino sugar content.

2.1.2 Polyhydroxy alkaloids (PHAs)

Polyhydroxy alkaloids (PHAs), or imino sugars, are small molecules. There are over 100 imino sugars known that have been isolated from natural sources including plants [4].The first natural PHA discovered was nojirimycin, which was isolated from a *Streptomyces* filtrate in 1966 [5]. Iminosugars can be considered as monosaccharides where the oxygen is replaced by nitrogen. Many of them are biological active, and anticancer, antiviral, antiinsect, and nematocidal activities have been reported [6]. They have also shown potential in a number of disease areas, such as diabetes, viral infections, and lysosomal storage disorders [6]. Thus, the discovery of new PHAs has become a growing area within the past two decades [6]. PHAs are classified as monocyclic and bicyclic polyhydroxylated derivatives of the

following five kinds of ring systems: pyrrolidine, piperidine, pyrrolizidines, octahydro-indolizine or indolizidine (fused piperidine and pyrrolidine systems), and nortropane (Figure1).

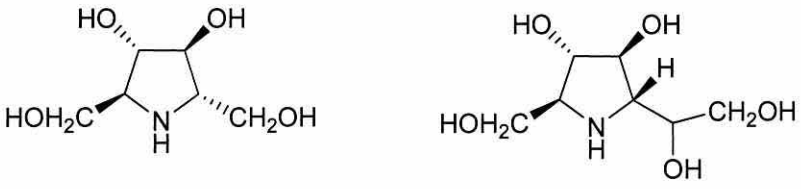

1 **2**

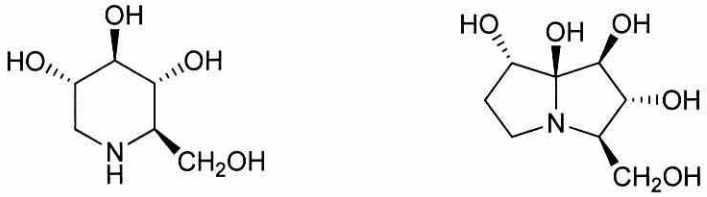

3 (DNJ) **4**

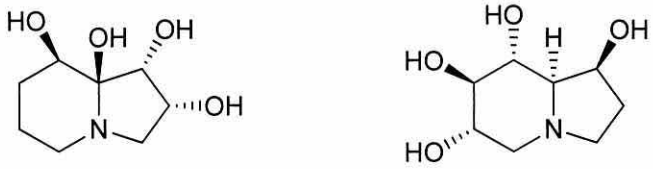

5 **6**

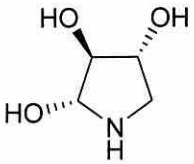

7

Figure 1: Some examples for pyrrolidine, piperidine, pyrrolizidines and indolizidine derived iminosugars: 2*R*, 5R-dihydroxymethyl-3*R*, 4R-dihydroxypyrrolidine (**1**, DMDP, pyrrolidine scaffold), 2,5-dideoxy-2,5-imino-DL-glycero-D-manno-heptitol (**2**, homo DMDP, pyrrolidine scaffold) 1-deoxynojirimycin (**3**, DNJ, piperidine scaffold) australine (**4**, pyrrolizidines scaffold), swainsonine (indolizidine scaffold) and castanospermine (**6**, indolizidine scaffold).

2.1.3 Glycosidase inhibitors

Imino sugars are considered as glycosidase inhibitors. Glycosidases are enzymes that catalyse the hydrolysis of complex carbohydrates and glycoconjugates, while glycosyltransferases are producing glycosidic linkages. Those enzymes exist in all living organisms and play an essential role for survival [7]. Large sugar polymers as cellulose can be broken by cellulases down to small sugar units that can easily be used by the organism. A wide range of glycosidases and glycosyltransferases is involved in the biosynthesis of the oligosaccharide portions of glycoproteins and glycolipids. These glycoproteins and glycolipids play a major role in the mammalian cellular structure and functions [8]. The biosynthesis of oligosaccharides of the *N*-linked glycoproteins in the endoplasmic reticulum (ER) and Golgi apparatus has very important effects on maturation, transport, and secretion of these glycoproteins [9]. There are two classes of glycosidases according to the two different fundamental mechanisms of the glycosidase catalysed hydrolysis. One is an inverting glycosidase, the other one is a retaining glycosidase. For the inverting glycosidases (Scheme 1, bottom), a carboxylic residue in the active site is deprotonating the water that in turn attacks the anomeric position. In the retaining mechanism a covalent bond between the active site and the sugar substrate is formed as an intermediate (Scheme 1, top).

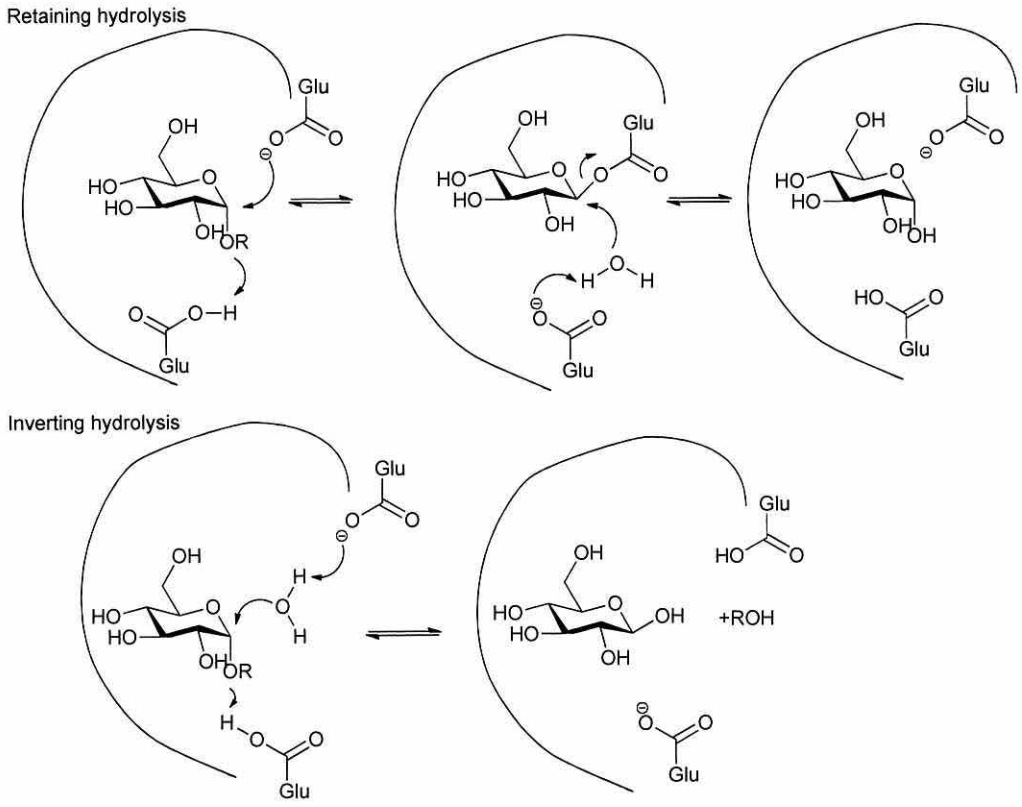

Scheme 1: Simplified enzymatic mechanism of hydrolysis.

The function of an inhibitor is often to block the active site. There are different ways to achieve this. One way is that the inhibitor is occupying the active site of the enzyme by having a stronger interaction with the active site than the substrate. Imino sugars have several structural features that make them suitable as glycosidase inhibitors.

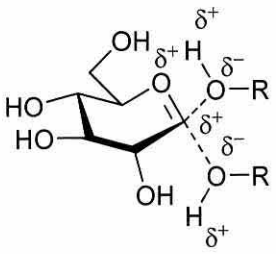

Figure 2: A simplified transition state during enzymatic cleavage.

Cleavage of the glycosidic bond gives the ring oxygen or the anomeric carbon a positive charged character. Thus, the protonated nitrogen with a positive charge on an imino sugar can mimic this. Also, double bonds flatten the cyclic system and are

therefore useful to mimic the conformation in the transition state. Possible stabilisation of the positive charge of the ring nitrogen, a trigonal anomeric center, a half chair conformation, and the specific configuration of the hydroxyl groups can affect the inhibitor properties of these imino sugars [12] (scheme 2). In summary, several structural factors including additional charges and the 3D-shape of the polyhydroxy alkaloids are crucial for their function as glycosidase inhibitiors [7].

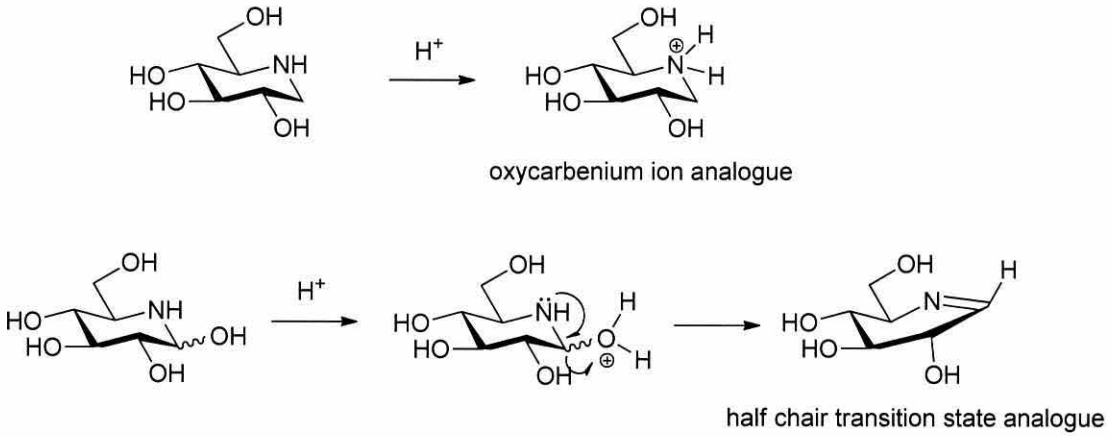

Scheme 2: This is the anticipated mechanism for the α-glucosidase inhibition by the iminosugars DNJ **3**, and nojirimycin.

2.1.4 Therapeutic use

Imino sugars have been considered for different therapeutic uses, such as anti-cancer agent, anti-diabetic agent, anti-viral agent, and immune stimulants. They are also used for treatment of glycosphingolipid lysosomal storage diseases [7]. Even though this area has attracted attention in recent years, and more imino sugar have been isolated from natural sources and synthesised, there are still not many imino sugars commercially available.

Several iminosugars have been investigated for therapeutic use, e.g. 1-deoxynojirimycin **3** (DNJ), 1,4-dideoxy-1,4-imino-D-arabinitol (DAB), castanospermine and swainsonine.

DNJ **3** (Figure 1) was first isolated from Mulberry leaves by Yagi in 1976 [13]. DNJ **3** was first synthesised by removing the anomeric hydroxyl group of nojirimycin that

was isolated from *Streptomycete strain* by Inouye and his group in 1968 [14]. Medicinal chemists used the DNJ **3** sugar for the development of other inhibitors, e.g. *N*-hydroxyethyl-DNJ (Miglitol). This compound was further developed by Bayer to make an anti-diabetic (Glyset®) agent that was the first imino sugar therapeutic to be used commercially [15]. DNJ was also adapted by Oxford University and Oxford Glycosciences to produce *N*-butyl-DNJ (Zavesca®), which is used for the treatment of type I Gaucher disease and Niemann-Pick type C disease, two lysosomal storage disorders [7] [16].

Swainsonine (**5**, Figure 1) has been isolated from both plants and microorganisms [7]. It has been shown to be an inhibitor of α-mannosidases and it also inhibits α-mannosidase II activity in the *N*-glycan biosynthesis pathway by blocking the production of complex-type oligosaccharides [7] Swainsonine has been used to study the function of *N*-glycans, and the anti-tumour activity of swainsonine has been previously examined [17]. Swainsonine is known for its anti cancer effect, it inhibits cancer cell metastasis, it can also be used as an adjuvant for anti-cancer drug. The main side effect is vacuolation caused by inhibition of lysosomal mannosidases. Swainsonine can be considered as a chemotherapeutic drug, and it will possibly be developed further and more possible applications may be discovered [7] [17].

Castanospermine (**6**, figure 1) was first isolated from the *Castanospermum australe*. It has been modified by the addition of a butanoyl group to form Celgosivir (6-*O*-butanoyl-castanospermine) [18]. Celgosivir has been identified to have anti-HIV activity and was evaluated in a phase II clinical trial. However, further development is required, because of the compound's toxicity profile and competition from other, less toxic anti-HIV drugs [19].

1,4-dideoxy-1,4-imino-D-arabinitol (**7**, DAB, figure 1) was isolated from *Angylocalyx braunii*. It is an inhibitor of glycogen phosphorylase [20]. DAB can reduce glucagon-induced and spontaneous hyperglycaemia. Inhibition of hepatic glycogen phosphorylase may benefit glycaemic control in patients with type 2 diabetes [21] [22].

2.2 Results and Discussion

The common method for polyhydroxy alkaloid extraction is extraction with methanol or ethanol. In general, alcohol-water solvent mixtures can increase the efficiency of the extraction, and 50 – 80 vol % alcohol solutions have been suggested. Water extraction can also be used because of the high solubility of PHAs in water [23].

Methanol or ethanol extraction can be used to extract PHAs from plant. This extraction method has the advantage that it is relatively easy to remove the solvents under reduced pressure. However, alcoholic solvents can also extract other polar constituents such as sugars and amino acids together with PHAs. Further separation of PHAs from crude extracts can be achieved by using ion exchange resins. Both cation and anion exchange resins can be used for the separation [3] [24] [25]. Dowex 50, Amberlite IR 120 and Amberlite CG 50 in their NH_4^+ or H^+ ion forms are the most common resins used for separation of PHAs [3] [24] [25].

Bluebell seeds (900 g) were extracted with 80% aqueous MeOH, and the extract was purified by using different ion-exchange resin columns to get a crude alkaloid mixture. The crude alkaloid mixture was analysed by NMR (500 MHz) and GLC- MS. Prior to GLC-MS analysis, the crude extract was silylated and purified by cation exchange chromatography.

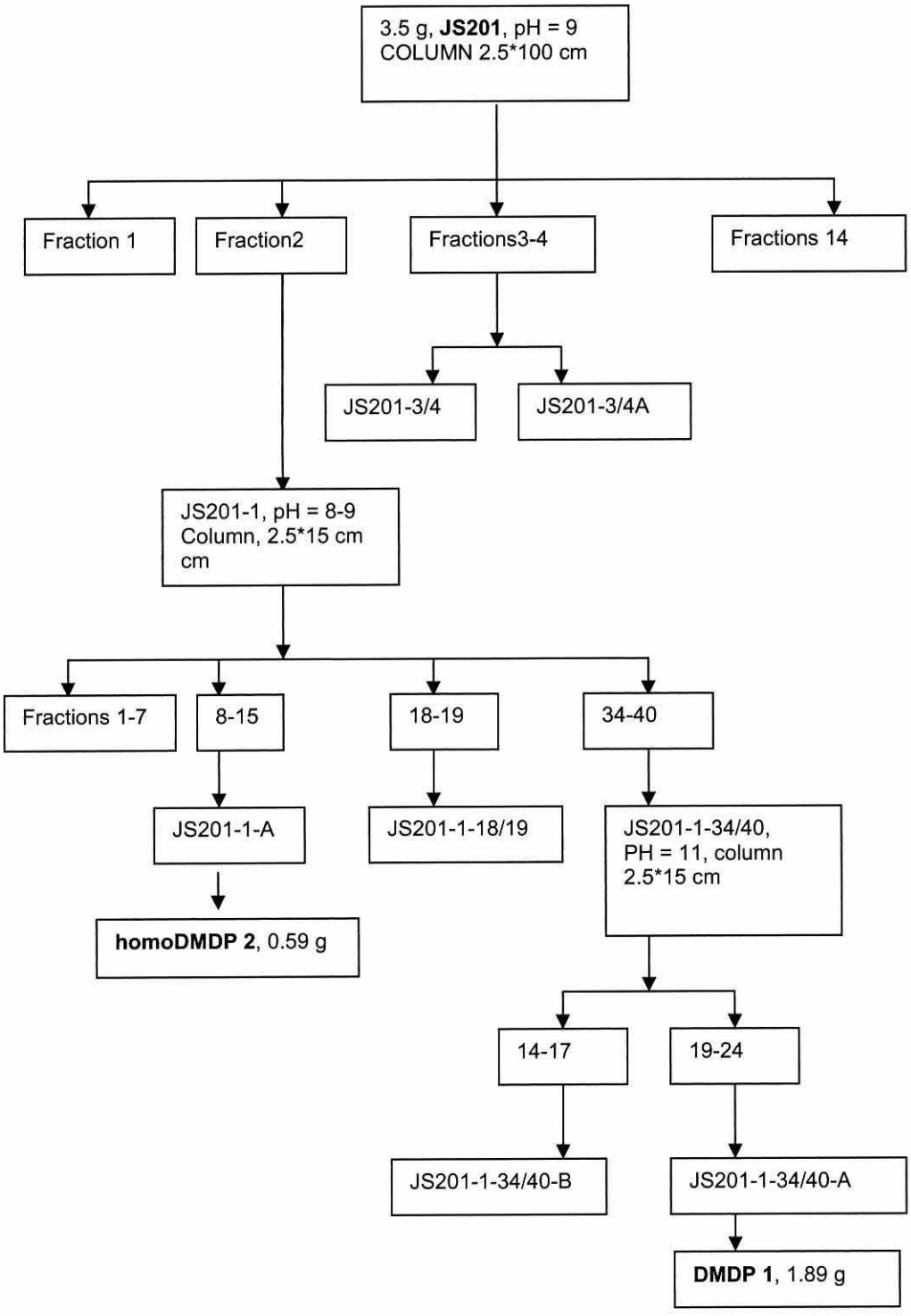

Figure 3: Ion exchange resin (Amberlite CG 50) flow scheme for the separation of the crude alkaloid mixture **JS201**.

The crude concentrate obtained from the methanolic extraction, was first purified by ion exchange chromatography (Amberlite IR 120, H^+ form). However, the obtained extract was viscous because of the high content of polymeric sugars. To circumvent frequent blocking of the column, 1 bar pressure had to be applied to get the

extraction solution to pass through. After this first column, a crude alkaloid extract (**JS201**, 3.5 g) of bluebell seeds was obtained. This material **JS201** was further purified by using Amberlite CG 50 (NH_4^+ form) according to the flow chart shown in Figure 3.

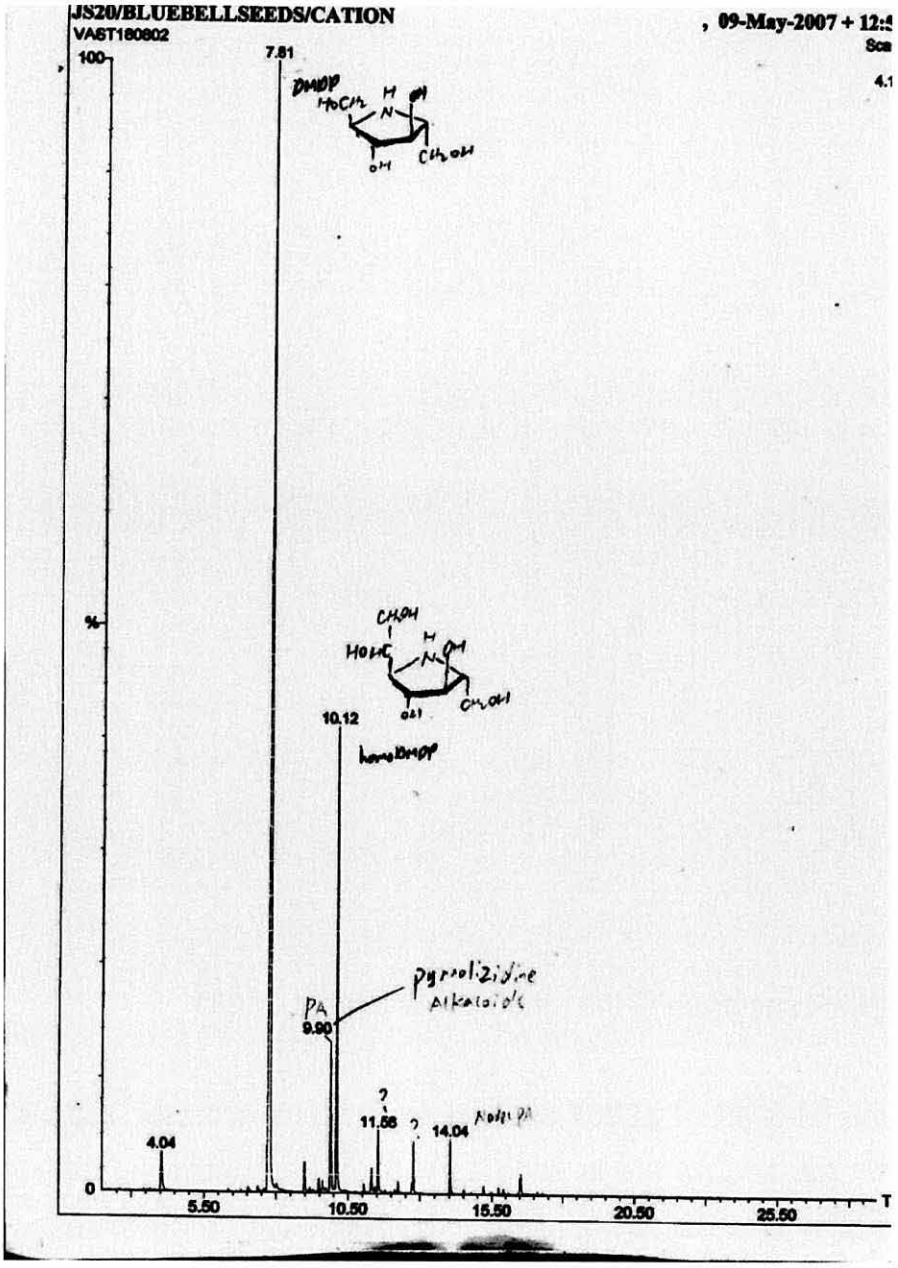

Figure 4: GC spectrums of crude PHAs extract mixture **JS201**.

Samples of the **JS201** crude alkaloid mixture were silylated for GC-MS analysis. Two major components (Figure 4) with retention times of 7.81 min and 10.12 min were assigned as possibly DMDP **1** and homoDMDP **2**. Compound **1** produced a tetra-*O*-trimethyl silylated (*O*-TMS) derivative with characteristic fragment ions at *m/z* 436

and 348 caused by the loss of CH_3 and CH_2O-TMS, respectively. Compound **2** gave a penta *O*-TMS derivative and characteristic fragment ions at *m/z* 538 $[M\text{-}CH_3]^+$ and 450 $[M\text{-}CH_2OTMS]^+$.

The GC spectrum also showed about twenty additional PHAs that will require further analysis.

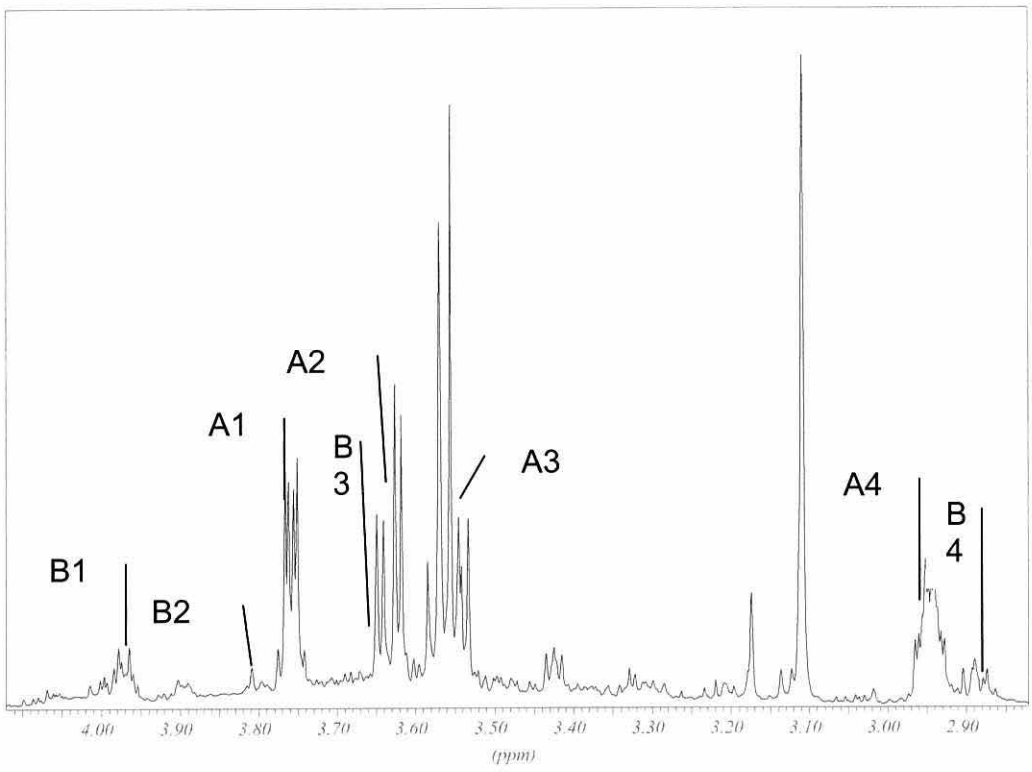

Figure 5:^{1}H-NMR spectrum of the crude PHAs extract **JS201**.

In addition, the ^{1}H-NMR of **JS201** showed several characteristic signals (Figure 5). Signal A1, A2, A3, and A4 are in good agreement with published data for DMDP **1** [26], while signal B1, B2, B3 and B4 corresponds to NMR data published for homoDMDP **2** [27]. Also the ^{13}C was in good agreement with the assumption that the two isolated compounds were DMDP **1** and homoDMDP **2** [27] [28] (Figure 6).
Pure DMDP **1** (1.85 g) was obtained from crude **JS201** by using Amberlite CG 50 ion exchange resin according to the flow scheme shown in Figure 2.

The ^{1}H-NMR spectrum of **1** in D_2O contains eight non-exchanging protons (Figure 7).

The compound produces only three carbon signals at 59.54, 62.06 and 75.72 ppm in the ^{13}C-NMR due to symmetry of the system (Figure 7).

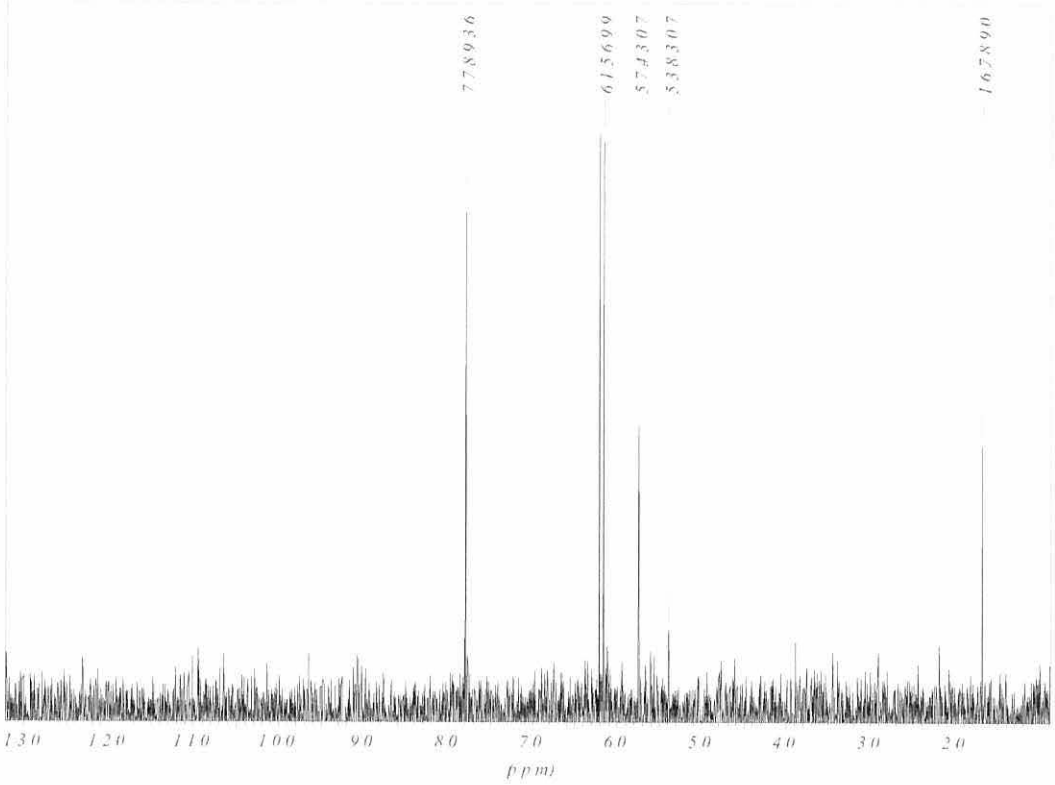

Figure 6: ^{13}C-NMR spectrum of the crude PHAs extract **JS201**.

Also pure homo DMDP **2** (0.59 g) was isolated and the structure confirmed by additional NMR experiments (Figure 9-10).

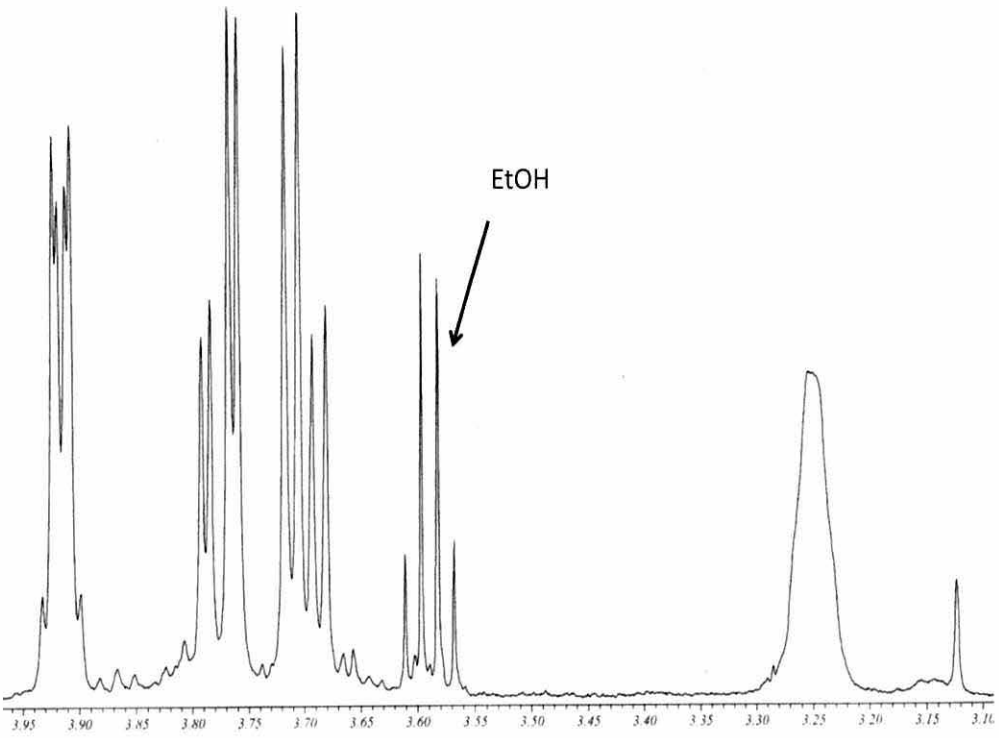

Figure 7: ^{1}H-NMR spectrum of DMDP **1**.

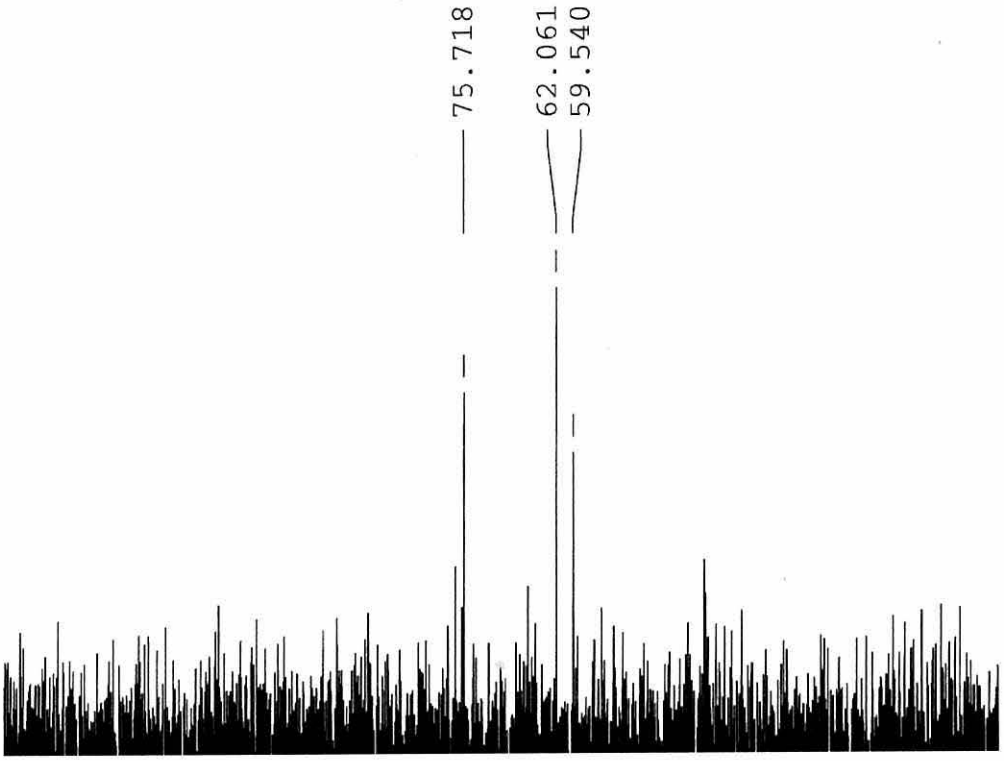

Figure. 8: ^{13}C-NMR spectrum of DMDP **1**.

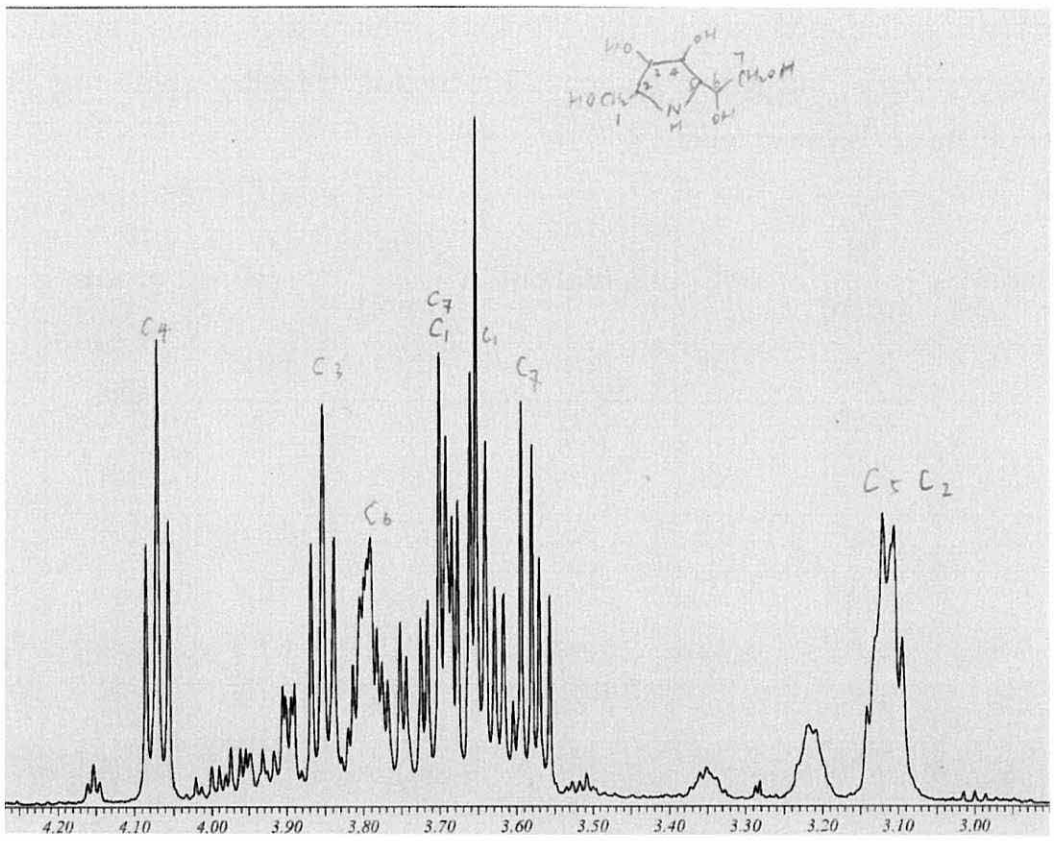

Figure 9: ^{1}H-NMR spectrum of homo DMDP **2**.

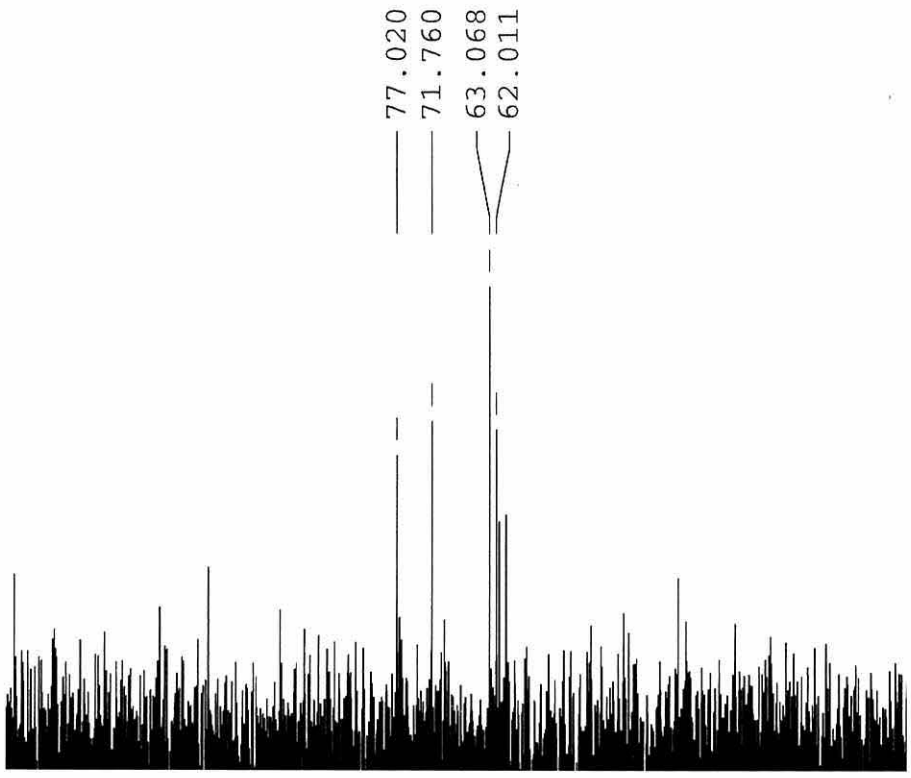

Figure 10: ^{13}C-NMR spectrum of homo DMDP **2**.

The ^{1}H-NMR spectrum of homoDMDP **2** in D_2O contains nine non-equivalent, non-exchanging protons and seven carbons. The proton chemical shifts and carbon chemical shifts are given in table 1 [27].

label	^{1}H [ppm]	ref	multiplicity	^{13}C [ppm]	ref	group
C1	3.75	3.74	*dd*	60.4	60.6	CH_2
	3.69	3.69	*dd*			
C2	3.13	3.16	*broad*	62.0	61.7	CH
C3	3.85	3.91	*t*	77.0	77.0	CH
C4	4.08	4.12	*t*	76.6	76.7	CH
C5	3.12	3.13	*broad*	61.0	61.3	CH
C6	3.79	3.84	*broad*	71.8	71.7	CH
C7	3.59	3.74	*dd*	63.0	62.9	CH
	3.56	3.64	*dd*			

Table 1. The NMR shifts obtained for the isolated and purified compounds **2** in comparison with published data [26] [27] [28] (ref = reference 28).

The above described isolation of bluebell seeds was also scaled-up at PhytoQuest Ltd. In contrast to the above described extractions, defatted seeds were used. Also some modifications were made to the overall process.

Defatted, grounded bluebell seeds were extracted with water instead of 80 % aqueous methanol. The crude extract was treated as described earlier on the small scale to get a mixture of DMDP **1** and homo DMDP **2** (Figure 11).

The seeds (1270 g) were extracted by soaking with 5 L water for 18 h at room temperature. Filtering off the soaked seeds using filter paper led to frequent blockage. To prevent this, the extraction solution was first passed over a cotton mesh to remove the coarse particles prior to filter paper filtration. The combined extracts (ca. 6 L) were applied to an Amberlite IR-120 column at a slow flow rate to ensure complete retention of the imino sugars. The crude imino sugars extract was eluted

NH_4OH. Another ion exchange column (Serdolit CG 400, OH^- form) was used to separate DMDP **1** and homoDMDP **2** from most of the other PHAs. The separation progress was monitored by GC-MS. The major imino sugar fraction from the bluebell seeds contained DMDP **1**. The compound showed the expected retention time (8.79 min), and homoDMDP with retention time 10.96. MS data confirmed the presence of **1** and **2** (Figure 12, Figure 13).

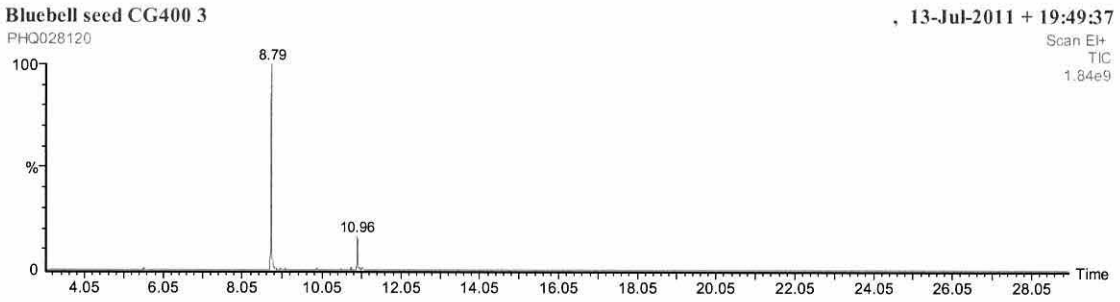

Figure 11: GC spectrum of bluebell seed extract (Serdolit CG 400 ion exchange resin column fraction).

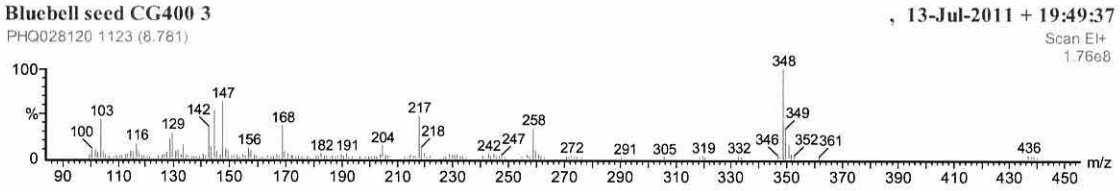

Figure 12: Mass spectrum of DMDP **1**.

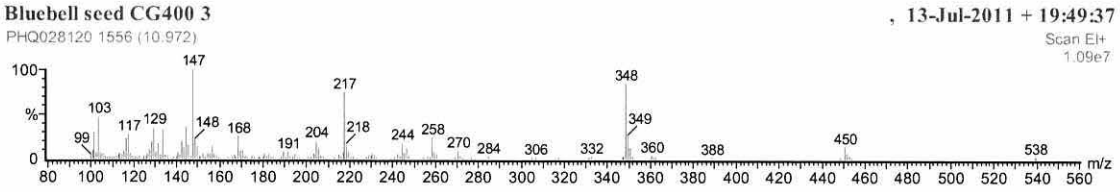

Figure 13: Mass spectrum of homoDMDP **2**.

Some additional imino sugars were also detected by GC-MS, such as pyrrolizidines DNJ **3** and DAB. The data indicated also the presence of some unknown compounds, possibly imino sugars, and further investigation should be done. In contrast to the lab scale extraction protocol, it turned out to be better to load the crude extract directly

onto the column without pre-concentration to avoid column blocking. Also a strong vacuum pump was required to increase the efficiency of large scale filtration and water evaporation.

2.3. Conclusions

Methanolic extracts from the seeds of grounded bluebells were subjected to various ion exchange resin columns to give crude PHAs mixtures (3.9 %). The major components of crude PHAs extract are 2R, 5R-dihydroxymethyl-3R, 4R-dihydroxypyrrolidine 1 (DMDP, 2.1 %) and 2,5-dideoxy-2,5-imino-DL-glycero-D-manno-heptitol 2 (homoDMDP, 0.65 %). The large scale extraction using water produced approximately the same amount the crude DMDP 1 and homo DMDP 2 mixtures (4.0 %). According to the experiments, there is now significant difference in using water or 80 % methanol except for the ease of removing large amounts of water. Also, no difference in PHA yield was observed, when comparing the extraction of defatted seeds with non-defatted seeds. It is, however, advantageous to load the ion exchange column with the extract solution without concentrating it. A slow flow rate is required to make sure that all PHAs are retained on the column but the risk of blockage is minimised. At present, the most useful analytical technique for PHAs is GC-MS in combination with NMR. Data obtained suggests that there are possibly some unknown PHAs.

2.4 Experimental

2.4.1 General methods

The purity of **JS201** was checked by HPTLC on Silica Gel $60F_{254}$ using the solvent system PrOH-AcOH-H_2O 4:1:1. Iodine vapours were used for detection. ^{1}H NMR and ^{13}C NMR experiments were recorded on a 500 MHz spectrometer (Bruker B-ACS 60). The ion exchange resin Amberlite IR-120 H^+ form was converted by soaking Amberlite IR-120 sodium form in HCl solution (1M) for 1 h and followed by washing with water. The ion exchange resin Amberlite CG 50 OH^- form was converted by soaking Amberlite CG 50 Cl^- form in NaOH (1M) for 1 h and follow by washing with water. All column dimensions are given in cm, W (width), H (length). Mass spectra were recorded on a Bruker Daltonics MicrOTOF using electrospray technique.

2.4.2 Plant material

Seeds of Hyacinthoides non-scripta were given by Dr. Vera Thoss, Bangor University/Vera Bluebell. A small amount of bluebell seeds were dried in an oven at 100 °C for 4 h and the moisture content of the seeds were determined to 14.2 ± 0.05 %. Seeds were grounded in a JK electronic grounder for about 5 min under liquid nitrogen. Seed powder was passed through metal sieves with 1mm mesh.

2.4.3 Extraction and isolation

Alcohol extraction and analysis (JS203 and JS205)

Grounded and sieved bluebells seeds (900 g) were extracted with 80 % aq. MeOH (5 L) for 72 h at room temperature. The mixture was filtered through filter paper (WHATMAN Grade 597: 4-7 µm, medium fast filter paper). The MeOH extract was collected and concentrated to a smaller volume (200 mL). Then, the seed residue was mixed with diluted 1M HCl (2 L) and left to extract for one additional hour to get the remaining alkaloids out of the substrate. After filtration, this HCl extract was collected and combined with the methanolic solution. The acidic aqueous solution was further concentrated by rotary evaporation to a volume of 150 mL. During the

evaporation, some solid product precipitated out from the saturated solution. Therefore, the solution was filtered again. This solid material was collected and named **JS 203**. The aqueous solution was applied to a column (2.5 W x 100 H) containing Amberlite IR- 120 (H^+ form), and eluted with 0.1M NH_4OH. The eluate was concentrated, and the residue dried under high vacuum to get crude imino sugars as dried yellow powder **JS201** (3.5 g).

For further separation, the crude alkaloid extract **JS201** (3.5 g) was applied to an Amberlite CG-50 column (2.5 W x 8 H, NH_4^+ form) with H_2O as eluant (fraction size 18 ml). TLC was used to detect product containing fractions. The content of the fractions were monitored by GC-MS analysis (Table 2).

RT / F	12.4	12.8	23.0	23.4	25.0	26.0	26.3	26.6	28.7	30.3
1										
2				90.88			0.560	8.09		
3			5.39	76.45	0.83	2.46	3.84	8.54	0.76	1.70
4			3.02	78.95	0.68	6.32	5.41	3.72	0.71	1.45
5		0.94	4.85	73.01		6.16	9.24	3.38	1.01	1.37
6		2.25	7.97	60.59		8.02	15.32	2.93	1.64	1.35
7	2.82	5.68	5.58	43.54		13.79	24.16	2.75	1.44	
8	12.65	18.07		36.18		11.30	26.78			
9	19.31	16.94		23.10		12.78	27.83			
10	33.92	36.99					29.07			
11	40.12	59.87								
12	45.35	54.64								
13	45.69	19.83								
14	8.12	9.88								

Table 2: Area % of GC of 1-14 fractions after Amberlite IR-120 clolumns (RT = retention time /min, F = name of column fractions)

The H_2O eluate was divided into 5 pools by combining the specified fractions: I

(fractions 2); II (fractions 3-4); III (fractions 5-7); IV (fractions 8-10); V (fractions 11-14). Each pool was further chromatographed with Amberlite CG-50.

Pool I was applied to a further column Amberlite CG-50 column (2.5 W x 15 H, NH_4^+ form) with H_2O as eluant (fraction size 10mL), and fractions were analysed by GC-MS. Fraction 8-15 (0.59 g) was identified as homo DMDP **2**, and fractions 18-40 (1.85 g) were confirmed as DMDP **1**.

2*R*, 5R-dihydroxymethyl-3*R*, 4R-dihydroxypyrrolidine (**1**, DMDP)
^{1}H NMR (500 MHz, D_2O) δ 3.85 (2H, dt, H-3, H-4), 3.70, 3.78 (4H, 2dd, H-1, H-1', H-6, 6'), 3.2 (2H, m, H-2, H-5) ppm. ^{13}C NMR (125 MHz, D_2O) δ 59.54, 62.06 and 75.72 ppm.

2,5-dideoxy-2,5-imino-DL-glycero-D-manno-heptitol (**2**, homoDMDP)
^{1}H NMR (500 MHz, D_2O) δ 4.08 (t, H-4), 3.85 (t, H-3), 3.79 (m, H-6), 3.75, 3.69 (2dd, H-1), 3.59, 3.56 (2dd, H-7), 3.13 (m, H-2), 3.12 (m, H-5) ppm. ^{13}C NMR (125 MHz, D_2O) δ 77.0 (C-3), 76.7(C-4), 71.7(C-6), 62.9(C-7), 61.7(C-2), 61.3(C-5), 60.6 (H-1) ppm.

2.4.4. Up-scaled extraction performed at Phytoqest, Aberystwyth

Defatted seeds of *Hyacinthoides non-scripta* were provided by Dr. Vera Thoss, Bangor University/Vera Bluebell. 1540 g ground-seed material had been defatted by extraction with hexane to give 1270 g defatted seed material [29]. Those seeds (1270 g) were extracted by soaking with 5 L water for 18 h at room temperature. Filtering off the soaked seeds using filter paper led to frequent blockage. To prevent this, the extraction solution was first passed over a cotton mesh to remove the coarse particles prior to filter paper filtration. The extraction solutions were stored at 4 °C, while the soaking procedure was repeated twice. The second and third extracts were concentrated to 500 mL in total. The combined extracts (ca. 6 L) were applied to an Amberlite IR-120 (5.5 W x 40 H, H^+ form) column. To ensure complete retention of the imino sugars, the flow rate was set to about 1 drop/2 s. The crude imino sugars extract was eluted using 2M NH_4OH. The eluate was concentrated to about

30 mL, and then passed onto a Serdolit CG 400 (4 W x 10 H, OH^- form) ion exchange resin column to separate DMDP **1** and homoDMDP **2** from most of the other PHAs by elution with water. The separation was monitored by GC-MS. According to GC-MS, Fractions 3-6 were considered as the major fractions containing the mixture of DMDP **1** and homo DMDP **2**. They were pooled, concentrated, and stored at 4 ^{o}C for future analysis.

2.5 References

1. *WCSP (Current Year). 'World Checklist of Selected Plant Families.* Facilitated by the Royal Botanic Gardens, Kew. Published on the Internet; http://apps.kew.org/wcsp/ Retrieved **2011-05-26**
2. Ingrouille, M., **1995**. Historical Ecology of the British Flora. Chapman & Hall, London.
3. Kato, A.; Adachi, I.; Miyauchi, M.; Ikeda, K.; Komae, T.; Kizu, H.; Kameda, Y.; Watson, A. A.; Nash, R. J.; Wormald, M. R.; Fleet, G. W. J.; Asano, N. *Carbohydr. Res,* **1999**, *316*, 95-104
4. Compain, P.; Martin, O. R. Imino sugars: From synthesis to therapeutic applications, Chichester, Wiley, **2007**, 25
5. Inouye, S.; Tsurouka, T.; Niida, T. *J. Antibiot*, **1966**, *19*, 288
6. Asano, N., *Glycobiology,* **2003**, *13*, 93
7. Watson, A. A.; Fleet, G. W. J.; Asano, N.; Molyneux, R. J.; Nash, R. *J. Phytochemistry*, **2001**, *56*, 265
8. Elbein, A.D., The effects of plant indolizidine alkaloids and related compounds on glycoprotein processing. In: James, L.F.; Elbein, A.D.; Molyneux, R.J.; Warren, C.D. (Eds.), *Swainsonine and Related Glycosidase Inhibitors*. Iowa State University Press, Ames, IA, **1989**, 15518
9. Dwek, R. A. *Chemical Rev,* **1996**, *96*, 683
10. Heightman, T. D.; Vasella, A. T. *Agnew. Chem. Int. Ed*, **1999**, *38*, 750
11. Jedrzejas, M. J.; Stern, R. *Proteins: Structure, Function, and Bioinformatics*, **2005**, *61*, 227
12. Sinnott, M. L. *Chemical Rev*, **1990**, *90*, 1171
13. Yagi, M.; Kouno, T.; Aoyagi Y. *Nippon Nogeikagaka Kaishi*, **1976**, *50*, 571-572
14. Inouye, S.; Tsurouka, T.; Ito T *Tetrahedron*, **1968**, *24*, 2125-2144
15. Asano, N. *Cell. Mol. Life Sci*, **2009**, *66*, 1479-1492
16. Winchester, B.G. *Tetrahedron Asym*, **2009**, *20*, 645-651
17. Hamaguchi, J.; Nakagawa, H.; Takahashi, M.; Kudo, T.; Kamiyama, N.; Sun, B.; Oshima, T.; Sato, Y.; Deguchi, K.; Todo, S.; Nishimura, S. *Mol. Cancer*, **2007**, *6*, 58-67
18. Sorbera, L. A.; Castaner, J.; Garcia-Capdevila, L. *Drugs Future*, **2005**, *30*, 545-552

19. Taylor, D. L.; Kang, M. S.; Brennan, T. M.; Bridges, C. G.; Sunkara, P. S.; Tyms, A. S. *Antimicrob. Agents Chemother*, **1994**, *38* (8), 1780-1787
20. Fleet, G. W. J.; Nicholas, S. J.; Smith, P. W.; Evans, S.V.; Fellows, L.E.; Nash, R.J. *Tetrahedron Lett*, **1985**, *26*, 3127-3130
21. Mackay, P.; Ynddal, L.; Anderson, J. V.; McCormack, J. G. *Diabetes Obes. Metab*, **2003**, *5*, 397-407
22. Kong, W-H.; Oh, S-H.; Ahn, Y-R.; Kim, K. W.; Kim, J. H.; Seo, S. W. *J. Agric. and Food Chem*, **2008**, *56*, 2613-2619
23. Liu, Y. H. *Chin. J. Clin. Rehabil,* **2005,** 6, 163-165
24. Asano, N.; Nishida, M.; Miyauchi, M.; Ikeda, K.; Yamamoto, M.; Kizu, H.; Kameda, Y.; Watson, A. A.; Nash, R. J.; Fleet, G. W. *J. Phytochemistry*, **2000**, *53*, 379
25. Kato, A.; Kato, N.; Miyauchi, S.; Minoshima, Y.; Adachi, I.; Ikeda, K.; Asano, N.; Watson, A. A.; Nash, R. *J. Phytochemistry*, **2008**, *69*, 1261
26. Welter, A.; Jadot, *J. Phytochemistry*, **1976**, *15*, 741-749
27. Card, P.J.; Hitz, W.D. *J. Org. Chem*, **1985**, *50*, 893-894
28. Watson, A. A.; Nash, R. J.; Wormald, M. R.; Harvey, D. J.; Dealler, S.; Lees, E.; Asano, N.; Kizu, H.; Kato, A.; Griffiths, R. C.; Cairns, A. J.; Fleet, G. W. *J. Phytochemistry*, **1997**, *46*, 255
29. Wilson, T, MSc thesis, **2011**, Bangor University.

Chapter 3 – Design, Synthesis, and Biological Evaluation of a Synthetic Glycoconjugate *Streptococcus pneumoniae* type 14 CPS Vaccine Candidate

3.1. Introduction

3.1.1 Bacterial cell wall

The bacterial cell wall can be divided into two categories; Gram-positive and Gram-negative. Gram's staining method was invented by Hans Christian Gram [1]. The difference between Gram-positive and Gram-negative cell walls is that Gram-positive bacteria have a thick layer constructed of peptidoglycans. This type of cell wall gives the bacteria a dark purple colour in the cell culture. In contrast, Gram-negative bacteria only have one thin peptidoglycan layer. Most of the staining agent washes away during the staining procedure, giving the stained cells a light pink colour. In addition, the Gram-negative membranes (Figure 1) also contain an outer membrane and an inner membrane [2] [3] [4].

The outer membrane contains lipopolysaccharides (LPS), lipoproteins and phospholipids. They play an important role in protecting bacteria from the outside environment. LPS consists of three parts: the O-antigen (*O*-polysaccharide), the core oligosaccharide, and lipid A. The O in the term O-antigen was originally referring to the behaviour of bacteria on agar plates and means 'without mist' from the German '**o**hne Hauch'. The *O*-polysaccharide is connected to the core and is made up by repeating units. It exists at the outside surface of bacteria as protective layer. The core contains an inner core and an outer core. The inner core contains unusual sugars such as heptose and Kdo. The outer core contains sugars such as D-glucose, D-mannose, D-galactose. The lipid A is a phosphorylated glucosamine disaccharide connected to fatty acids. These fatty acid chains anchor the LPS to the other membrane [2] [3] [4].

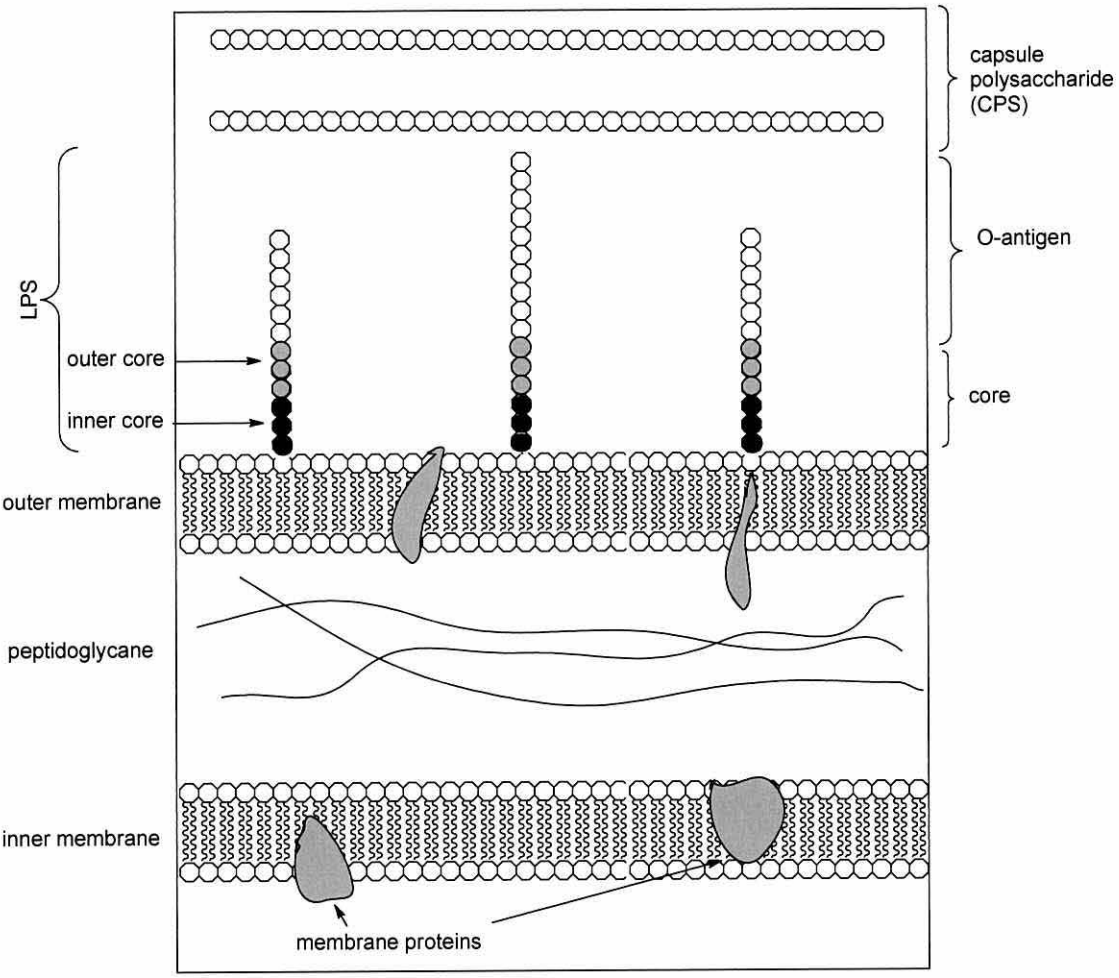

Figure 1: Schematic cross section of the cell wall of a Gram-negative bacteria.

3.1.2 Streptococcus pneumoniae

Streptococcus pneumoniae is a species of Streptococcus that is a major human pathogen [5]. It was recognized as a major cause of pneumonia in the late 19th century [6]. There are many different types of *S. pneumoniae*. About 90 different serotypes are known so far [6]. The structures of the capsular polysaccharide of the bacteria are used for serotyping the bacteria. Serotypes 6, 14, 18, 19 and 23 are common. *S. pneumonia* type 14 is one of the most common serotypes. Many very young children and very old people suffer from diseases caused by *S. pneumoniae* [5].

3.1.3 Capsular polysaccharide

Many bacteria are surrounded by a network of polysaccharides, called capsular polysaccharides (CPS). Usually oligosaccharides form the repeating unit of the CPS but homopolymers consisting of a monosaccharide unit are also known, *e.g.* the CPS of *N. meningitis* consists of α-(1-8) linked sialic acids. The CPS can be classified by the type of carbohydrates it consists off. The CPS is usually of high molecular weight, water soluble, and often containing acidic groups. There are about 80 serotypes of CPSs known in *E.coli* and about 90 serotypes for *S. pneumoniae* [7] [8].

The CPSs play an important role in bacteria. They act as evolutionary adaptation to protect bacteria from the outside environment. In some cases the CPS mimic host structures. The hyaluronic acid CPS of *Streptococcus, as an example,* mimics the mammalian structure. More important, CPS can act as adhesion receptor. Some CPSs are well known as the major virulence factors of bacteria such as in *Streptococcus pneumoniae* [8].

3.1.4 Bacterial infection and immunology

The human body is constantly exposed to a microorganism-containing environment. Although most bacteria are beneficial, some bacteria can cause bacterial infection. These bacteria are pathogenic bacteria. Bacterial infections often begin with bacteria entering the human mucosal membranes found at different places in the body such in the nose, mouth, pharynx, eyes, but also the genito-urinary and the respiratory system. Some pathogens growing at host cells cause infection, some pathogens may just colonise the host [4] [9].

The human immune systems combine many interdependent cell types to protect body from bacterial infections. An immune response can be specific or non- specific. The non-specific immune response can be achieved by phagocytes. When a bacterial cell gets attached to the phagocytes cell surface receptor, phagocytes can stretch around the bacterium and engulf it [4] [9].

Lymphocytes can be divided into two major cell types: B cells and T cells. The function of B cells is to produce specific antibodies in response to foreign bacterial material, and to signal other cells to engulf the bacteria. There is also a type of B cells that produces antibodies in response to T cell activation. Those B cells are called B memory cells. T cells contain specific antigens receptors on their surface, and they can recognise fragments of antigens on the surface of bacterial cells. T cells are divided into two major types, the T killer subset (T_C) (CD8 + T cell) and T helper subset (T_H) (CD4 + T cell). T helper cells communicate with other cells and activate them to destroy and remove bacteria. T helper cells also stimulate both the production of B memory cells and B cells to produce antibodies. T killer directly destroy cells carrying certain foreign molecule on their surface [4] [9].

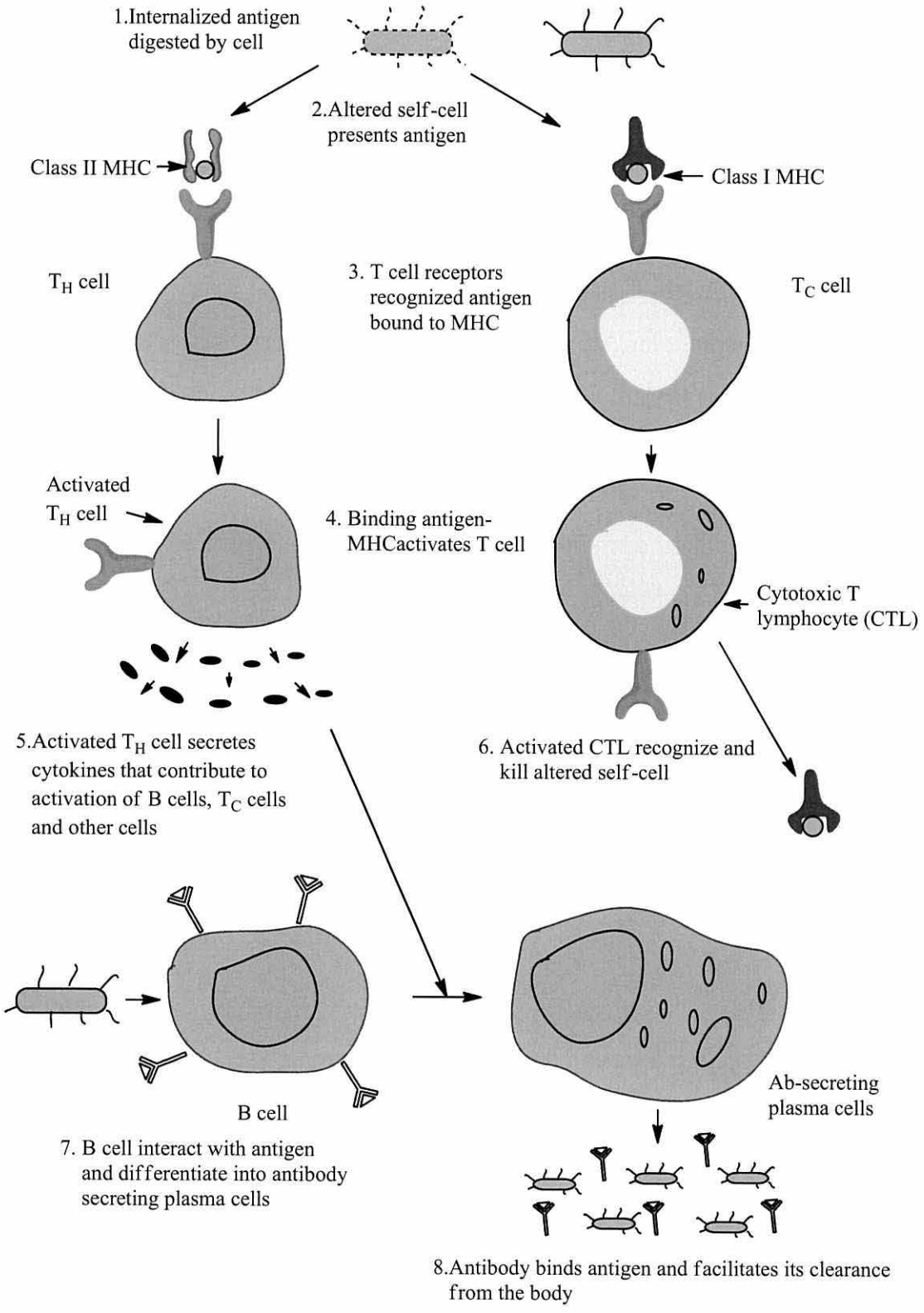

Figure 2: Overview of the humoral and cell mediated branches of the immune system, modified from [4].

Immune responses can be divided into a humoral and cell-mediated one. The

humoral respone is that a B cell interacts with an antigen to produce serum antibody to protect the body from bacteria. The cell mediated immunity is that T cells interact with antigesn and present it to T cells in order to activate the immune response [9].

B cell and T cell can recognise discrete sites (normally on the antigen surface), called antigenic determinants, or a specific epitopes. There are four major cell-membrane molecules responding to antigen to be recognised by the immune system: membrane-bound antibodies on B cells, T cell receptors, class I MHC (**m**ajor **h**istocompatibility **c**omplex) molecules, and class II MHC molecules. The Class I MHC is present on almost all cells in the human body. An infected cell presents fragments of a bacterium or a virus on the Class I MHC. The T_C cell recognises the combination of this antigen and the Class I molecule. The Class II MHC is present on many cells belonging to the immun system. T_H cells recognise antigens that are presented by Class II MHC. The T_H cells will initiate the secretion of small chemical compounds, the cytokines. Those molecules increase the phagocytosis but also the production of B-memory cells. B cells can directly recognise an antigen, while a T cell can only recognise an antigen when it is bound to MHC molecules on the surface of an antigen-presenting cell or an altered self-cell [4].

3.1.5 Vaccines

There are two major types of vaccines against *S. pneumoniae* commercially available. One type are the pneumococcal polysaccharide vaccines (PPV), the other are pneumococcal conjugate vaccines (PCV) [9]. Compared to the large number of 90 different sero types of *pneumococci*, the available vaccines are not enough to cover all these serotypes. However, the number of serotypes in the vaccines has increased from 4 to 23 [11] [12] [13]. The oldest pneumococcal vaccine, the 23-valent vaccine is active against 23 different types of pneumococcal serotypes (1, 2, 3, 4, 5, 6B, 7F, 8, 9N, 9V, 10A, 11A, 12F, 14, 15B, 17F, 18C, 19F, 19A, 20, 22F, 23F and 33F) [14]. This vaccine can be used for adults and children [14]. However, the 23-valent vaccine does not work on children under two-year age [15]. Therefore PCV vaccines are developed to protect young children under the age of 2 years from *S. pneumoniae*. These conjugated vaccines consist of a sugar part and a protein. The

protein is necessary to get the T-cell dependent immune response. In the conjugated vaccines, the parts are connected by a covalent bond. Recently, several new PCV vaccines have been developed, e.g. the PCV7 vaccine [17] against serotypes 4, 6B, 9V, 14, 18C, 19F, and 23F strains and the 13-valent Prevnar 13 vaccine [18] that is active against six additional strains, 1, 3, 5, 6A, 19A and 7F [16].

3.1.6 Aim of this project

Many young children and old people suffer from diseases caused by *S. pneumoniae*. A problem is that antibiotics do not work always because the bacteria have become resistant to the antibiotics. There are vaccines available that are made from mixtures of the polysaccharides. These vaccines do not work in young children under two years because young children do not have mature B cells. They need a vaccine that produces a T-cell dependent immunity. There are conjugate vaccines available that can be used for young children. Both types of vaccines are using polysaccharides obtained from the bacteria. The problems are batch variation and presence of impurities, and added adjuvants that can lead to severe side reactions after immunisation [19].

The aim of this project is the development of a totaly synthetic carbohydrate-based vaccine against *Streptococcus pneumoniae* type 14 to avoid the above mentioned problems.

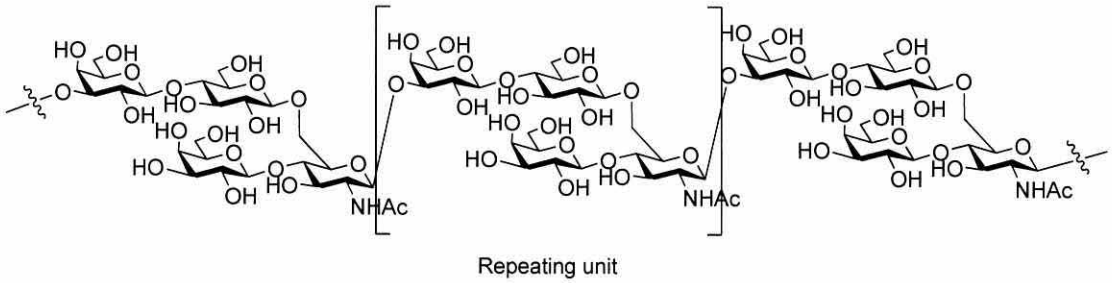

Figure 3: The tetrasaccharide repeating unit of the capsular polysaccharide of *S. pneumoniae* type 14.

In previous studies it was found, that a tetrasaccharide portion of the capsular polysaccharide of *S. pneumoniae* type 14 is sufficient to produce an immune

response [20]. This tetrasaccharide is a repeating unit of the capsular polysaccharide (Figure 3). This structure might be a good starting point to develop a totaly synthetic conjugate vaccine. For this purpose, a spacer-equipped tetrasaccharide has to be synthesised. The syntheses of the protected tetrasaccharide and the building blocks have been described earlier [21]. In addition, a biotin labelled tetrasaccharide will be useful to study the immune response in detail (Figure 4).

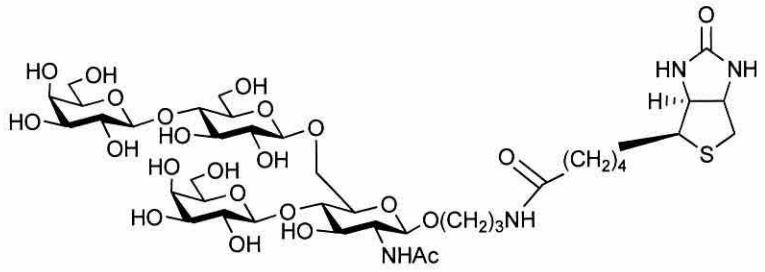

11

Figure 4: The biotin labelled tetrasaccharide.

3.2 Results and discussions

3.2.1 Synthesis of a spacer equipped tetrasaccharide corresponding to a repeating unit of the *S. pneumoniae* type 14 CPS

To produce a totaly synthetic carbohydrate-based conjugated vaccine several pieces were required. The immunogenic tetrasaccharide had to be prepared, a carrier had to be found, and a decision about the protein required for the T-cell dependent immune response had to be made. It was decided to use gold nanoparticles with a very small diameter (2 nm). This size of nanoparticles has been found to be soluble in aqueous systems and to be non-toxic [22]. A sequence of ovoalbumin was chosen as T-cell triggering component. A common way to link molecules to gold particles is to use thiol-functionalised compounds [23].

The ω-amino linker equipped tetrasaccharide **5** was intended to be used for nanoparticle and biotin conjugation. The ethylthio tetrasaccharide **1** [21] was available (Scheme 1). Azidopropanol was coupled to compound **1** using *N*-

iodosuccinimide (NIS) and silver trifluoromethanesulfonate (AgOTf) as promoter to yield spacer glycoside **2** (90 %). The reaction mixture had to be kept as dry as possible by using molecular sieves (4 Å). Only the β anomer was formed due to neighbouring group participation of the phthalimido group [24].

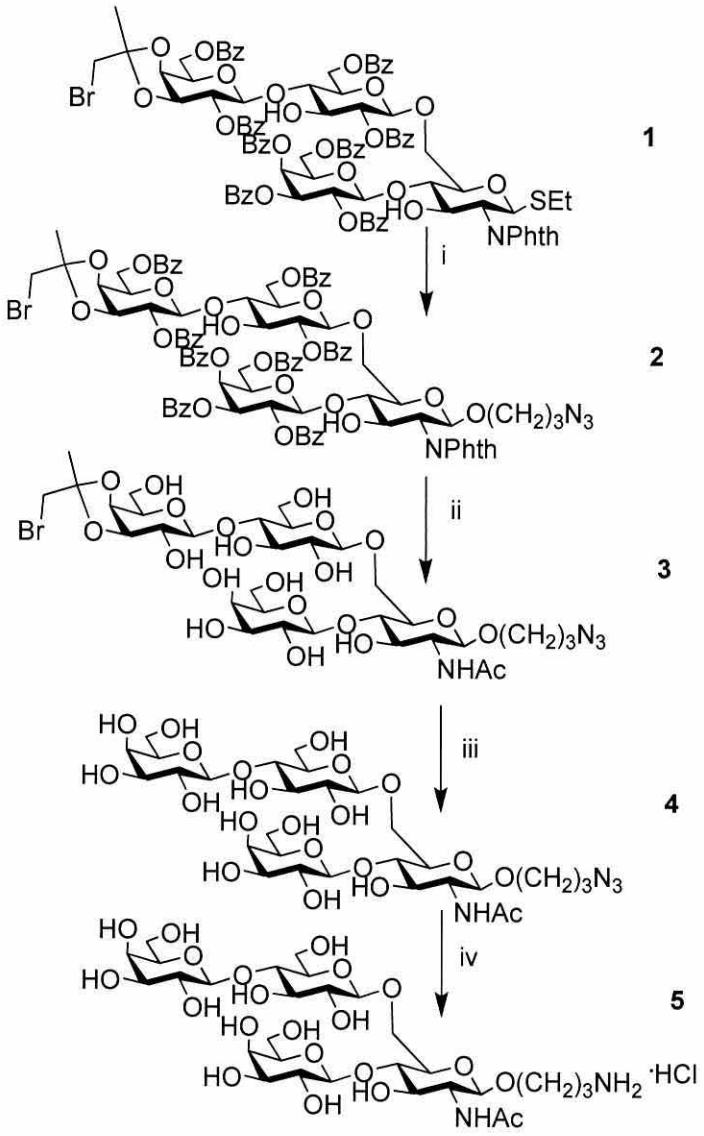

Scheme 1: i: 1 azidopropanol, dry DCM, NIS, RT, 15min 2. AgOTf , 0°C, 3. RT, 1h, 90 % ii: 1. dry ethanol, EDA, 60 °C, overnight, 70 % 2. Dry MeOH, Ac_2O, 1h, RT, 3. NaOMe, dry MeOH, 95 % iii: 90%TFA, RT, 3h. iv: water/MeOH 1:1, HCl, Pd/C, hydrogen atmosphere, RT, overnight, 93 %.

The deprotection was tried in different ways. If the bromoisopropylidene group was removed first followed by cleavage of the phthalimido group and *N*-acetylation and

debenzoylation, a side product was formed. This was isolated and identified as ethylene diacetamide (EDA) [25]. It was found that it was difficult to remove this side product from the partially unprotected tetrasaccharide.

Therefore, the phthalimido group was removed using ethylenediamine in dry ethanol under reflux giving the derivative with the free 2-amino group. Some of the benzoyl groups were also cleaved off at this step, and the products therefore not characterised. Then *N*-acetylation was carried out with acetic anhydride in MeOH, converting the amino group into the desired acetamido group. After that, complete debenzolyation was performed under Zemplén conditions [26] (sodium methoxide and methanol) to afford the azido-spacer derivative **3** in 70 %.

Then the bromoisopropylidene group was removed by acid hydrolysis using 90 % trifluoroacetic acid (TFA) to yield compound **4** in 95 % yield. The spacer equipped tetrasaccharide hydrochloride salt **5** (93 %) was formed by treatment of **4** using 1 equivalent HCl and a catalytic amount of Pd/C under a hydrogen atmosphere [27]. The reaction was carried out overnight. The addition of a small amount of HCl readily converted the produced amine into the ammonium salt. This way, the reaction was not slowed down due to poisoning of the catalytic system.

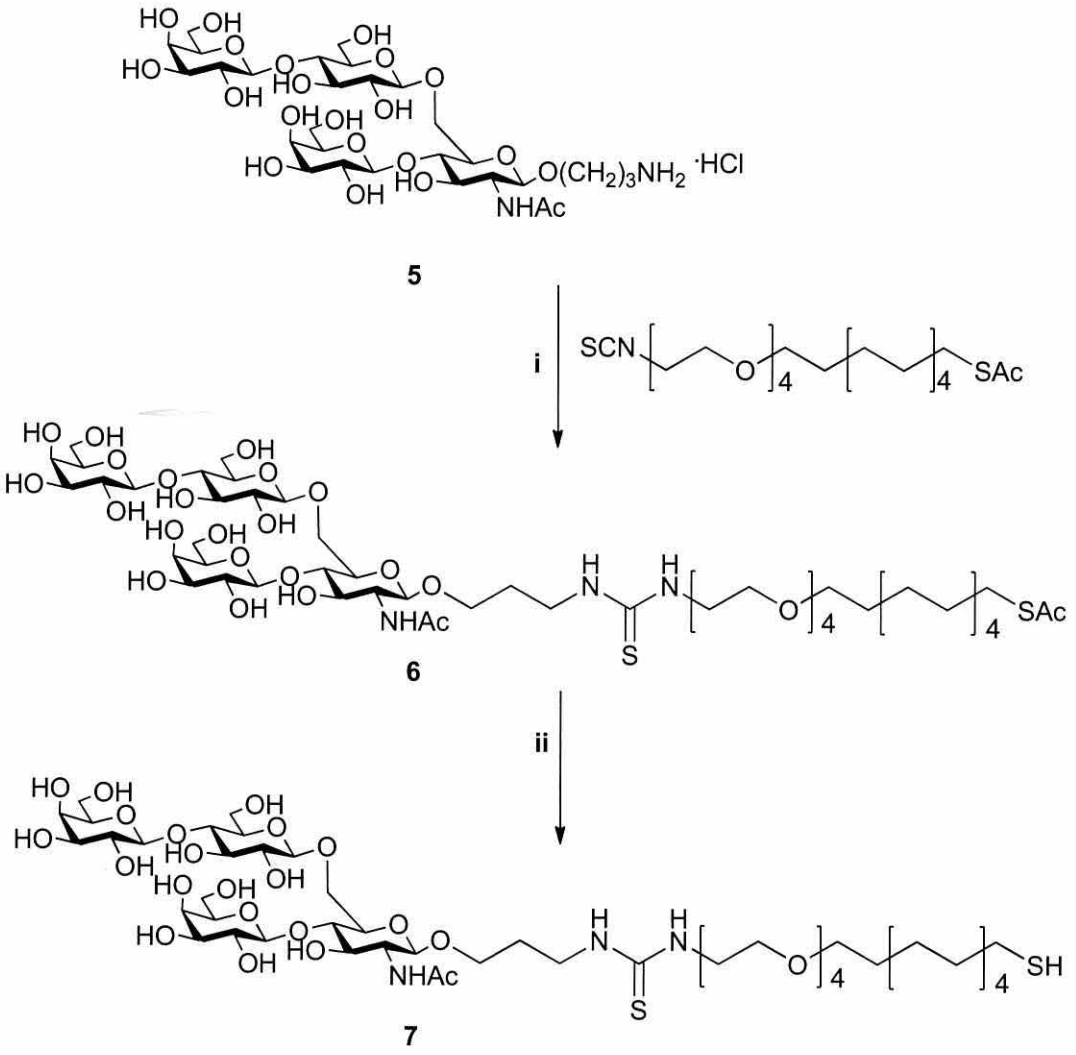

Scheme 5: i Et_3N, H_2O/PrOH/CH_3CN, 17 h, 25°C, ii MeONa/MeOH, 4 h, 25°C [28].

The GNPs were finally constructed using the linker equipped tetrasaccharide unit **7**, monosaccharide glucoside **8**, and the synthetic $OVA_{323-339}$-peptide **9**. Glucose (**8, figure 5)** and $OVA_{323-339}$-peptide (**9, figure 5)** worked as inert components to control the density of the recognised epitope. In addition, the specially designed long linkers made that the epitopes were pointing outwards, thus not being wrapped around the GNPs. Both factors make the recognised epitopes more accessible to the antibodies [29].

The required further conjugation reaction (scheme 5) was done by our collaborators [28]. Tetrasaccharide **5** was reacted with an isothiocyanate linker in a water/isopropanol/acetonitrile solution, containing triethylamine [28]. The reaction gave thioacetyl-protected neoglycoconjugate **6** (71%). Compound **6** was further

deprotected to produce **7** as a mixture of disulfide and thiol (2.5:1, 81%). Compound **7** was used to prepare Gold glyconanoparticles (GNPs) (Figure 5) [28].The glucose conjugate **8** was prepared according to literature [23].

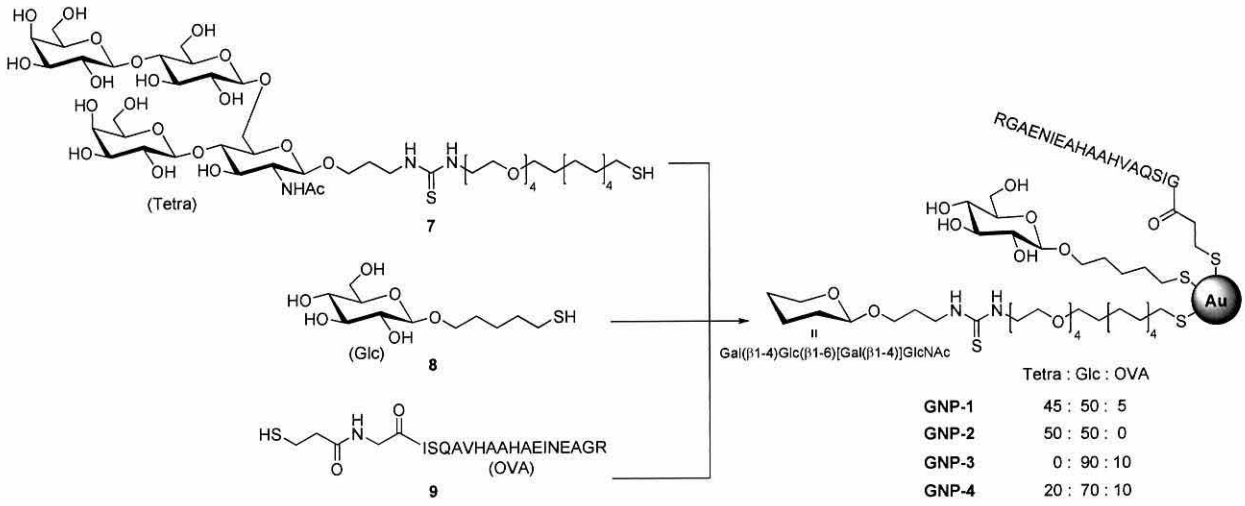

Figure 5: One-step synthesis of hybrid gold glyconanoparticles (GNPs) incorporating different molar ratios of branched tetrasaccharide **7** (Tetra = Gal-Glc-(Gal-)GlcNAc), D-glucose (Glc) conjugate **8**, and $OVA_{323-339}$-peptide (OVA) conjugate **9** [28].

3.2.2 Biological results

Several types of GNPs were prepared in different molar ratios of the tetrasaccharide conjugate **7**, the glucose conjugate **8**, and the $OVA_{323-339}$-peptide fragment **9** (Table 1).

GNPs	Mean metal core diameter [nm][a]	Average number of gold atoms[b]	Average MW (KDa)	Molar ratio of conjugates Tetra : Glc : OVA[c]	Estimated average molecular formula
GNP1[d]	1.8 ± 0.5	201	95	45 : 50 : 5	$Au_{201}(Tetra)_{32}(Glc)_{35}(OVA)_4$
GNP-2	1.9 ± 0.3	225	97	50 : 50 : 0	$Au_{225}(Tetra)_{36}(Glc)_{35}$
GNP-3	1.9 ± 0.5	225	76	0 : 90 : 10	$Au_{225}(Glc)_{64}(OVA)_7$
GNP-4	1.7 ± 0.7	201	84	20 : 70 : 10	$Au_{201}(Tetra)_{14}(Glc)_{50}(OVA)_7$

[a]Diameter of the gold nanocluster (as measured by TEM). [b]Average number of gold atoms per nanoparticle was calculated from the size of the gold cluster obtained by TEM, as reported previously [18] [c]Molar ratio of conjugates per nanoparticle was determined by analyzing the mixtures using NMR before and after nanoparticle formation. [d]Two different batches of **GNP-1** were independently prepared and displayed the same physicochemical and immunochemical properties [28].

Table 1. Physicochemical properties of the hybrid gold nanoparticles prepared in the study [28].

These GNPs were injected into mice. Specific IgG antibodies against native Pn14PS were determined by ELISA. According to the data (Figure 6), **GNP-1**, **GNP-1**, **GNP-2**, **GNP-3** and **GNP-4** produced different levels of specific IgG antibodies against native Pn14PS. Overall, it was found that GNPs coated with the tetrasaccharide and $OVA_{323-339}$ peptide induce specific IgG antibodies that recognize the branched tetrasaccharide homologue β-D-Gal*p*-(1→4)-β-D-Glc*p*-(1→6)-[β-D-Gal*p*-(1→4)-]β-D-Glc*p*NAc-(1→3)-β-D-Gal-(1→) [xxxiv] and the native polysaccharide of Pn14PS.

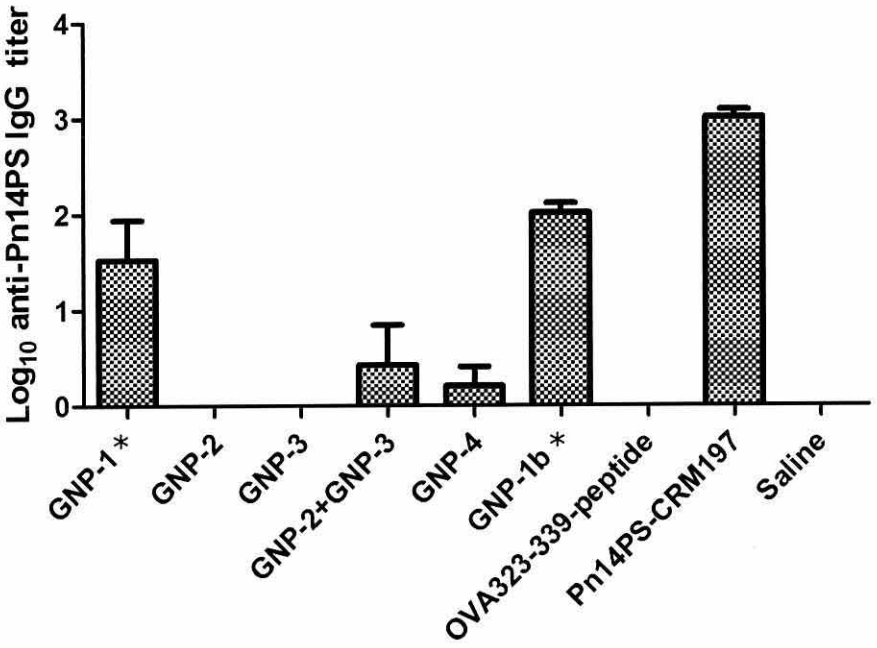

Figure 6. Specific anti-*S. pneumoniae* type 14 polysaccharide (Pn14PS) IgG antibodies determined by ELISA [28].

3.3 Synthesis of a biotin labelled tetrasaccharide corresponding to a repeating unit of the *Streptococcus pneumoniae* type 14 capsular polysaccharide

The biotin labelled tetrasaccharide was intended to visualize specific B cells. Target **10** was made by reacting **5** with Et_3N, NHS-activated biotin in Millipore water (83% yield) (scheme 6). The compound was isolated and submitted for biological evaluation.

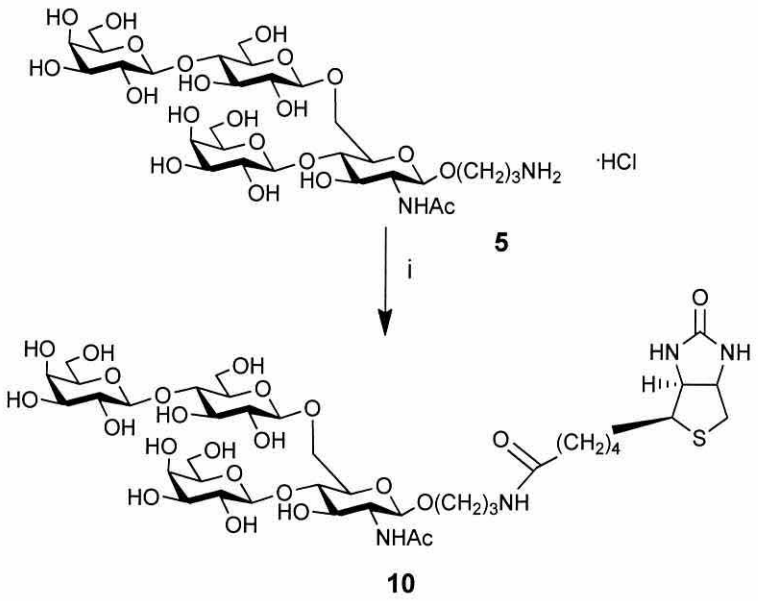

Scheme 6: i: Millipore water, Et_3N, NHS activated biotin, 83 %.

3.4 Conclusions

In conclusion, synthesis of the linker-equipped tetrasaccharide unit **5** was achieved. Gold nanoparticles (GNPs) were coated with the linker-equipped tetrasaccharide unit **7**, glucoside **8** and the synthetic $OVA_{323-339}$-peptide **9**, and injected to mice. Biological results showed that GNPs constructed with 45 % of tetrasaccharide structure **7**, 5 % of $OVA_{323-339}$-peptide and inert glucosides 8 were able to induce IgG antibodies against polysaccharide of *S. pneumoniae* type 14. A biotin labelled conjugate **10** was also successfully prepared, and is under biological evaluation.

3.5 Experimental

3.5.1 General procedures

DCM was distilled from calcium hydride before use. Dry methanol was kept over molecular sieves 3 Å; all other chemicals were used as purchased. TLC was perfomed on 0.25 mm precoated silica gel glass plates (Merck silica gel 60 F_{254}) with detection by UV-light (254nm) or charring with 10% sulphuric acid solution followed by heating. Organic solvent were evaporated with rotary evaporator under reduced pressure at approximately 40°C (water bath). Silica gel (Amicon 0.041 – 0.063 mm) was used for column chromatography.

MALDI-TOF spectra were recorded on a Bruker Reflex IV using 2, 4, 6- trihydroxy-acetophenone monohydrate (THAP) as matrix.

NMR-spectra were recorded at 250MHz or 500 MHz, respectively, in $CDCl_3$, D_2O or CD_3OD. NMR-experiment in $CDCl_3$ were referred to the chloroform signal (δ = 7.31 ppm) or (δ = 77.16 ppm).

3-Azidopropyl 3,4-O-(1-bromomethylethylidene)-β-D-galactopyranosyl-(1→4)-β-D-glucopyranosyl)-(1→6)-[β-D-glucopyranosyl-(1→4)]-2-acetamido-2-deoxy-β-D-glucopyranoside (**3**).

Compound **1** (150 mg, 82 µmol) was dissolved in dry DCM (2 mL), and then molecular sieves (4 Å, 200 mg), 2-azidopropanol (30 µL, 0.32 mmol) and *N*-iodosuccinimide (30 mg, 0.13 mmol) were added. The reaction mixture was stirred at room temperature for 15 min. After that, the mixture was cooled down to 0 °C in an ice bath, and a catalytic amount of AgOTf was added. The reaction was monitored by TLC (toluene/ EtOAc 6:1), while stirring of the reaction mixture continued for 1 h at room temperature. After complete conversion, the mixture was concentrated and purified by flash column chromatography (toluene → toluene/EtOAc, 15:1→10:1→7:1→5:1) to give 3-azidopropyl [2,6-di-*O*-benzoyl-3,4-*O*-(1-bromomethylethylidene)-β-D-galactopyranosyl]-(1→4)-(2,3,6-tri-*O*-benzoyl-β-D-

glucopyranosyl)-(1→6)-[(2,3,4,6-tetra-*O*-benzoyl-β-D-glucopyranosyl)-(1→4)]-2-deoxy-2-phthalimido-β-D-glucopyranoside as diastereomeric mixture (138 mg, 71 µmol, 90 %). MALDI-TOF MS for $C_{101}H_{89}BrN_4O_{31}$: Calcd. 1933.4767 $[M+H]^+$, 1955.4586 $[M+Na]^+$. Found 1933.5150 $[M+H]^+$ ± 20 ppm, 1955.5625 $[M + Na]^+$ ± 25 ppm. NMR data were in agreement with the previously reported ones [12].

This material (138 mg, 71 µmol) was dissolved in dry ethanol (5 mL), and after addition of ethylenediamine (500 µL, 7.4 mmol) the reaction mixture was stirred at 60 °C overnight. After complete consumption of the starting material (TLC: 6:1, DCM/MeOH), the mixture was concentrated and the residue co-evaporated 2 times with toluene. Then dry methanol (5 mL) and acetic anhydride (250 µL) was added to the residue, and the resulting mixture was stirred for 1 h at room temperature, concentrated, co-evaporated with toluene, and again dissolved in dry methanol (10 mL). Then NaOMe (approx. 1 M solution in MeOH, 10 drops) was added, and the reaction mixture was stirred at room temperature overnight. The progress of the reaction was monitored by MALDI-TOF MS. After complete conversion, the mixture was neutralized using H^+-ion-exchange resin (Dowex-50WX-8). The resin was filtered off the reaction solution, and the filtrate was concentrated before the residue applied onto a column. Flash chromatography (DCM/MeOH 15:1 → 10:1 → 8:1 → 6:1 → 3:1 → 1:1→ methanol) gave compound **5** as diastereomeric mixture (48 mg, 53 µmol, 74 %).

^{13}C NMR (CD_3OD) δ 173.6 ($NC(O)CH_3$), 110.1 ($C(CH_3)(CH_2Br)$), 104.9, 104.6, 104.2, 103.1 ($C\text{-}1^{I\text{-}IV}$), 81.8, 81.5, 81.0, 80.5, 77.0, 76.5, 76.5, 76.0, 75.9, 75.5, 75.4, 74.9, 74.4, 74.1, 72.8, 70.5, 68.7, 67.5, 62.6, 62.5, 62.0, 56.8 ($C\text{-}2^{I\text{-}IV}\text{-}6^{I\text{-}IV}$, $OCH_2CH_2CH_2N_3$), 37.0 ($C(CH_3)(CH_2Br)$), 30.2 ($OCH_2CH_2CH_2N_3$), 25.0, 23.1 ($C(CH_3)(CH_2Br)$) and ($NC(O)CH_3$). ($OCH_2CH_2CH_2N_3$) undetected (under CD_3OD signals) ppm; HR-MS for $C_{32}H_{53}BrN_4O_{21}$: Calcd. 931.2278 $[M+Na]^+$. Found 931.1931 $[M+Na]^+$ ± 37 ppm.

3-Aminopropyl-β-D-galactopyranosyl-(1→4)-β-D-glucopyranosyl-(1→6)-[β-D-glucopyranosyl-(1→4)]-2-acetamido-2-deoxy-β-D-glucopyranoside·HCl salt (5).

Compound **3** (48 mg, 53 µmol) was dissolved in 90% trifluoroacetic acid (1.8 mL). The reaction mixture was stirred at room temperature for 3 h and the progress of the reaction monitored by TLC (DCM/MeOH, 6:1) and MALDI-TOF. After complete consumption of the starting material, the mixture was co-evaporated with toluene (2 x 5 mL). Purification by size-exclusion chromatography (Bio-Gel P-2 column, 1% *n*-BuOH in purified water) provided 3-azidopropyl β-D-galactopyranosyl-(1→4)-β-D-glucopyranosyl)-(1→6)-[β-D-glucopyranosyl-(1→4)]-2-acetamido-2-deoxy-β-D-glucopyranoside (40 mg, 51 µmol, 96 %).

^{1}H NMR (D_2O) δ 4.49-4.42 (m, 3H, 3xH-1); 4.36 (d, 1H, *J* = 7.8 Hz, H-1); 4.20 (d, 1H, *J* = 9.8 Hz); 3.94-3.82 (m, 5H); 3.81-3.54 (m, 15H), 3.54-3.49 (m, 1H); 3.49-3.42 (m, 1H); 3.33-3.24 (m, 2H), 1.96 (s, 3H, NAc); 1.79-1.72 (m, 2H, $OCH_2CH_2CH_2N_3$). ^{13}C NMR (D_2O) δ 174.5 ($NC(O)CH_3$), 103.0, 102.8, 102.4, 101.2 (C-1^{I-IV}), 78.4, 77.9, 75.4, 75.3, 74.7, 74.3, 73.5, 72.7, 72.5, 72.3, 71.0, 68.6, 67.4, 67.3, 61.1, 61.0, 60.1, 55.1 (C-2^{I-IV}-6^{I-IV}, $OCH_2CH_2CH_2N_3$), 47.8 ($OCH_2CH_2CH_2N_3$), 28.1 ($OCH_2CH_2CH_2N_3$), and 22.2 ($NC(O)CH_3$). HR-MS for $C_{29}H_{50}N_4O_{21}$: Calcd. 813.2860 $[M+Na]^+$. Found 813.2754 $[M+Na]^+$ ± 13 ppm.

This material (40 mg, 51 µmol) was dissolved in water/MeOH (1:1, v/v) and 2 M HCl (1 equiv., 30 µL), and a catalytic amount of Pd/C was added. The reaction mixture was stirred under a hydrogen atmosphere at room temperature. When complete conversion had taken place, as indicated by Maldi-TOF, the catalyst was removed by filtration over a filter sandwich. The solvents were then removed by evaporation. The residue was dissolved in water (2 mL), and freeze-dried to obtain compound **5** (36 mg, 45 µmol, 89%).

^{1}H NMR (D_2O) δ 4.41-4.33 (m, 3H, 3xH-1); 4.29 (d, 1H, *J* = 7.8 Hz, H-1); 4.14 (d, 1H, *J* = 9.0 Hz); 3.88-3.77 (m, 3H); 3.76 (sb, 2H); 3.72-3.47 (m, 15H), 3.47-3.42 (m, 1H); 3.41-3.35 (m, 2H); 3.25-3.18 (m, 1H), 2.92 (t, 2H, *J* = 6.8 Hz, $OCH_2CH_2CH_2NH_2$), 1.88 (s, 3H, NAc); 1.78 (dt, 2H, J = 13.0 Hz, $OCH_2CH_2CH_2NH_2$). ^{13}C NMR (D_2O) δ 174.7 ($NC(O)CH_3$), 103.0, 102.8, 102.4, 101.3 (C-1^{I-IV}), 78.4, 77.7, 75.4, 75.3, 74.7,

74.3, 73.4, 72.7, 72.5, 72.1, 71.0, 68.6, 68.1, 61.0, 61.0, 55.1 (C-2^{I-IV}-6^{I-IV}, $OCH_2CH_2CH_2NH_2$), 37.7 ($OCH_2CH_2CH_2NH_2$), 26.6 ($OCH_2CH_2CH_2NH_2$), and 22.1 ($NC(O)CH_3$). HR-MS for $C_{29}H_{52}N_2O_{21}$: Calcd. 787.2955 $[M+Na]^+$. Found 787.3105 $[M+Na]^+$ ± 19 ppm.

Biotinylation (10)

Compound **5** (10 mg, 0.1 mmol) was dissolved in Millipore water (800 µL), then Et_3N (8 µL) and NHS-activated biotin (12 mg, 0.05 mmol) was added and the mixture stirred at room temperature for 30 min. The reaction was monitored by Maldi. After complete conversion, the mixture was concentrated and purified by RP C18 column chromatography (water→10%MeOH→20%MeOH→30%MeOH→40%MeOH) to get product (**10**) (10 mg, 86%). ^1H NMR (D_2O) δ 4.51 (m, 1H, H_{biotin}), 4.47-4.42 (dd, 3H, J = 8.0 Hz, J = 15.0 Hz, 3xH-1); 4.40-4.33 (m, 3H); 4.20 (br d, 1H, J = 11.3 Hz); 3.92-3.82 (m, 5H); 3.79-3.70 (m, 3H); 3.70-3.56 (m, 13H), 3.55-3.50 (m, 2H); 3.49-3.43 (m, 2H); 3.32-3.24 (m, 3H), 3.23-3.16 (m, 1H, H_{biotin}), 3.14-3.07 (m, 2H), 2.92 (dd, 1H, H_{biotin}), 2.70 (dd, 1H, H_{biotin}), 2.39 (br s, 1H), 2.17 (t, 2H, J = 7.3 Hz), 1.96 (s, 3H, NAc); 1.80-1.70 (m, 4H), 1.68-1.56 (m, 4H), 1.44-1.38 (m, 2H), 1.28 (t, 2H). MALDI-TOF Calcd for $C_{39}H_{66}N_4O_{23}S$ MS: 990.38 [M]; 1013.38 $[M+Na]^+$. Found: 1013.32 $[M+Na]^+$ ± 59 ppm.

3.6 References

1. Gram, C. *Fortschr. Med*, **1884**, *2(*6), 185-189
2. Wheelis, M., *Principles of Morden Microbiology. 1st edition,* Jones & Bartlett Publishers, **2007**
3. Shagam, J. *Introduction to Microbiology*, Pearson Education Limited, **2006**
4. Goldsby, R. A.; Kindt, T. J.; Osborne, B. A.; Kuby, Janis. *Immunology,fifth edition*, England, W.H. Freeman and company, **2003**
5. Winslow, C., and Broadhurst, J. *J. Bacteriol*, **1920**, *5* (3), 191–229
6. Watson, D. A.; D. M. Musher, J. W. Jacobson, and J. Verhoef. *Clin. Infect. Dis,* **1993**, *17*, 913–924
7. Verez-Bencomo, V.; Fernández-Santana, V.; Hardy, E.; Toledo, M. E.; Rodríguez, M. C.; Heynngnezz, L.; Rodriguez, A.; Baly, A.; Herrera, L.; Izquierdo, M.; Villar, A.; Valdés, Y.; Cosme, K.; Deler, M. L.; Montane, M.; Garcia, E.; Ramos, A.; Aguilar, A.; Medina, E.; Toraño, G.; Sosa, I.; Hernandez, I.; Martínez, R.; Muzachio, A.; Carmenates, A.; Costa, L.; Cardoso, F.; Campa, C.; Diaz, M.; Roy, R. *Science* **2004**, *305*, 522.
8. Ajit, V.; Richard, D. C.; Jeffrey, D. E.; Hudson, H. F.; Pamela, S.; Carolyn, R. B.; Gerald, W. H.; and Marilynn, E. E, *Essencial of Glycobiology, 2nd Edition*, Cold Spring Harbor, **2009**, 322-325
9. Madigan, M. T; Martinko, J. K; Parker, J, *Broke Biology of Microorganisms 10 th Edition*, Carlson, G, Ed, **2003**, 79-94
10. Barocci, M. A.; Censini, S. and Rappuoli, R. *Vaccine*, **2007**, *25*, 2963-2973
11. Macleod, C. M.; Hodges, R. G.; Heidelberger, M.; Bernhard, W.G. *J. Exp. Med,* **1945**, *82*, 445
12. Austrian, R.; Douglas R.M.; Schiffman, G, Coetzee, A. M.; Koornhof, H. J.; Hayden, S. S.; Reid, R. D. *Trans. Assoc. Am. Physicians,* **1976**, *89*, 184
13. Klein, J. O.; Plotkin, S. A.; Austrian, R. *Clin. Infect. Dis*, **2007**; *45*, 2
14. Obrien, K, L.; Hochman, M, Goldblatt, D. *Lancet Infect. Dis*, **2007**, 7, 597-606
15. Bruyn, G. A. W.; Van Furth, R. *Eur. J. Clin.Microbiol.Infect. Dis*, **1991**, *10*, 897–910
16. CDC home [Internet]. [Updated: October 1st, 2011]. Centers for Disease Control and Prevention, [cited October 12th, 2011]. Available from http://www.cdc.gov/

17. Black, S.; Shinefield, H.; Fireman, B.; Lewis, E.; Ray, P.; Hansen, J.R. Elvin, L.; Ensor, K. M.; Hackell, J.; Siber, G.; Malinoski, F.; Madore, D.; Chang, I.; Kohberger, R.; Watson, W.; Austrian, R.; Edwards, K. *Pediatr. Infect. Dis. J*, **2000**, 19 **(**3), 187–195
18. HHS home [Internet]. [Update: October 2nd, 2011] The Department of Health and Human Services (HHS), [cited October 12th, 2011]. Available from http://www.hhs.gov/
19. Herberts, C.; Melgert, B.; van der Laan, J. W.; Faas, M. *Expert. Rev. Vaccines*, **2010**, *9* (12), 1411-1422
20. Safari, D., Dekker, H. A. T.; Joosten, J. A. F.; Michalik, D.; Carvalho de Souza, A.; Adamo, R.; Lahmann, M.; Sundgren, A.; Oscarson, S.; Kamerling, J. P.; Snippe, H. *Infect. Immun*. **2008**, *76*, 4615
21. Sundgren, A.; Lahmann, M.; Oscarson, S. *J. Carbohydr. Chem,* **2005**, *24*, 379
22. Rojo, J.; Diaz, V.; De la Fuente, J.M.; Segure, I.; Barrientos, A.G.; Riese, H. H.; Bernard, A.; Penades, S. *Chem. Bio. Chem*, **2004**, *5*, 291-297
23. Martinez-Avila, O.; Hijazi, K.; Marradi, M.; Clavel, C.; Campion, C.; Kelly, C.; and Penades. *Chemistry*, **2009**, *15*, 1806-1809
24. Demchenko, A. V.; Wolfert, M. A.; Santhanam, B.; Moore, J. N.; Boons, G. J. *J. Am. Chem. Soc,* **2003**, *125*, 6103
25. Sundgren, A., Sythesis of antigenic oligosaccharides from the human pathogenic bacteria *Streptococcus pneumoniae, Haemophilus influenza* and *Vibrio cholerae*, **2005**, Göteborg University
26. Zemplén, G.; Pacsu, E. *Ber. Dtsch. Chem. Ges*, **1929**, 62, 1613–1614
27. Lahmann, M.; Bülow, L.; Teodorovic, P.; Gybäck, H.; Oscarson, S *Glycoconjugate J,* **2004**, *21*, 251
28. Safari, D.; Marradi, M.; Chiodo, F.; Dekker, H. A. T.; Shan, Y.; Adamo, R.; Oscarson, S.; Rijkers, G. T.; Lahmann, M.; Kamerling, J. P. S.; Snippe, P. H. *Nanomedicine UK*, **2011**, DOI:10.2217/NNM.11.151
29. Ojeda, R.; de Paz, J. L.; Barrientos, A. G.; Martín-Lomas, M.; Penadés, S. *Carbohydr. Res,* **2007**, *342*, 448

Chapter 4 – Synthesis of regioselectively sulfated lactose and *N*-acetyl lactosamine derivatives to be used in binding studies with the FedF and the lectin of *E. coli*

4.1 Introduction

4.1.1 *Escherichia coli*

Escherichia coli (*E. coli*) are common bacteria which can be found in the intestines of human and animal bodies. Most strains are harmless and they have beneficial functions such as producing vitamin K2 [1], which prevents harmful bacteria from establishing themselves in the intestines. Some serotypes like serotype O157:H7 can cause several diseases such as diarrhea and abdominal cramps [1]. Recently, a serious public health problem caused by *E.coli* serotype O104:H4 occurred in Germany and France. More than 50 people died [2]. *E.coli* was first discovered by Theodor Escherichin in 1885 [3].

4.1.2 2-Deoxy-2-amino sugars

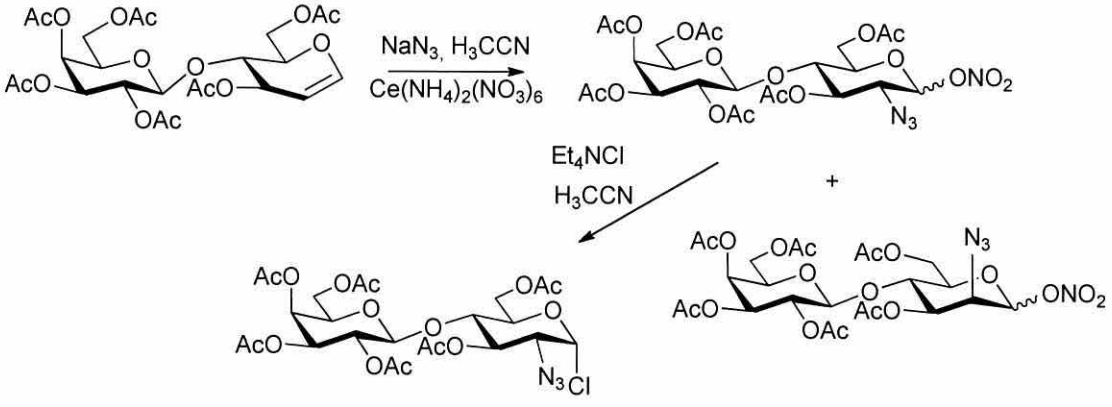

Scheme 1: Azidonitration of peracetylated lactal.

2-Deoxy-2-amino sugars are sugars where the OH group at the C-2 position has been replaced by an amino group. These sugars play an important role in living

organisms. They are widely distributed as building blocks in glycoconjugates such as glycosaminoglycan and peptidoglycans [4]. 2-*N*-acetamido-2-deoxyglycosides such as *N*-acetyl lactosamine (LacNAc, **13**) are very common classes of 2-deoxy-2-amino sugars [5]. Several key reactions are involved in the synthesis of 2-acetamido-2-deoxyglycosides such as LacNAc **13** (scheme 10). One is the azidonitration reaction of glycals (scheme 1) which has been described by R. Lemieux in 1979 [6]. The azido group is introduced at the C-2 position of a glycal producing 2-deoxy-2-azido derivatives with a nitrate group in the anomeric position. This group can be further hydrolysed or replaced by a halide to give a non-participating glycosyl donor for the synthesis of 2-deoxy-2-amino sugar-containing oligosaccharides. A disadvantage is that the introduction of the azido group is not completely stereoselective. The selectivity is highly dependent on the reaction conditions but always produces epimeric mixtures.

In addition, azidoselenation (scheme 2A) was developed as one step synthesis of 2-azido-2-deoxy sugars [7].

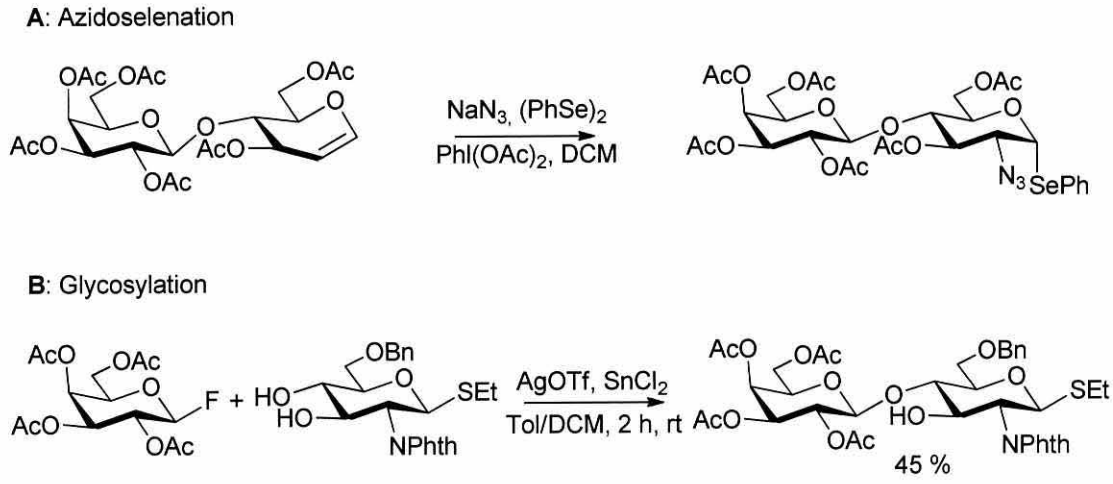

Scheme 2: **A**: Azidoselenation of lactal; **B**: A LacNAc derivative produced by glycosylation [8].

A common way is otherwise to produce LacNAc derivatives by glycosylation [8]. This can be useful if a special protecting group pattern is desired (scheme 2B).

It is often difficult to use 2-acetamido sugars as glycosyl donors due to competing formation of the oxazoline. In many cases a different protecting group is required on the nitrogen [9]. However, it is an option to use oxazolines. This is not always a very high yielding reaction but is very useful for introducing small linkers [10]. Stable 1,2-oxazolines can be formed as a glycosyl donor (scheme 3) [7]. Other glycosylation methods are also used for the synthesis of LacNAc **13** (scheme 10) derivatives.

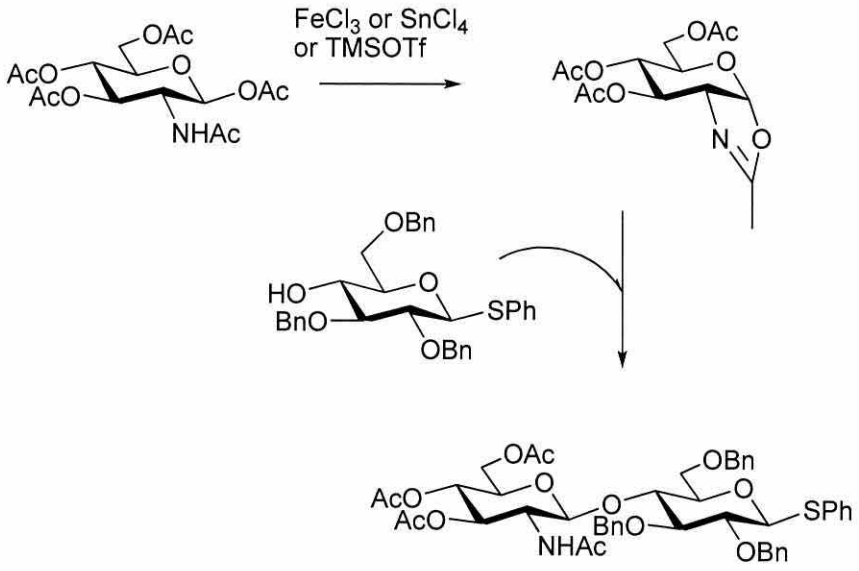

Scheme 3: Oxazolines as glycosyl donors for the synthesis of a LacNAc derivative.

4.1.3 The Heyns rearrangement

The Heyns rearrangement was reported by Heyns and Koch in the 1950s [11]. He described how D-fructose reacted with ammonia to form D-glucosamine (scheme 4).

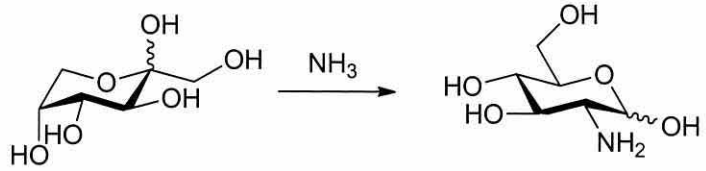

Scheme 4: The Heyns rearrangement of D-fructose.

However, ketoses reacting with amines to form ketosylamines followed by isomerisation to the corresponding 2-amino-2-deoxy-1-aldoses was first reported by E. Fischer [12]. This type of reactions was then further investigated by Heyns and

Koch in 1952 [11]. They found that D-fructose reacts with ammonia to form D-glucosamine. After that, the scope of the reaction was extended by Carson [13] and Heyns' group [14] using a wide range of different primary and secondary amines to produce the corresponding *N*-substituted glucosamines. Because of problems during the reaction, all these reactions gave relatively low yields (about 20 %) [15]. Competition of an Amadori rearrangement [16] (scheme 5) as side reaction can affect the product formation when using primary amines. Also, there is a competition between hydrolysis and rearrangement of the initial condensation product [17]. In 1999, an efficient synthetic method of selected *N*-substituted D-lactosamine derivatives starting from lactulose was reported by Tanja M. Wrodnigg [17] [18] [19].

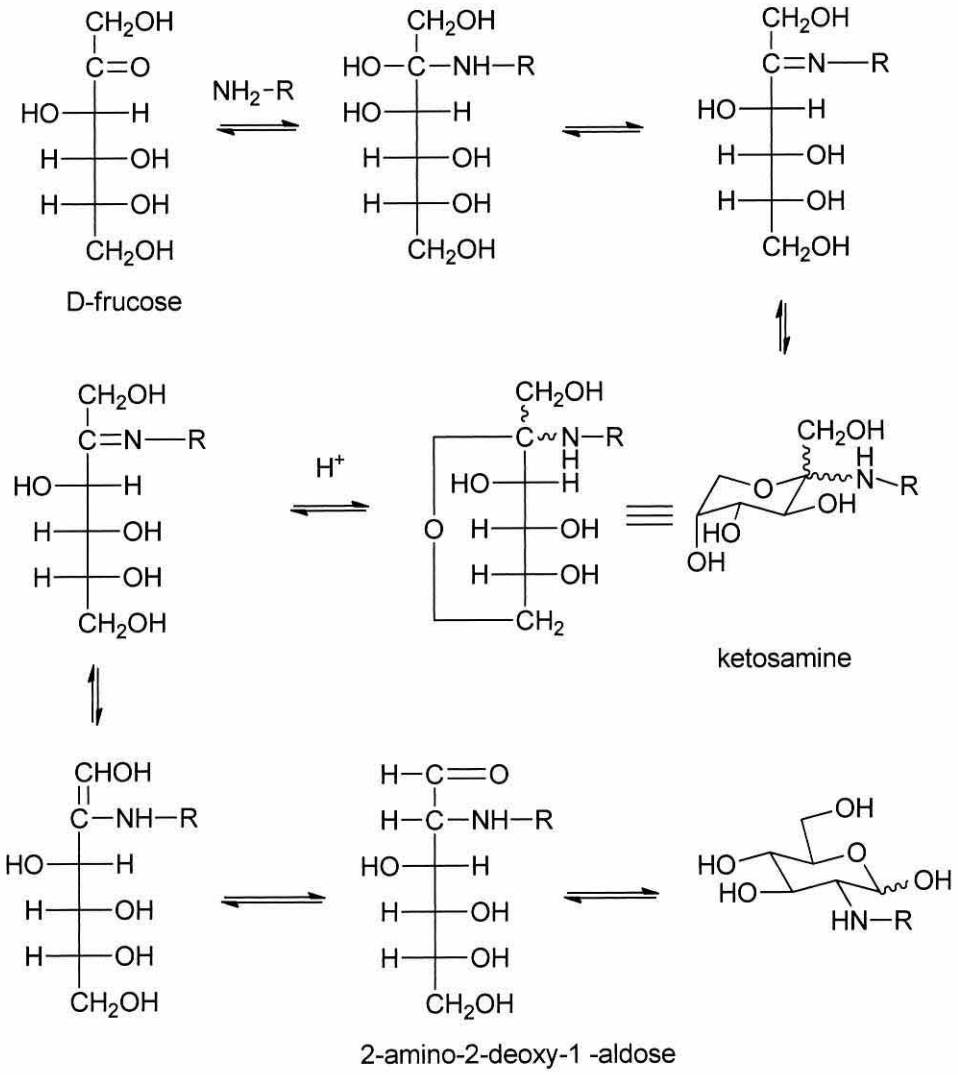

Scheme 5: Heyns rearrangement of D-fructose shown with intermediate steps.

D-fructose condenses with amines (scheme 5) in the same way as other ketones and

amines. In the case of D-fructose, the open-chain form of the reducing sugar reacts with the amino group in an addition-elimination mechanism producing a Schiff base. A keto-enol type isomerisation gives the enamine that at the same time is an enol. The enol tautomerises then, making it possible to form the 2-amino-2-deoxy-1-aldoses under slightly acid conditions [20].

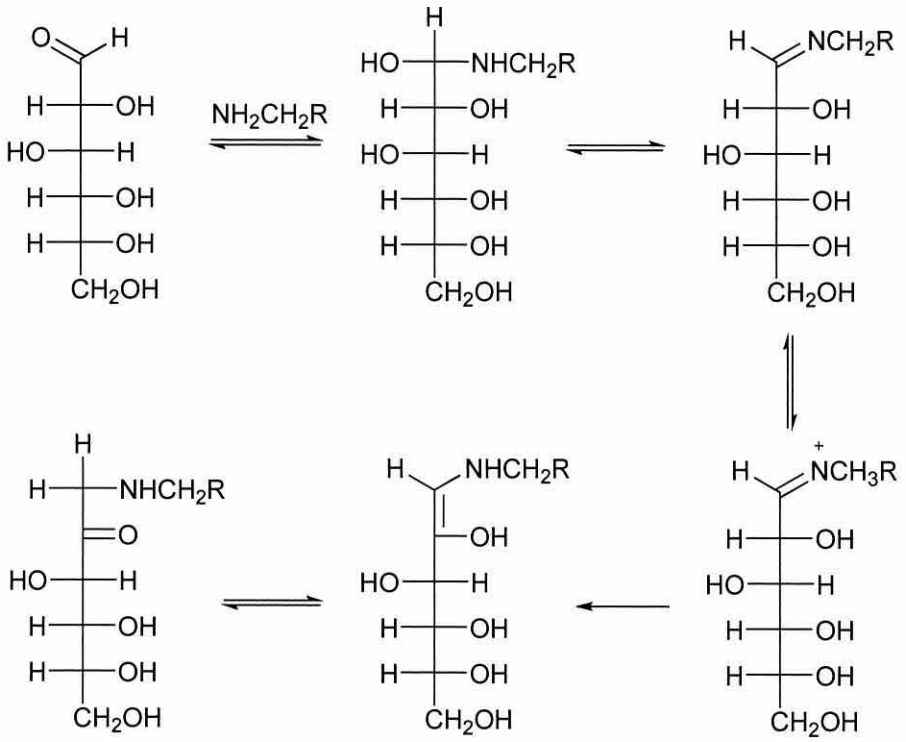

Scheme 6: The Amadori rearrangement.

4.1.4 Aim of the project

FedF is the sticky end of the F18 fimbriae of enterotoxigenic bacterium *Escherichia coli*. TheFedF receptor binds to carbohydrate ligands on intestinal microvilli, causing diarrhoea and oedema disease in newly weaned baby pigs. It also induces the secretion of Shiga toxins [22]. The FedF receptor-binding domain was found to bind to sulfated *N*-acetyllactosamine (LacNAc) and sulfated lactose, but the exact ligands are not known. It seems that the carbohydrate ligands might be disulfated [23].To further study the binding site, sulfated derivatives are required. The aim of this project was twofold. First, an efficient source of LacNAc should be found. Second, various sulfatation patterns should be introduced with minimal use of protecting

group chemistry. Six sulfated *N*-acetyllactosamine and lactose derivatives were the targets for this project (Figure 1).

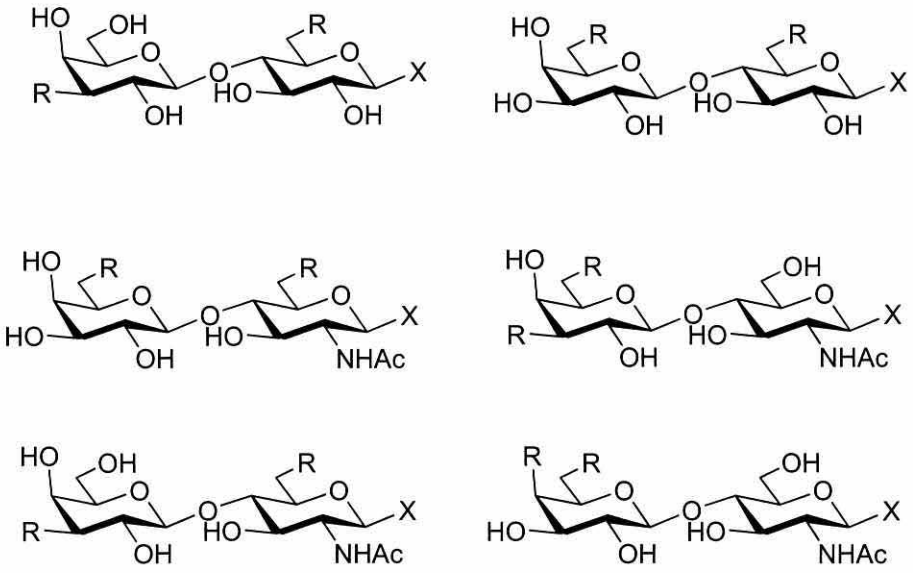

Figure 1: Disulfated structure targets. **R** = OSO_3H, **X** = OMe or $O(CH_2)_3N_3$

4.2 Results and discussion

4.2.1 Synthesis of di-*O*-sulfated-azidopropyl lactosides

The plan was to make the sulfated structures with as little protecting group manipulations as possible. It is known that certain hydroxyl groups are more reactive than others in the sugar system. The primary hydroxyl groups often react regioselective in the presence of the secondary hydroxyl groups. It is also known that the 3'-position in the lactose system can be sulfated regioselective (Figure 2) [23].

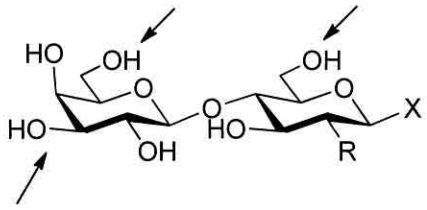

Figure 2: The arrows indicate positions that can be sulfated in the presence of the other unprotected OH-groups.

These considerations led to two protecting group patterns (Figure 3). 4,6-Benzylidene protection could be used for pattern **B**, while 3,4-isopropylidene protection could be used for pattern **A**. The isopropylidenation reaction can be done under kinetic and thermodynamic conditions [24]. The kinetic conditions give the 4,6 protecting pattern, while the thermodynamic conditions give the 3,4 protecting pattern. In any case, the anomeric position has to be protected first.

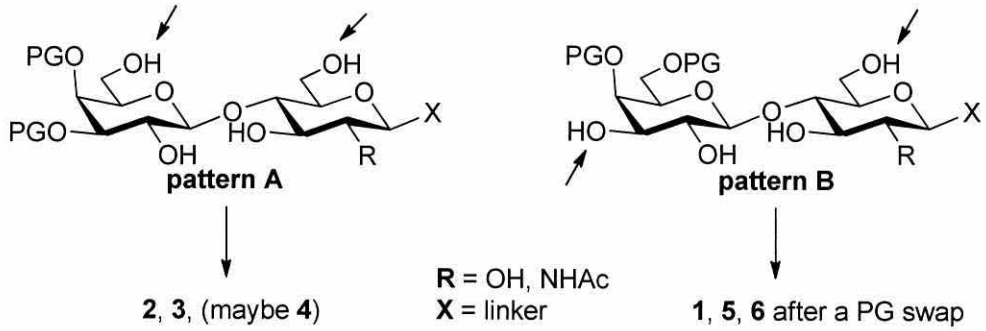

Figure 3: Protecting pattern **A** and **B** could give access to five or possibly all six target structures.

Thus, the synthesis of methyl lactosides was first attempted. The methyl group was expected to be easily introduced using methanol and boron triflouride etherate. This did not work well. Instead, the 3-azidopropyl linker was used. This linker has a slightly longer spacer arm and is in terms of chemical modifications a more flexible group than the methyl group. The azido function can be used, *e.g.*, for click reactions. The azido group reacts with an alkyne under catalysis of copper(I) giving a heterocycle. This reaction can be done in water or buffer systems. This is good for making glycoconjugates in water. Further, the azide can be reduced to an amine. This is good because an amide can easily be formed to make a glycoconjugate, *e.g.* the sugar can be linked to a label or a protein.

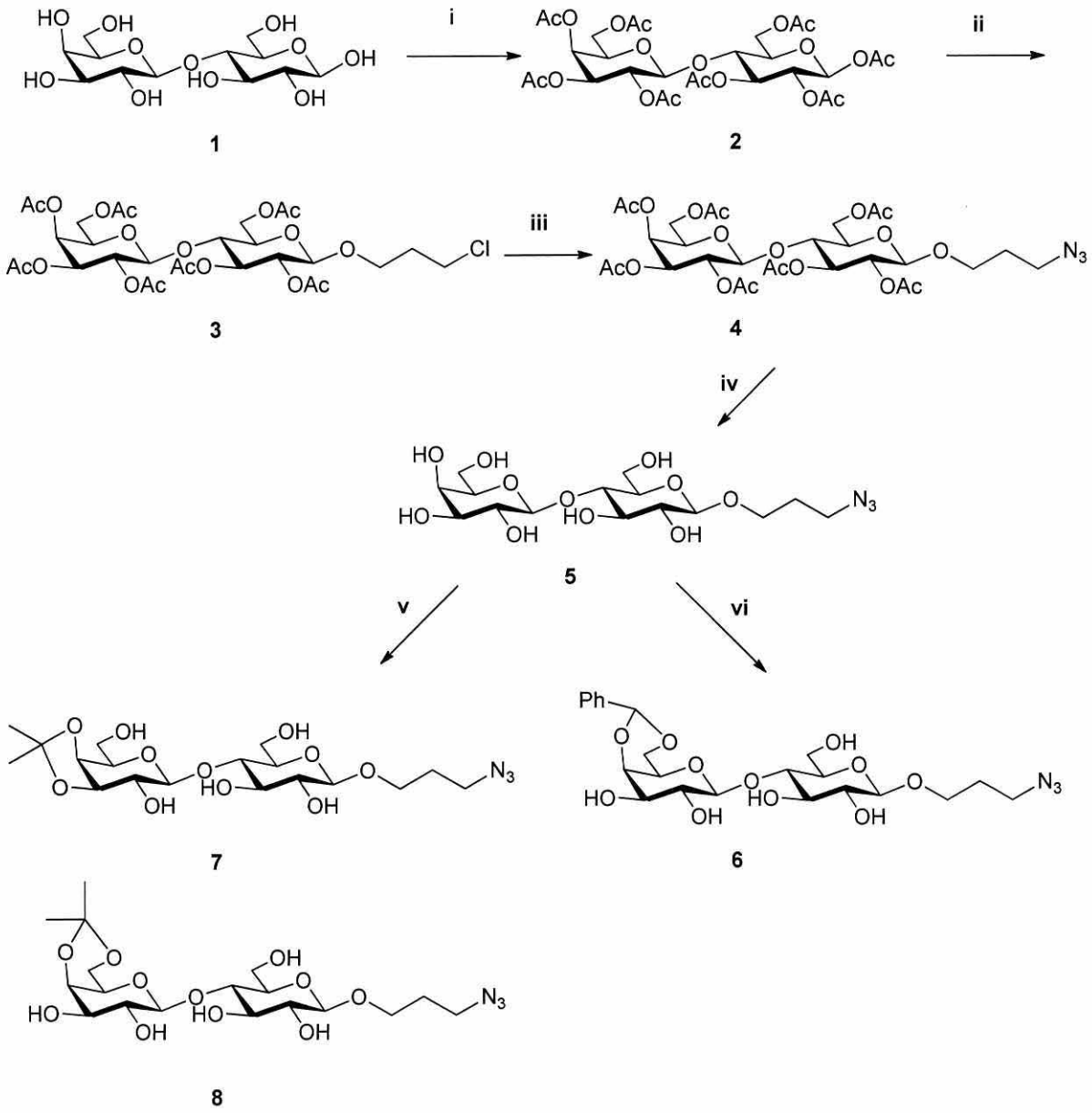

Scheme 7: **i**: Ac_2O, NaOAc, reflux, 30min, 81 %; **ii**: 3-chloropropan-1-ol, $BF_3.Et_2O$, dry DCM, RT, 2h, 82 %; **iii**: 1. NaI, dry DMF, 140°C, 1h, 2. NaN_3, dry DMF, reflux, 1 h, 80 %; **iv**: 1. NaOMe, dry MeOH, RT, 1h, 88 %; **v**: dry acetonitrile, 2,2-dimethoxy propane $VO(OTf)_2$, RT, 2d, 69%; **vi:** Dry acetonitrile, benzaldehydedimethylacetal, CSA, 30°C, overnight, 62 %.

Thus, D-Lactose **1** was converted using standard reaction into derivatives 6, 7 and 8.

Sulfation was attempted under different conditions. However, additional work is required. Sulfation was carried out by using $Py{\cdot}SO_3$ in dry pyridine while stirring at room temperature. These conditions led to exhaustive sulfation. To achieve a lower

degree of sulfation, the reaction was conducted at –10 to –20 °C (selective sulfation) for 2-3 h until TLC showed no further reaction. At this point, the reaction was stopped by addition of $NaHCO_3$. Warming up the reaction without quenching at low temperature gave exhaustive sulfation rapidly. After quenching, the reaction mixtures were always diluted with MeOH, filtered and washed with MeOH twice. After concentration, the non-carbohydrates were removed by size exclusion chromatography (Sephadex LH-20) [23]. The major problem was that selective sulfation seemed to be sensitive to temperature. Temperature control (-10 to -20 °C) was attempted by using a cooling bath (NaCl/ice 1:3). No equipment was available to maintain a constant lower temperature over longer periods of time. Several test reaction was done with the available equipment. However, no decent regioselectivity was achieved. Further investigations are necessary to solve this problem.

4.2.2 Synthesis of D-Lactosamine from Lactulose

Lactosamine is a rather expensive building block. Azidonitration is one of the standard reactions to produce lactosamine but the overall yields are often low. A problem is also the upscaling. The azidonitration reaction has to be run at low temperature to achieve high stereoselectivity. Otherwise a large amount of the 2-azido epimer is formed [7]. Also, this reaction is not without risk due to the large amount of sodium azide required. The Heyns rearrangement looked like a straightforward alternative. However, the published procedures were known to be difficult to be reproduced, and a working procedure had to be developed [18] [19].

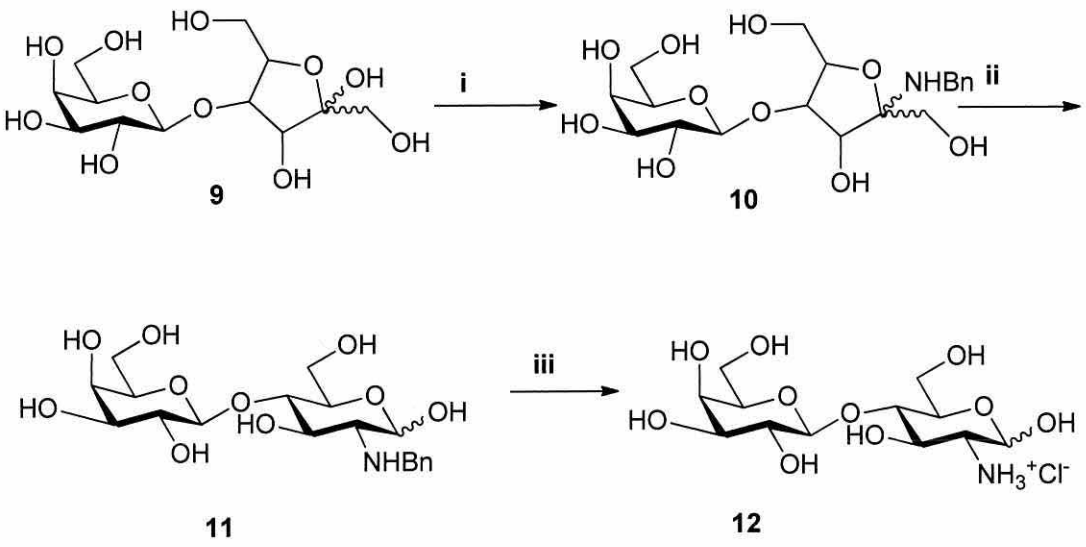

Scheme 9: **i**: Benzylamine, 40°C 3 days; **ii**: methanol, glacial acetic acid, RT, 2 h; **iii**: HCl, pH 1-2, $Pd(OH)_2/C$, H_2, 6 bars, 60 %; **iv**: methanol, NaOMe, Ac_2O, 40°C 1 day, 82 %.

For this purpose, lactulose **9** was reacted with benzyl amine to produce ketosyl amine **10** as described [18]. The reaction progress was monitored by TLC, and ketosyl amine **10** was produced as the major product while some unreacted lactulose remained (scheme 9). The crude mixture was then precipitated from diethyl ether. The rearrangement reaction was then carried out with the crude mixture using glacial acetic acid in methanol at room temperature. During this step, *N*-benzyl lactosamine **11** was formed. Removal of the *N*-benzyl group by hydrogenolysis was achieved by dissolving **11** in water at pH 1-2 with Pearlman's catalyst (20%) under hydrogen atmosphere producing **12** (crude yield, 74 %) [28].

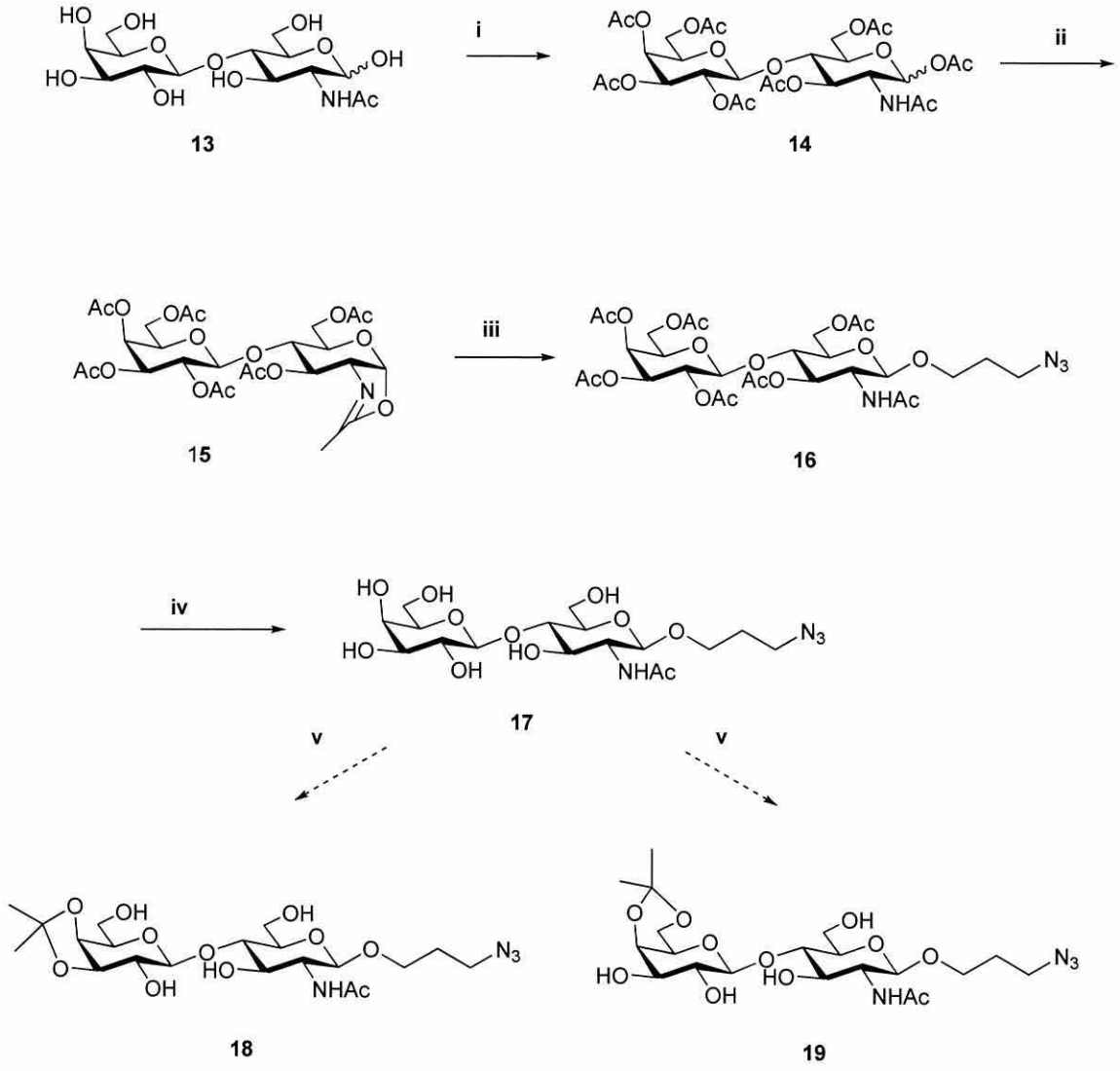

Scheme 10: **i**: Ac_2O, pyridine, RT, overnight, 67 %; **ii**: dry dichloroethane (DCE), trimethylsilyl trifluoromethanesulfonate (TMSOTf), 50°C, 4 h; 71 % **iii**: DCE, 3-azidopropanol, PPTS, 70°C, 3 h, 76 %; **iv**: methanol, NaOMe, RT, 1 h; **v:** dry acetonitrile, $VO(OTf)_2$, RT, 2d, 94 %.

This reaction can also be carried out at ambient pressure. However, extended reaction times were required (at least 5-6 days). In order to increase the efficiency of the reaction, 6 bars pressure of H_2 was applied. At this point, it was possible to remove remaining lactulose **9** from the reaction mixture by cation exchange chromatography giving **13** in an overall 60 % yield starting from **9**. However it was found that this extra purification step did not significantly increase the overall yield.

Next, compound **12** was *N*-acetylated by adding sodium methoxide and acetic

anhydride to the crude material obtained from the hydrogenolysis reaction to produce LacNAc **13** (crude yield, 82%).

Crude LacNAc **13** was then peracetylated by using acetic anhydride in pyridine to form peracetylated LacNAc **14** (scheme 10) [28]. At this step, the material was purified by flash column chromatography providing the target compound **14** as an anomeric mixture in a total yield of 48 % on a 25 g scale with regards to starting material **9**. Compound **14** was then converted to oxazoline **15** using trimethylsilyltriflate (TMSOTf) (76%) [28]. Then the spacer was introduced at the anomeric position to produce **16** using 3-azidopropanol and a catalytic amount of pyridinium *p*-toluenesulfonate (PPTS) [29]. Compound **16** was deacetylated by using methanol and sodium methoxide to form **17**. This material is now available for the required transformations.

4.3 Conclusions

Compared with the published procedure [17], lactulose was reacted with slightly increased excess of benzylamine (8 eq. vs 7.7 eq. in the published procedure). Also a smaller amount of diethyl ether was used to precipitate compound **10** and **11** (2000 ml vs 2500 ml in the published procedure). The diethylether mixture was then kept in the refrigerator at 4 ^{o}C for 2 – 4 h. The storage time in the refrigerator was not reported. However, it was found that the material had to be kept at least 2 h to avoid loss of material. During the filtration the crystalline material started to melt and became sticky. The filtration had to be done quickly and washing had to be carried out with ice-cooled ether. Further it was also found, that 6 bars pressure of H_2 during hydrogenolysis was important. Lower pressure, such as the reported 3 bars and even ambient pressure worked but those conditions required extended reaction times longer than the reported 5 to 6 days. Cation exchange chromatography (Amberlite 120) was applied to purify LacNAc from crude LacNAc-lactulose mixture, however, this step turned out to be not important for the procedure.

4.4 Experimental

4.4.1 General procedures

DCM was distilled from calcium hydride before use. Dry methanol was kept over molecular sieves 3 Å; all other chemicals were used as purchased. TLC was performed on 0.25 mm pre-coated silica gel glass plates (Merck silica gel 60 F_{254}) with detection by UV-light (254nm) or by charring with 10% sulphuric acid solution followed by heating. Organic solvent were evaporated by a rotary evaporator under reduced pressure at approximately 40°C (water bath). Hydrogenation reactions were carried out on a WHXINGYU jacket hydrogenation reactor. Lab water was purified by a Millipore water system. Sandwich filter consist of three filters (20 µm - 10 - µm - 5µm). Silica gel (Amicon 0.041 – 0.063 mm) was used for column chromatography. MALDI-TOF spectra were recorded on a Bruker 2, 4, 6- trihydroxy-acetophenone monohydrate (THAP) as matrix.

NMR-spectra were recorded at 500 MHz (Bruker B-ACS 60), respectively, in $CDCl_3$, D_2O or CD_3OD. NMR-experiment in $CDCl_3$ were referred to the chloroform signal (^1H, δ = 7.31 ppm) and (^{13}C, δ = 77.16 ppm).

2,3,4,6-Tetra-*O*-acetyl-β-D-galactopyranosyl-(1→4)-1,2,3,6-tetra-*O*-acetyl-β-D-glucopyranose (2)

A suspension of anhydrous sodium acetate (2 eq, 25.0 g, 0.31 mol) and acetic anhydride (10.7 eq, 175 ml, 1.85 mol) was heated to reflux temperature, then D-lactose **1** (1 eq, 50.0 g, 0.15 mol) was added in portions, so that the reaction mixture continued to reflux. After complete addition, the mixture was stirred under reflux for 30min, and then the reaction mixture was poured onto 500ml crushed ice and stirred over night. The precipitated produce was filtered off, washed with water, dried in vacuum and recrystallised from 600 ml ethanol to yield the peracetylated lactose **2** (80.6 g, 81 %) as colourless crystals. ^1H-NMR2.(500 MHz, $CDCl_3$ = 7.31 ppm) δ = 5.66 (d, 1H, H-1, $J_{1,2}$ = 8.4 Hz), 5.33 (dd, 1H, J = 1.2Hz, J = 3.6 Hz H-4'), 4.46 (d, 1H, J = 7.6 Hz, H-1'), 4.42 (d, 1H, H-6' a), 4.13-4.04 (m, 3H, H-5', H-6A, H-6'B), 3.88-

3.85 (m, 2H, H-4', H-6b) 2.14, 2.10, 2.08, 2.05, 2.04, 2.02, 2.01, 1.95 (8s, 24H, $8CH_3$) ppm;^{13}C-NMR (125 MHz, $CDCl_3$ =77.16): δ = 170.48, 170.44, 170.26, 170.18, 169.74, 169.68, 169.14, 168.98 (8C, 8C=O), 101.68 (C-1'), 91.67 (C-1), 75.81, 73.63, 72.76, 71.09, 70.87, 70.65, 69.14, 66.74, (8C), 61.87 (C-6), 60.98 (C-6'), 20.95, 20.93, 20.87, 20.75, 20.73, 20.71, 20.62, 18.53 (CH_3) ppm. The NMR spectra of compound **2** matched previously reported data [25].

3-Chloropropyl-2,3,4,6-tetra-o-acetyl-β-D-galactopyranosyl-(1→4)-2,3,6-tri-*O*-acetyl-β-D-glucopyranoside (3)

The peracetylated β-D-lactose 2 (1 eq., 10.0 g 14.7 mmol) was co-evaporated with toluene and dissolved in dry DCM. Then 3-chloropropanol (2 eq., 2.5mL, 29.4 mmol) and BF3.Et2O (2.5 eq, 4.7 mL, and 36.8 mmol) were added to the mixture. The reaction was stirred under nitrogen atmosphere at room temperature for 3h. The reaction was monitored by TLC (toluene/EtOAc, 1:1). After the reaction was completed, the reaction mixture was poured onto crushed ice and stirred for 30 min, thenthe organic layer was separated and washed with NaHCO3 and brine, and concentrated under reduced pressure. The crude product was purified by silica gel column chromatography (toluene →toluene/ EtOAc, 10:1→8:1→6:1→3:1) to give the spacer-equipped lactoside 3 (8.2 g, 82 %). ^{1}H-NMR(500 MHz, CDCl3 = 7.31 ppm) δ=5.33 (dd, 1H, J =1.2 Hz, J =4.4 Hz, H-4'), 5.14 (dd = t, 1H, H-3), 5.10 (dd, 1H, H-2'), 4.94 (dd, 1H, J = 3.6 Hz, J = 10.4 Hz, H-3'), 4.87 (dd, 1H, , J = 8.0 Hz, J = 9.6 Hz, H-2), 4.50-4.45 (m, 3H, H-1', H-6a, H-1), 4.14-4.04 (m,3H, H-5', H-6a, H-6'b), 3.96-3.91 (m, 1H, -OCH2a-), 3.88-3.84 (m, 1H, H-6b), 3.80-3.75 (dd = t, 1H, H-4), 3.69-3.55 (m, 4H, H-5, -OCH_2b, -CH_2N_3), 2.14, 2.11, 2.05, 2.04, 2.03, 2.29, 1.95 (7s, 21H, -$COCH_3$) ppm; ^{13}C-NMR (125 MHz, $CDCl_3$ = 77.16 ppm): δ = 170.50, 170.47, 170.27, 170.18, 169.86, 169.83, 169.19 (C=O), 101.21 (C1), 100.93 (C1'), 76.4, 72.84, 72.80, 71.79, 71.13, 70.83, 69.25 (7C), 66.74 (-O*C*$H_2$$CH_2$$CH_2$Cl), 66.50, 62.11, 60.95 (3C), 41.43 (2C, -OCH_2CH_2*C*H_2Cl), 32.29 (-OCH_2*C*$H_2$$CH_2$Cl), 20.99, 20.93, 20.94, 20.82, 20.77, 20.76, 20.74 (CH_3) ppm. MALDI-TOF MS: Calcd for $C_{29}H_{41}ClO_{18}$ 713.08 [M]; 736.08 [M+Na] +. Found: 737.06 [M+Na]+ ± 27 ppm.

3-Azidopropyl-2,3,4,6-tetra-*O*-acetyl-β-D-galactopyranosyl-(1→4)-2,3,6-tri-*O*-acetyl-β-D-glucopyranoside (4)

Lactoside **3** (1 eq, 4.0 g, 5.6 mmol) and NaI (2 eq, 1.7 g, 11.3 mmol) were dissolved in dry DMF, and stirred at 50°C for 1 h. Then NaN_3 was added in portions, and the dark brown reaction mixture was refluxed at 140°C for 1 h. After that, the reaction mixture was poured into ice water to give a yellow-brown solution. EtOAc was added and the organic layer was separated. The water phase was extracted with EtOAc twice. The combined organic layers were washed with water and brine, and evaporated. The yellow product was purified by silica gel flash column chromatography (toluene →toluene/ EtOAc, 10:1→5:1→3:1→2:1) to give the colourless product **4** (3.2 g, 80 %).^{1}H-NMR(500 MHz, $CDCl_3$ = 7.31 ppm) δ=5.39 (dd, 1H, J = 1.2 Hz, J = 3.6 Hz H-4'), 5.23 (dd = t, 1H, H-3), 5.15 (dd, 1H, H-2'), 5.00 (dd, 1H, J = 3.6 Hz, J = 10.4 Hz, H-3'), 4.93 (dd, 1H, H-2), 4.55-4.50 (dd, 1H, H-6'a), 4.52 (d, 1H, H-1'), 4.51 (d, 1H, H-1), 4.18-4.09 (m, 3H, H-5', H-6a, H-6'b), 3.97-3.89 (m, 2H, H-6b, -OCH_2^a-), 3.83 (dd = t, 1H, J =9.6 Hz, H-4), 3.66-3.59 (m, 2H, H-5, OCH_2^b-), 3.41-3.36 (m, 2H, -CH_2N_3), 2.19, 2.16, 2.10, 2.09, 2.08, 2.01, 2.00 (7s, 21H, -CH_3), 1.90-1.82 (m, 2H, -$CH_2CH_2CH_2N_3$) ppm; ^{13}C-NMR (125 MHz, $CDCl_3$ = 77.16 ppm): δ = 170.40, 170.39, 170.19, 170.10, 169.80, 169.68, 169.12 (C=O), 101.22 (C1), 100.71 (C1'), 76.38 (C-4), 72.89 (C-3), 72.81 (C-5), 71.79 (C-2), 71.12 (C-5'), 70.83 (C-3'), 69.24 (C-2'), 66.74 (C-4'), 66.59 (-$OCH_2CH_2CH_2N_3$), 62.06 (C-6'), 60.93 (C-6), 48.08 (-$OCH_2CH_2CH_2N_3$), 29.11 (-$OCH_2CH_2CH_2N_3$), 20.98-20.64 (7 CH_3) ppm. MALDI-TOF MS: Calcd for $C_{29}H_{41}N_3O_{18}$ 719.24 [M]; 742.24 $[M+Na]^+$. Found: 742.21 $[M+Na]^+$ ± 40 ppm. NMR data were in agreement with the previously reported ones [26].

3-Azidopropyl-β-D-galactopyranosyl-(1→4)-β-D-glucopyranoside (5)

Lactoside **5** (1eq, 1.0 g, 1.38 mmol) was dissolved in dry methanol (10 ml, 10 ml/g sugar). Sodium methoxide solution (1 M, 100 µl) was added and the light brown reaction was stirred over night at room temperature. The reaction was monitored by TLC (DCM/MeOH, 3:1). After that, Dowex H^+ ion exchange resin was added and the mixture was stirred for 30 min. After neutralization (monitored by pH paper) the resin was filtered off, washed with methanol, and the filtrate solution was concentrated to

get light yellow crystals **5** (510 mg, 88 %).^{1}H-NMR(500 MHz, D_2O = 4.80 ppm) δ = 4.49 (2xd, 2H, H-1', H-1), 4.04-3.98 (m, 2H), 3.95 (m, 1H), 3.84 (m, 1H), 3.81-3.77 (m, 3H), 3.75 (m, 1H), 3.70-3,65 (m, 3H), 3.64-3.60 (m, 1H), 3.58-3.54 (m, 1H), 3.48 (m, 2H), 3.35-3.31 (m,1H), 1.93 (m, 2H, -$OCH_2CH_2CH_2N_3$) ppm; ^{13}C-NMR (125 MHz, D_2O, TMS = ppm): δ = 102.91 (C-1'), 102.11 (C-1), 78.37, 75.33, 74.75, 74.36, 72.79, 72.50, 70.93, 68.52, 67.35 (-$OCH_2CH_2CH_2N_3$), 61.00, 60.06, 47.85 (-$OCH_2CH_2CH_2N_3$), 28.21 (-$OCH_2CH_2CH_2N_3$) ppm. MALDI-TOF MS: Calcd for $C_{15}H_{27}N_3O_{11}$ 425.16 [M]; 448.16 $[M+Na]^+$. Found: 448.18 $[M+Na]^+$ ± 45 ppm. NMR data were in agreement with the previously reported ones [26].

3-Azidopropyl-4,6-*O* -benzylidene-β-D-galactopyranosyl-(1→4)-β-D-glucopyranoside (6)

Compound **5** (1 eq., 1 g, 1.95 mmol) was dissolved in dry acetonitrile (10 mL), then benzaldehyde dimethylacetal (2 eq., 800 µL) and a catalytic amount of camphorsulfonic acid were added. The reaction mixture was stirred at 30 °C overnight. The reaction was monitored by TLC (EtOAc/MeOH/water, 7:2:1). After complete reaction, triethylamine (330 µL) was added. The reaction mixture was concentrated and purified by flash column (EtOAc/MeOH 20:1→15:1→10:1→5:1 to obtain product **6** (1 g, 83 %). MICRO-TOF MS: Calcd for $C_{12}H_{23}NO_{10}$ 341.312 [M]. Found: 341.326 M ± 41 ppm. NMR data were in agreement with the previously reported ones [30].

3-Azidopropyl-3,4-*O*-isopropylidene-β-D-galactopyranosyl-(1→4)-β-D-glucopyranoside (7)

A round bottomed flask was charged with vanadyl triflate (0.05 eq, 40 mg), then acetonitrile (1.77 mL) was added into the flask to dissolve the catalyst. 2, 2-Dimethoxypropane (10 eq., 2.9 mL) was added to the solution and the mixture was kept stirring for 10 min. The colour of the solution changed from faint blue to brown. After that, compound **5** (50 mg, 118 mmol) was added to the reaction mixture. The reaction mixture was stirred at room temperature for 2 days, while the reaction was monitored by TLC (EtOAc/MeOH, 4:1). After complete conversion, the reaction mixture was concentrated and applied onto a flash column (EtOAc/MeOH

20:1→15:1→10:1→5:1) to give product **7** (36 mg, 69 %). No NMR data available due to NMR quench.

N-Benzyl-D-lactosamine (11)

Commercial available lactulose **9** (1eq, 25 g, 73.0 mmol) was reacted with benzylamine (8 eq, 62.5 mL, 572 mmol) at 40°C for 3 days. The reaction was monitored by TLC (DCM/MeOH/NH_4OH, 2:2:1) and stopped when the TLC showed the expected product as the major spot. Then the reaction mixture was poured into diethyl ether (2000 ml) and kept in the refrigerator (4°C) for 2 h. The precipitate was filtered off and dried under reduced pressure to give a yellow solid (35 g) containing a mixture of **10** and residual starting material **9**. This mixture was used for the next step without further purification. The crude compound **10** was then dissolved in a mixture of methanol (125 mL) and glacial acetic acid (15 mL). The resulting solution was kept stirring at room temperature (20°C) for 2 h, then added slowly into diethyl ether (2000 mL) and kept for additional 4 h in the refrigerator at 4°C. The formed precipitate was filtered off and dried under reduced pressure to produce crude **11** still containing a small amount of unreacted lactulose **9**. The crude product **11** (40.2 g) was used in the next step without purification.

D-Lactosamine Hydrochloride (12)

Crude *N*-Benzyl-D-lactosamine**11** (mixture containing a small amount of lactulose, 40.2 g) was dissolved in Millipore water (160 mL), and the pH was adjusted to 1 using concentrated HCl. Then Pearlman's catalyst (palladium hydroxide on carbon, 20 %, 5 % by weight, 1.5 g) was added. The reaction was kept in a hydrogenation gas apparatus at 6 bars pressure for 1 day until TLC (MeOH/DCM/NH_4OH, 2:1:1) and MICRO-TOF data showed that the reaction was completed. The reaction mixture was filtered through a sandwich filter to give crude **12**. This material was then applied to a cation exchange column (Amberlite H-120, 8.5 W x 25 H cm), eluted with 0.1 M NH_4OH, the elute was then adjusted pH to 2 with 1 M HCl and dried under reduce pressure to give **12** (20 g, 60 % from lactulose **9**). MICRO-TOF MS: Calcd for $C_{12}H_{23}NO_{10}$ 364.311 $[M+Na]^+$. Found: 364.313 $[M+Na]^+$ ± 5 ppm. The NMR spectra of compound **12** matched with previous report data [28].

2-Acetamido-2-deoxy-4-(*O*-β-D-galactopyranosyl)-D-glucose (13)

D-Lactosamine hydrochloride **12** (1 eq, 3 g, 8.8 mmol) was dissolved in dry methanol (20 ml) and sodium methoxide solution (1.3 eq, 1 M, 11.4 mL, 11.4 mmol) was added. The mixture was stirred at 40°C for 30 minutes, and then acetic anhydride (1.8 eq, 15 mL, 15.9 mmol) was added. Stirring was continued overnight at room temperature. The reaction progress was monitored by TLC (MeOH/DCM/NH_4OH, 2:1:1), then Dowex H^+ ion exchange resin was added and the mixture was stirred for 30 min. After neutralization the resin was filtered off, washed with methanol and the filtrate was concentrated. Then, the product was purified by flash column to give LacNAc **13** (2.5 g, 82 %) as α, β mixture. MICRO-TOF MS: Calcd for $C_{14}H_{25}NO_{11}$ 406.348 $[M+Na]^+$. Found: 406.365 $[M+Na]^+$ ± 42 ppm. The NMR spectra of compound **13** corresponded to published values [31]

2-Acetamido-1,3,6-tri-*O*-acetyl-2-deoxy-4-*O*-(2,3,4,6-tetra-*O*-acetyl-β-D-galacto pyranosyl)-D-glucopyranose (14)

Compound **13** (1 eq, 4 g, 10.6 mmol) was dissolved in dry pyridine (15 mL). Acetic anhydride (21.6 eq, 21.6 mL, 229.0 mmol) was added, and the reaction was stirred

at the room temperature overnight. The reaction was monitored by TLC (Toluene /Ethyl acetate, 1:6). The product was purified by flash column to get **14** (4.7 g, 67 %). α-**14**: ^{1}H NMR (500 MHz, $CDCl_3$ = 7.31 ppm): δ = 6.07 (d, $J_{1,2}$ = 3.52 Hz, 1H, H-1), 5.68 (br d, 1H, NH), 5.42 (dd, 1H, H-4'), 5.31(br dd, 1H, H-3), 5.19 (dd, 1H, H-2'), 5.04 (dd, 1H, H-3'), 4.59 (d, J = 7.89 Hz, 1H, H-1'), 4.39–4.51 (m, 2H, H-2, H-6b), 4.10–4.26 (m, 3H, H-6a', H-6b' and H-6a), 3.90–3.98 (m, 3H, H-4, H-5 and H-5'), 1.98–2.18 (8s, 24H, Ac) ppm. β-**14**: ^{1}H NMR (500 MHz, $CDCl_3$ = 7.31 ppm):δ = 6.02 (br d, N*H*$COCH_3$), 5.76 (d, I-H'), 5.42 (dd, 4-H), 5.22 (dd. 2-H), 5.18 (dd, 3-H'), 5.10 (dd, 3-H), 4.60 (d, I-H), 4.57 (dd, 6'-H'), 4.38 (ddd, 2-H'), 4.18-4.31 (m. 6-H', 6-H, 6'-H), 4.01–4.06 (m, 5-H), 3.94 (dd, 4-H'), 3.87 (ddd, 5-H'), 2.06-2.27 (8 s's, $COCH_3$) ppm. MICRO-TOF MS: Calcd for $C_{28}H_{39}NO_{18}$ 700.605 $[M+Na]^+$. Found: 700.558 $[M+Na]^+$ ± 67 ppm. The NMR spectra of compound **12** matched reported data [28].

2-Methyl-{3,6-di-*O*-acetyl-1,2-dideoxy-4-*O*-(2,3,4,6-tetra-*O*-acetyl-β-D-galactopyranosyl)-α-D-glucopyrano}-[2,1-d]-oxazoline (15)

Peracetylated LacNAc **14** (50 mg, 73.8 μmol) was dissolved in dry DCE (750 μL) and trimethyl-silyltrifluoromethanesulfonate (TMSOTf) was added. The reaction was stirred at 50 °C for 3 h. The progress of the reaction was monitored by TLC (Toluene/ethyl acetate, 1:6). After the reaction was completed, triethylamine (Et_3N) (50 μL) was added to the reaction solution to quench the reaction. Then the reaction mixture was concentrated and applied onto a flash column to get **15** (32 mg, 71%). MICRO-TOF MS: Calcd for $C_{26}H_{35}NO_{16}$ 640.553 $[M+Na]^+$. Found: 640.530 $[M+Na]^+$ ± 36 ppm. The NMR spectra of compound **12** corresponded to publish report [28].

3-Azidopropyl-2,3,4,6-tetra-*O*-acetyl-β-D-galactopyranosyl-(1→4)-2-acetamido-2-deoxy-3,6-di-O-acetyl-β-D-glucosamine (16)

Compound **15** (77 mg, 0.125 mmol) was dissolved in 1,2-dichloroethane (DCE) (3 mL), pyridinium *p*-toluenesulfonate (PPTS) (3.2 mg, 0.0125 mmol) and 3-azidopropanol (91 μL) were added. The reaction was stirred at 70 °C for 2 h, until TLC showed that the reaction was completed. After that, the reaction solution was cooled down to room temperature, then pyridine (200 μL) was added to neutralize. Dichloromethane (5 mL) was added into reaction flask, and the resulting solution

poured into ice water. The organic layer was washed subsequently with $NaHCO_3$ and brine, and dried with $MgSO_4$. The filtered solution was concentrated under reduce pressure, and applied to a flash column to get product **16** (68 mg, 76 %).
^{1}H-NMR (500 MHz, $CDCl_3$ = 7.31 ppm) δ = 5.63 (br d, 1H, J = 9.5 Hz, NH), 5.25 (dd, 1H, J = 0.8 Hz, J = 3.5 Hz, H-4'), 5.00 (dd, 1H, J = 8.0 Hz, J = 10.5 Hz, H-2'), 4.94 (dd, 1H, J = 8.0 Hz, J = 9.5 Hz, H-3), 4.96 (dd, 1H, J = 3.5 Hz, J = 10.5 Hz, H-3'), 4.39 (dd, 2H, H-6a,b), 4.31 (d, 1H, J = 7.5 Hz, H-1), 4.05-3.91 (m, 5H), 3.83-3.75 (m, 2H), 3.67 (t, 1H, J =8.6 Hz, H-4), 3.52-3.49 (m, 1H, OCH_2^a-), 3.45-3.41 (m, 1H, OCH_2^b-), 3.25 (td, 2H, $-CH_2N_3$), 2.04, 2.00, 1.96, 1.95, 1.94, 1.86, 1.85 (7s, 21H, $-CH_3$), 1.78-1.68 (m, 2H, $-CH_2CH_2CH_2N_3$) ppm; ^{13}C-NMR (125 MHz, $CDCl_3$ = 77.16 ppm): δ = 170.70, 170.37, 170.32, 170.12, 170.07, 170.00, 169.30 (C=O), 101.18 (C1), 100.00 (C1'), 75.72 (C-4), 72.69 (C-3), 72.47 (C-5), 70.84 (C-5'), 70.76 (C-3'), 69.12 (C-2'), 66.65 (C-4'), 66.01 ($-OCH_2CH_2CH_2N_3$), 62.23 (C-6'), 60.82 (C-6), 53.24 (C-2), 48.02 ($-OCH_2CH_2CH_2N_3$), 28.92 ($-OCH_2CH_2CH_2N_3$), 23.24 (CH_3), 20.83-20.48 (6 CH_3) ppm. MICRO-TOF MS: Calcd for $C_{29}H_{42}N_4O_{17}$ 741.660 $[M+Na]^+$. Found: 741.606 $[M+Na]^+$ ± 72 ppm.

3-Azidopropyl-β-D-galactopyranosyl-(1→4)-2-acetamido-2-deoxy-β-D-glucopyranoside (17)

Compound **16** (120 mg, 167 µmol) was reacted with NaOMe (1M, 15 µL) and MeOH (2 mL) to form product **17** (73 mg, 94%). MICRO-TOF MS: Calcd for $C_{17}H_{30}N_4O_{11}$ 489.440 $[M+Na]^+$. Found: 489.461 $[M+Na]^+$ ± 43 ppm.

4.5 References

1. Bentley, R.; Meganathan, R. *Microbiol. Rev*, **1982**, *46*, 3, 241–80
2. WHO European [Internet]. [Update: October 21st, 2011]. World Health Organization, Regional office for Europe, [cited October 22th, 2011]. Available from http://www.euro.who.int/en/home
3. CDC home [Internet]. [Updated: October 1st, 2011]. Centers for Disease Control and Prevention, [cited October 12th, 2011]. Available from http://www.cdc.gov/
4. Banoub, J.; Boullanger, P.; Lafont, D. *Chem.Rev*, **1992**, *92*, 1167
5. Bongat, A.; Demchenko, A. *Carbohydr. Res*, **2007**, *342*, 374–406
6. Lemieux, R. U.; Ratcliffe, R. M. *Can. J. Chem*, **1979**, 57, 1244
7. Benjamin G. D.; Chambers, D.; Cumpstey, I.; France, R.; Gamblin, D. *Carbohydrates*, **2003**, 69-120
8. Zhang, Yong-Min.; Brodzky, A.; Sinaÿ, P.; Saint-Marcoux, G.; Perly, B. *Tetrahedron: Asym.*, **1995**, *6* (5), 1195-1216
9. Banoub, J.; Boullanger, P.; Lafont, D. *Chem. Rev*, **1992**, *92*, 1167.
10. Westerlind, U.; Westman, J.; Toernquist, E.; Smith, C. I. E.; Oscarson, S.; Lahmann, M.; Norberg, T. *Glycoconjugate. J*, **2004**, *21*, 227-241
11. Heyns, K.; Koch, W. *Z. Naturforsch*, **1952**, *7b*, 486–488
12. Fischer, E. *Ber*, **1884**, *17*, 579–584
13. Carson, J.F. *J. Am. Chem. Soc*, **1955**, *77*, 1881–1884
14. Heyns, K.; Meinecke, K. H. *Chem. Ber*, **1953**, *86*, 1453–1462
15. Wrodnigg, T.M.; Eder, B. The amadori and heyns rearrangements: landmarks in the history of carbohydrate chemistry or unrecognized synthetic opportunities? In Glycoscience – epimerization, isomerization, rearrangement reactions of carbohydrates; Stütz, A.E. Ed.; Springer: Heidelberg, **2000**, 115–152
16. Amadori, W., Atti. *reale accad. nazl. Lincei,* **1925**, *6* (2), 337
17. Stütz, Arnold E.; Brigitte Eder, G. D.; Illaszewicz, C.; Wrodnigg,T. M. *J. Carbohydr. Chem*, **2003**, *22*, 253
18. Wrodnigg, T. M. *J Carbohydr Chem,* **2006**, *25*, 33
19. Wrodnigg, T. M.; Stütz, A. E. *Angew. Chem. Int. Ed*, **1999**, *38*, 827
20. Lindhorst, T. K., *Essentials of carbohydrate chemistry and biochemistry*, Germany, **2002**, 97-100

21. Bertschinger, H. U.; Bachmann, M., Mettler, C.; Pospischil, A., Schraner, E.M.,Stamm, M.; Sydler, T.; Wild, P. *Vet. Microbiol*, **1990**, *25*, 267–281
22. De Kerpel M, V. M. *Acta. Crystallogr. Sect F. Struct. Biol. Cryst. Commun,* **2006**, *62*, 1278
23. Galina V. Pazynina, V. V. S., Maxim L. Maisel, Ivan M. Belyanchikov and Nicolai V. Bovin, *Mendeleev. Commun,* **2008**, *18*, 238
24. De, S.K.; *J. Mol. Catal. A: Chem.*, **2005**, *226*, 77
25. Su, Yehua.; Wang, Yanguang.; Lin, Xianfu.; Xie, Jiansheng.; Hu, Xun. *Eur. J. Med. Chem*, **2010**, *45* (7), 2713-2718
26. Yu, Hai.; Chokhawala, Harshal.; Karpel, Rebekah.; Yu, Hui.; Wu, Bingyuan.; Zhang, Jianbo.; Zhang, Yingxin.; Jia, Qiang.; Chen, Xi. *J. Am. Chem. Soc*, **2005**, *127* (50), 17618–17619
27. Hanaya, T.; Sato, N.; Yamamoto, H. *Carbohydr. Res,* **2005**, *340* (16), 2494-2501
28. Range, G.; Krähmer, R.; Welzel, P.; Müller, D.; Herrmann, G. F.; Kragl, U.; Wandrey, C.; Markus, A.; Van Heijenoort, Y.; Van Heijenoort, J. *Tetrahedron*, **1997**, *53*, 1695
29. Gao, Y.; Eguchi, A.; Kakehi, K.; Lee, Y. C. *Bioorg. Med. Chem. Lett*, **2005**, *13*, 6151
30. Sundgren, A., Synthesis of antigenic oligosaccharides from the human pathogenic bacteria *Streptococcus pneumoniae, Haemophilus influenza* and *Vibrio cholerae*, **2005**, Göteborg University.
31. Herrrnann, G. E; Krugl, U,; and Wundrey, C. *Angew. Chem. Int. Ed. Engl.* **1993**, *105,* 1399.

Chapter 5 – Development of a separation protocol for subfucosylated Leb oligosaccharides and synthesis of a Lewis b hexasaccharide conjugate for multivalent binding studies of *Helicobacter pylori* BabA

5.1 Introduction

5.1.1 Helicobacter pylori

Helicobacter pylori (*H. pylori*) are one of most common bacteria that cause gastritis, peptic ulcer disease and cancer [1]. More than 50 % of the world's population is infected by this bacterium but not all infected individuals develop symptoms [2]. The infection is initiated by *H. pylori* recognising and attaching to the Lewis b (Le^b) blood group antigen (Figure 1) found on the stomach epithelial surface. This is mediated by the bacterial blood group antigen binding adhesin (BabA) [3]. BabA is found on the outer membrane of *H. pylori* [4]. Several syntheses of Le^b antigen structures have been reported, e.g. [5] [6] [7] [8] [9].

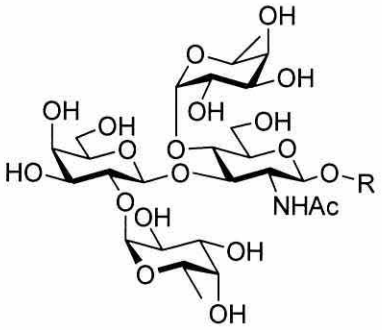

Figure 1: The Lewis b (Le^b) blood group antigen.

5.1.2 Aim of the project

BabA recognition and binding to Le^b antigen is crucial for the pathophysiology of *H. pylori* infections. In order to investigate the binding and also for isolation purpose, Le^b hexasaccharide protein conjugates have been synthesised earlier [10]. The

introduction of the two α-linked fucoses, the last synthetic step prior to complete deprotection, is often leading to side products due to incomplete fucosylation. The necessary purification at this step was known to be difficult. Due to the high value of the material, it was thought that the development of a separation protocol would be attractive. Therefore, the aim of this project was to elaborate a protocol for the purification and separation of the Le^b hexasaccharide from a mixture of the Le^b hexasaccharide and monofucosylated pentasaccharides. This material was then conjugated to produce an alkyne terminated conjugate intended for studying multivalent binding effects.

5.2. Results and discussions

5.2.1 Purification of the synthetic Lewis^b hexasaccharide

Material **1**, a mixture of partially deprotected Lewis^b hexasaccharide and pentasaccharides, was provided. According to MALDI-TOF data (Figure 2), the major compounds of this mixture were hexasaccharides carrying 5 to 9 benzyl ether protecting groups. Other compounds of the mixture were pentasaccharides with 1-7 benzyl ether protecting groups.

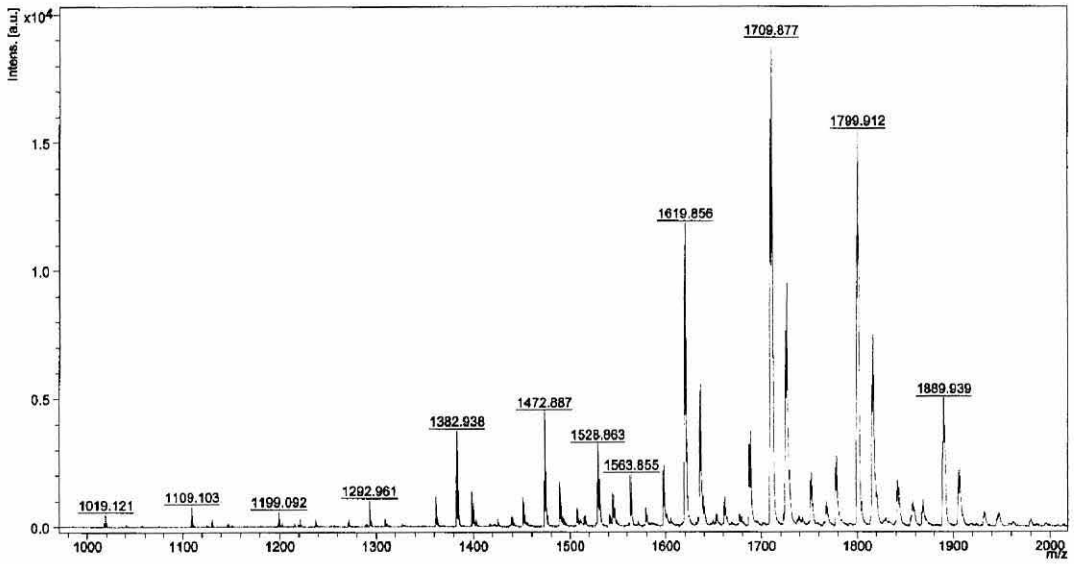

Figure 2: MALDI-TOF spectrum of the available material **1**.

First of all, mixture **1** was reacted with EtOH, Pd/C, and one equivalent HCl under the H_2 atmosphere to remove all remaining benzyl ethers to get product **2** (scheme 1). The MALDI-TOF spectrum (Figure 2) showed that the mixture **1** had been successfully deprotected, and no further degradation was observed. The addition of HCl was required to reduce the overall reaction time. One equivalent HCl converts the quickly formed amino group into the ammonium salt. This avoids that the catalytic system gets poisoned [8]. Extended reaction times can however also hydrolyse the labile fucose linkages. As an alternative, larger amounts of acetic acid are often used as additive for the hydrogenation instead of the equivalent HCl [11]. However, complete debenzylation without loss of fucosyl residues is not always achievable with highly benzylated oligosaccharides [8]. Compound mixture **2** contained a mixture of hexasaccharides and pentasaccharides (Figure 3).

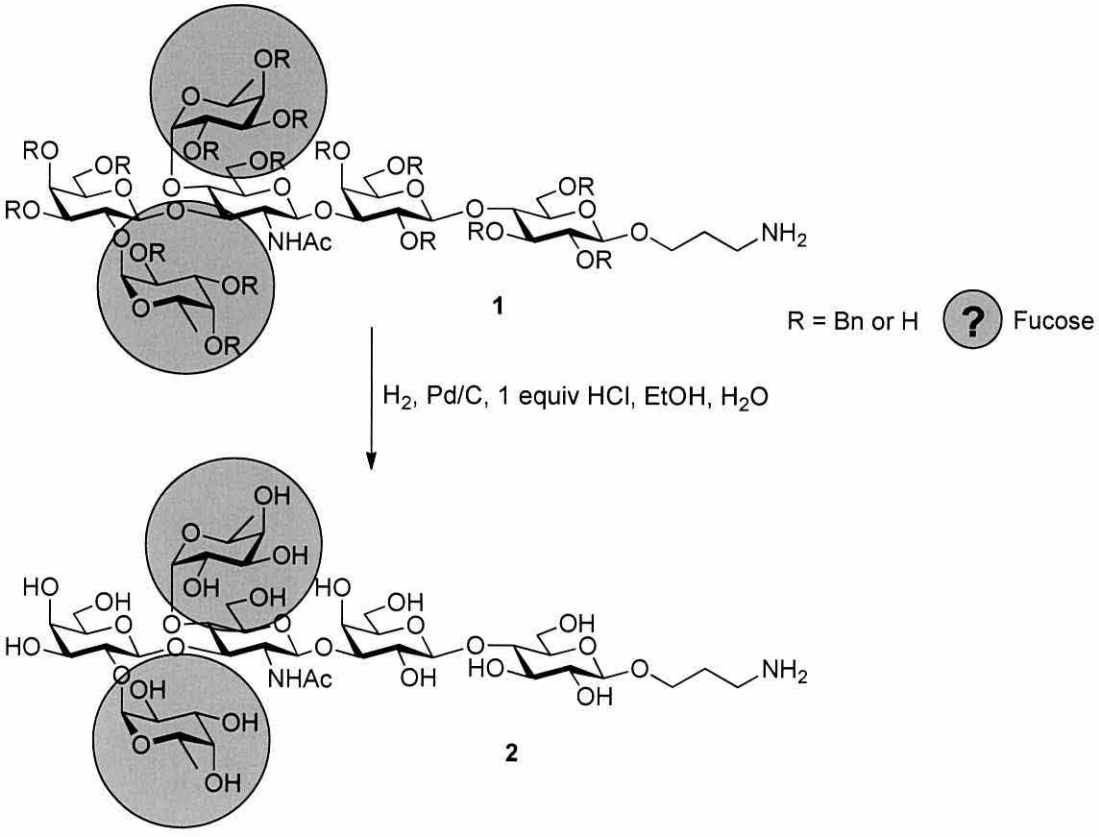

Scheme 1: Deprotection reaction of mixture **1**.

Mixture **2** was further purified by using size exclusion chromatography (P2 column)

and reversed phase chromatography (C18 column) to get pure hexasaccharide **3**. The P2 column was mainly used for de-salting. The reversed C18 column gave the separation using a step-gradient (water/MeOH). This procedure gave the pure hexasaccharide **3** as the hydrochloride salt.

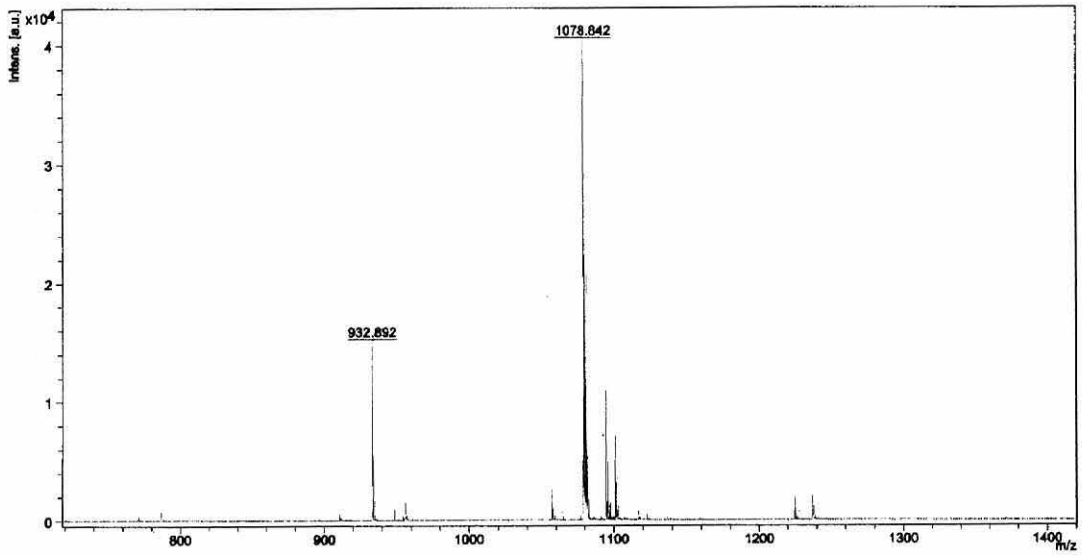

Figure 3: MALDI TOF spectrum of compound mixture **2**.

5.2.2 Conjugation of the synthetic Lewis^b hexasaccharide

The conjugation step was done by reacting hexasaccharide **3** with Et_3N and linker **4** to get product **5** (scheme 2, 93 % yield).

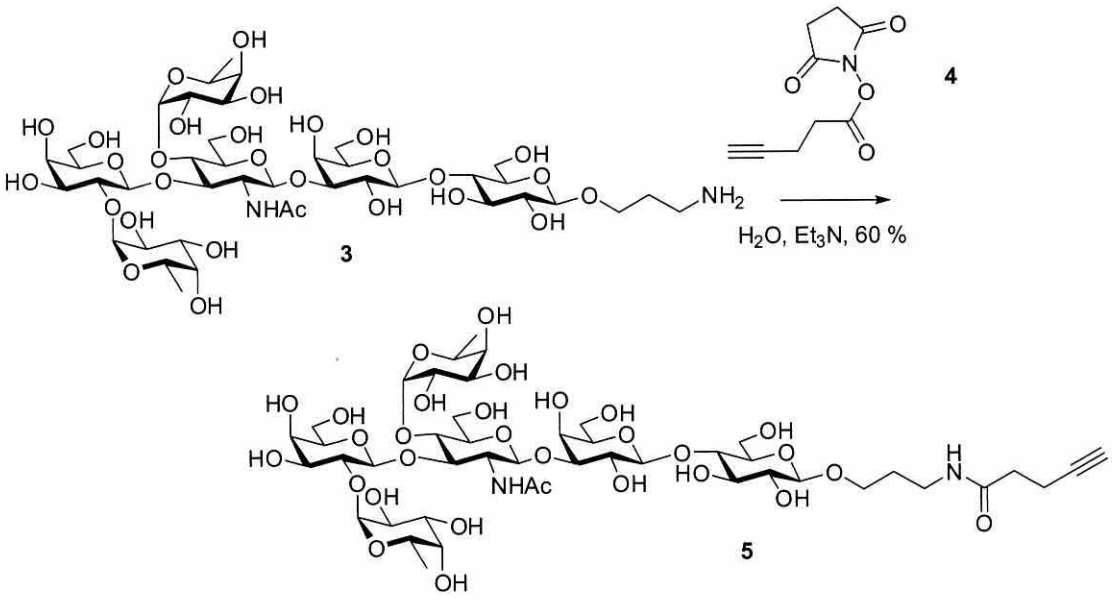

Scheme 2: Conjugation reaction of hexasaccharide **3**.

Compound **5** has been submitted to collaborators (Trinity College, Dublin) to do click reactions with porphyrin systems (scheme 3) [12], and further biological investigations.

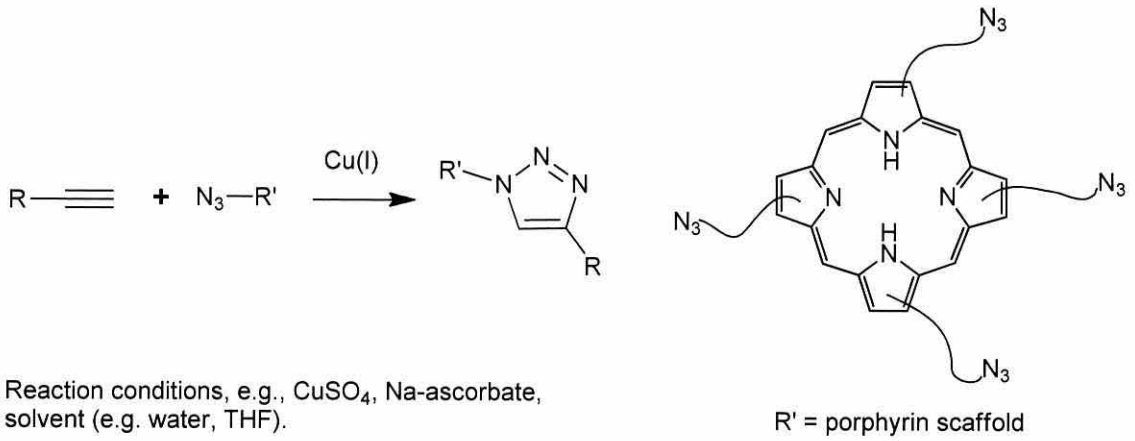

Scheme 3: A schematic representation of a click reaction and the porphyrin core to be used for the conjugations with **5**.

5.3 Conclusions

In conclusion, a separation protocol for incomplete fucosylated Le^b structures has been elaborated using a combination of a desalting column and reversed phase chromatography. Conjugation of compound **3** to an alkyne linker giving compound **5** for the preparation of porphyrin based multivalent structures was straight forward.

5.4 Experimental

5.4.1 General procedures

Dry methanol was kept over molecular sieves 3 Å; all other chemicals were used as purchased. TLC was perfomed on 0.25 mm precoated silica gel glass plates (Merck silica gel 60 F_{254}) with detection by UV-light (254 nm) or charring with 10% sulphuric acid solution followed by heating. Organic solvent were evaporated with a rotary evaporator under reduced pressure at approximately 40°C (water bath). Sandwich filter consist of three filters (20 µm - 10 - µm - 5µm). Silica gel (Amicon 0.041 – 0.063 mm) was used for column chromatography. All column dimensions are given in cm, W (width), H (length).

MALDI-TOF spectra were recorded on a Bruker Reflex IV instrument, using 2, 4, 6-trihydroxy-acetophenone monohydrate (THAP) as matrix.

Deprotection of hexasaccharide (2)

Mixture **1** (70 mg, 42 µmol) was dissolved in THF (2 mL), EtOH (2 mL) and H_2O (66 µL), then HCl (1M, 42 µL) and Pd/C (5 %, 60 mg) was added to the reaction solution. The reaction was carried on under H_2 atmosphere for 6 hours using a hydrogen filled balloon at room temperature. Then 1 mL water and additional 10 mg Pd/C were added. Stirring was continued overnight until the reaction was completed. The reaction progress was monitored by MALDI-TOF. The reaction solution was filtered through a sandwich filter, concentrated and purified by P2 and RP-C18 columns. First, the concentrated mixture was applied onto a P2 column (Bio-Gel P-2 column, 3.5 W x 75 H), then eluted with water (1% *n*-BuOH in purified water). Each collected fraction was analysed by MALDI-TOF. Sugar containing fractions were then collected and dried under reduce pressure to give crude **2** (30 mg, 17 % pentasaccharides content). After that, crude **2** was applied to a RP-C18 column (1.5 W x 8 H). The RP-C18 column was prewashed with a step-gradient using 2 mL for each step (MeOH→80%MeOH→60%MeOH→40%MeOH→20%MeOH→water). Crude **2** was dissolved in water (1 mL). This solution was applied to the column. Then fractions were eluted with a water/MeOH step-gradient using 4 ml for each step

(Water→10%MeOH→20%MeOH→30%MeOH→40%MeOH). The fractions were checked by MALDI-TOF. The product containing fractions were collected, concentrated, and dried under reduced pressure to give product **2** (25 mg). MALDI-TOF MS: Calcd for $C_{35}H_{62}N_2O_{25}$ 933.865 $[M+Na]^+$. Found: 933.853 $[M+Na]^+$ ± 13 ppm.

Conjugation reaction of hexasaccharide (5)

Compound **3** (16 mg, 15.1 μmol) was dissolved in MeOH/water (1:1, 500 μL). Et_3N (4 μL) and linker **4** were added. The reaction was stirred overnight at room temperature, and monitored by MALDI-TOF. After the reaction was completed, the solution was concentrated and applied a C18 column. The RP-C18 column was prewashed with a step-gradient using 2 mL for each step (MeOH→80%MeOH→60%MeOH →40%MeOH→20%MeOH→water).Concentrated solution was passed through C18 column, and then eluted with water/MeOH. (Water→10%MeOH→20%MeOH →30%MeOH→40%MeOH, 4 mL of each elute). The fractions were checked by MALDI-TOF. The fractions were collected and concentrated to give compound **5** (16 mg, 93%) MALDI-TOF MS: Calcd for $C_{46}H_{76}N_2O_{30}$ 1160.091 $[M+Na]^+$. Found: 1159.729 $[M+Na]^+$ ± 31 ppm.

5.5 References

1. Feldman, R.A.; Eckersley, A.J.; Hardie, J.M. *Br. Med. Bull*, **1998**, *54*, 39-53
2. Ernst, P. B.; Gold, B. D. *J. Pediatr. Gastroenterol. Nutr*, **1999,** *28*, 462-473
3. Boren, T.; Falk, P.; Roth, K.; Larson, G. Normark, S. *Science*, **1993**, *262*, 1892.
4. Kusters, J. G.; Van Vliet, A. H.; Kuipers, E. J. *Clin. Microbiol. Rev*, **2006**, *19* (3), 449–90
5. Randolph, J.T.; Danishefsky, S. *Angew. Chem. Int. Ed. Engl*, **1994**, *33*, 1470–1473
6. Randolph, J.T.; McClure, K.F.; Danishefsky, S. *J. Am. Chem. Soc*, **1995**, *117* 5701–5711, 5712–5719
7. Chernyak, A.; Oscarson, S.; Turek, D. *Carbohydr Res,* **2000**, *329*, 309.
8. Lahmann, M.; Bülow, L.; Teodorovic, P.; Gybäck, H.; Oscarson, S. *Glycoconjugate. J,* **2004**, *21*, 251
9. Eklind, K. R.; Gustafsson, A.; Tidén, K.; Norberg, T.; Åberg, P. M. *J. Carbohydr. Chem*, **1996**, *15*, 1161-1178
10. Mammen, M.; Choi, S. K.; Whitesides, G.M. *Angew. Chem. Int. Ed. Engl*, **1998**, *37*, 2754–2794
11. Glorius. F. *Org. Biomol. Chem,* **2005**, *3*, 4171-4175
12. Kolb, H. C.; Finn, M. G.; Sharpless, K. B. *Angew. Chem. Int. Ed,* **2001,** *40* (11), 2004-2021.

Supplementary Information

The following paper has been accepted for publication:
Nanomedicine UK, **2011**, DOI:10.2217/NNM.11.151

Title: Gold nanoparticles as carriers for a synthetic *Streptococcus pneumoniae* type 14 conjugate vaccine

Authors names & affiliations: Dodi Safari[1], Marco Marradi[2,3], Fabrizio Chiodo[2], Huberta A. Th. Dekker[1], **Yulong Shan[4]**, Roberto Adamo[5], Stefan Oscarson[6], Ger T. Rijkers[7], Martina Lahmann[4], Johannis P. Kamerling[5], Soledad Penadés[2,3]*, Harm Snippe[1]*

[1]*Department of Medical Microbiology, University Medical Center Utrecht, Utrecht, The Netherlands;* [2]*Laboratory of GlycoNanotechnology, Biofunctional Nanomaterials Unit, CIC biomaGUNE and* [3]*Networking Research Centre on Bioengineering, Biomaterials and Nanomedicine (CIBER-BBN), San Sebastián, Spain;* [4]*School of Chemistry, Bangor University, Bangor, United Kingdom;* [5]*Bijvoet Center, Department of Bio-Organic Chemistry, Utrecht University, Utrecht, The Netherlands;* [6]*Center for Synthesis and Chemical Biology, University College Dublin, Belfield, Dublin 4, Ireland;* [7]*Department of Medical Microbiology and Immunology, St. Antonius Hospital, Nieuwegein, The Netherlands*

*Corresponding authors:

Harm Snippe
Department of Medical Microbiology
University Medical Center Utrecht
Heidelberglaan 100, 3584 CX Utrecht, The Netherlands
Tel: +31 (0) 887553890; Fax: +31 (0) 302541770
Email: h.snippe@umcutrecht.nl

Soledad Penadés
Laboratory of GlycoNanotechnology,

Biofunctional Nanomaterials Unit
CIC biomaGUNE / CIBER-BBN
Paseo Miramón 182, 20009 San Sebastián, Spain
Tel: +34 943 00 53 07; Fax: +34 943 00 53 01
E-mail: spenades@cicbiomagune.es

Abstract

Aims: Carbohydrates are poorly immunogenic and coupling of capsular polysaccharides of pathogens to immunogenic protein carriers (conjugate vaccines) have been developed to improve their immune response. Our idea is to explore the use of gold nanoclusters as carrier to prepare fully synthetic carbohydrate vaccines against *Streptococcus pneumoniae* and test their immunogenic efficacy.

Material & Methods: Gold nanoclusters (~2 nm) coated with different amounts of a synthetic tetrasaccharide epitope related to the *S. pneumoniae* type 14 capsular polysaccharide (Pn14PS), the T-helper $OVA_{323-339}$ peptide, and D-glucose were prepared by a one pot method and characterized by transmission electron microscopy, IR, UV, and NMR. The immunogenicity of these gold glyco-nanoparticles (GNPs) was studied in mice and the levels of antibody against the tetrasaccharide, Pn14PS, and $OVA_{323-339}$ in sera measured by ELISAs. Spleen cells from immunised mice were stimulated *in vitro* with $OVA_{323-339}$ and the supernatant was analysed using a luminex-multiplex cytokine assay to determine IL-2, TNF-α, and IFN-γ (Th1 cytokines); IL-4 and IL-5 (Th2 cytokines); and IL-17 (Th17 marker). The capacity of the evoked antibodies to promote the uptake of heat inactivated and FITC-labelled *S. pneumoniae* type 14 by human polymorphonuclear leukocytes (PMNL) was assessed *in vitro*.

Results & Discussion: Water soluble GNPs containing 45% of tetrasaccharide and 5% of $OVA_{323-339}$ were able to trigger significant titer of specific anti-Pn14PS IgG antibodies. Cytokines levels confirmed that GNPs led to helper Th cells activation. The anti-saccharide antibodies were able to promote the phagocytosis of *S. pneumoniae* type 14 bacteria by human PMNL, indicating the functionality of the antibodies.

Conclusions: This study presents the first example of a fully synthetic carbohydrate vaccine against *S. pneumoniae* based on gold nanoclusters. The current results demonstrate the usefulness of gold nanoparticles as a versatile carrier for the development of a great diversity of synthetic carbohydrate-based vaccines.

Keywords

gold nanoparticles, tetrasaccharide epitope, $OVA_{323-339}$ peptide, *Streptococcus pneumoniae,* mice immunization, antibodies, synthetic carbohydrate vaccine

Introduction

Since carbohydrates are usually poorly immunogenic, strategies have been developed to improve their immune response. One such strategy is the coupling of capsular polysaccharides of pathogens to suitable immunogenic protein carriers (conjugate vaccines) [i]. With the exception of zwitterionic polysaccharides [ii], [iii] carbohydrates are T cell independent antigens and conjugate vaccines convert the immune response into one with a T cell dependent character [iv]. Although carbohydrate conjugate vaccines have been prepared against malaria [v] and prostate cancer [vi], and used successfully to prevent invasive pneumococcal [vii] and *Haemophilus* type b [viii] diseases, there are still many challenges and problems to be addressed in the area of carbohydrate vaccine design. One of these is the identification of the smallest protective epitopes for many pathogens. Furthermore, a main concern for synthetic vaccines is the risk of carrier-induced epitopic suppression [ix].

Current advances in the identification and synthesis of carbohydrate epitopes have opened new ways to rationalize vaccine design [x]. Several strategies for the production of synthetic carbohydrate-based vaccines have been developed to overcome the hurdles encountered with the use of protein carriers and complex bacterial capsular polysaccharides [i], [xi]. These strategies include the use of liposomes [xii, xiii] dendrimers [xiv], peptides [xv], micrometric beads [xvi] and polymeric nanoparticles, [xvii] as scaffolds to obtain multivalent conjugate vaccines [i]. Recently, three-component synthetic vaccines containing a tumour-associated glycopeptide, a peptide T-helper epitope, and a toll-like receptor 2 (TLR2) agonist [xii] or L-rhamnose [xviii] were found to elicit high titers of IgG antibodies in mice. Based on our experience in the preparation of multicomponent biofunctional gold nanoclusters [xix], we reasoned that a synthetic vaccine could be also constructed using gold nanoparticles as carrier of the vaccine components.

Nanotechnology offers an alternative to conventional vaccine technologies and can improve vaccine development [xvii, xx]. The opportunity of modifying the surface of nanoparticles to achieve simultaneous antigen-loading, adjuvant co-delivery, improved circulation times, and targeting properties has increased the interest in nanoparticle-based vaccines. Micrometric gold particles have been used to administer DNA vaccines directly into cells of the skin in humans by "gene gun" inoculations [xxi] that facilitate DNA delivery and gene expression in order to induce protective levels of antibody against hepatitis B virus [xxii] and influenza [xxiii]. It has also been reported that small metallic nanoparticles (5-10 nm) coated with tiopronine [xxiv] or Cys-modified peptides [xxv] can trigger macrophage activation *in vitro*, demonstrating the possibility to modulate cell-mediated immune responses with suitable nanotools.

This study explores the preparation and potential application of hybrid gold glyconanoparticles (GNPs) as vaccine candidates against the native polysaccharide of *Streptococcus pneumoniae*, a major cause of invasive respiratory tract infections in both children and the elderly [xxvi]. We have previously developed a simple and versatile method to prepare sugar-functionalized gold nanoclusters (glyconanoparticles [GNPs]) with a polyvalent carbohydrate display and a globular shape [xxvii, xxviii]. This method allows the generation of complex gold GNPs by combining different molecules on the same nanoplatform in a controlled fashion [xix]. GNPs are water-soluble, non-cytotoxic, and stable under physiological conditions and have turned out to be useful tools with which to study and intervene in carbohydrate-mediated biological processes [xxix, xxx].

A polysaccharide vaccine against the 23 most prevalent pneumococcal serotypes is currently available. This vaccine elicits a poor antibody response in high-risk groups, especially neonates and children. [xxxi] It has been shown, however, that conjugate vaccines of natural capsular polysaccharides coupled to a carrier protein such as diphtheria toxin are immunogenic in young children and protect against invasive pneumococcal disease [xxxii]. In subsequent studies, synthetic fragments of *S. pneumoniae* capsular polysaccharides conjugated to protein carriers have also been investigated for their effectiveness as vaccine candidates [xxvi]. The synthetic branched tetrasaccharide β-D-Gal*p*-(1→4)-β-D-Glc*p*-(1→6)-[β-D-Gal*p*-(1→4)-]-β-D-Glc*p*NAc-(1→), which corresponds to a single repeating unit of the *S. pneumoniae* type 14 capsular polysaccharide (Pn14PS), was identified as the smallest structure capable of evoking opsonophagocytic antibodies against *S. pneumoniae* type 14 when conjugated to cross-reactive material of diphtheria toxin (CRM197) protein [xxxiii, xxxiv]. In the present study, a series of 2 nm hybrid gold nanoparticles (GNP-1-4) displaying different ratios of the branched tetrasaccharide unit of Pn14PS [xxxiv], the T-helper ovalbumin $OVA_{323-339}$ peptide [xxxv, xxxvi], and the monosaccharide D-glucose, were prepared (**Figure 1**). Subsequent studies on the immunogenicity of these hybrid gold nanoparticles showed that they do induce a specific immune response against Pn14PS after intracutaneous administration to BALB/c mice. Furthermore, spleen cells of immunised mice were stimulated *in vitro* and cytokine profiles were determined. Cytokines are important mediators of a number of critical steps during the immune response [xxxvii, xxxviii]. The capacity of elicited antibodies to promote phagocytosis of *S. pneumoniae* type 14 by human polymorphonuclear leukocytes *in vitro* was also evaluated.

Materials & methods

Preparation of thiol-armed conjugates

In order to prepare the gold GNPs, thiol-armed conjugates of the branched tetrasaccharide, D-glucose, and $OVA_{323-339}$ have been synthesized. The synthesis of 1-{3-[β-D-Gal*p*-(1→4)-β-D-Glc*p*-(1→6)-[β-D-Gal*p*-(1→4)-]β-D-Glc*p*NAc]propyl)}-3-(23-mercapto-3,6,9,12-tetraoxatricosyl)thiourea (**1**) has been carried out following a modified protocol [xxxix] and is reported in the **Supplementary Material**. 5-(Thio)pentyl β-D-glucopyranoside (**2**) was synthesized as previously described [xxviii]. The $OVA_{323-339}$ peptide with an additional glycine and mercaptopropionic acid linker at the *N*-terminus $HS(CH_2)_2C(O)$GISQAVHAAHAEINEAGR (**3**) was obtained from GenScript Corp (Piscataway, NJ, USA).

Preparation of hybrid gold nanoparticles

A slight modification of an earlier reported single-step procedure [xix] was applied to prepare the GNPs. A solution of tetrachloroauric acid ($HAuCl_4$, Strem Chemicals, 0.025 M, 1 equiv.) in water was added to a 0.012 M (5 equiv.) methanolic solution of the appropriate mixture of thiol-armed compounds **1**, **2** and **3** (**Figure 1** and **Supplementary Figure S1**) in different ratios. An aqueous solution of $NaBH_4$ 1M (21 equiv.) was then added in four portions, with vigorous shaking. The black suspension formed was shaken for an additional 2 h at 25 °C after which the supernatant was removed and analysed. The residue was dissolved in a minimal volume of Nanopure water and purified by dialysis or by centrifugal filtering. For the ligand analysis, ^{1}H NMR spectra of the initial mixtures used for the GNPs synthesis and of the unreacted conjugates from the supernatants after GNPs formation were recorded (**Figures S3-S6**). The ratio of the ligands in the GNPs (**Table 1**) was evaluated by integrating the signals of the anomeric protons of tetrasaccharide **1** with those of the anomeric proton of glucoside **2** and the methyl groups of isoleucine (Ile) and valine (Val) of $OVA_{323-339}$ peptide conjugate **3**. The particle size distribution (average gold diameter) of the gold nanoparticles was evaluated from transmission electron microscopy (TEM) micrographs (**Figure S9**). The average number of gold atoms were calculated on the basis of the average diameter obtained by TEM micrographs, and molecular formulas of the GNPs were estimated according to a previous work [xl] (**Table 1**). Details of the chemical syntheses and analytical data (^{1}H NMR, IR, TEM, and UV-vis) of the hybrid GNPs are provided in the **Supplementary Material**.

Mouse immunization studies

Inbred 6-week-old female BALB/c mice were immunized intracutaneously with a series of GNPs (6 μg) which contain the tetrasaccharide (approx. 3 μg per dose) and/or $OVA_{323-339}$ peptide (approximately 3 μg per dose), using a mixture of MPL and Quil-A as adjuvants [10 μg monophosphoryl lipid-A (MPL derived from S. minnesota R595 LPS; Ribi ImmunoChem Research Inc., Hamilton, MT, USA) and 20 μg Quil-A (Quil-A was a gift from Dr. Erik B. Lindblad, Brenntag Biosector , Vedbaek, Denmark)] as described previously [xxxiv] (**Supplementary Table S1**). The GNPs were injected at four different sites in the proximity of the lymph nodes of the axillae and the groins. The following antigens served as positive controls: *S. pneumoniae* type 14 polysaccharide conjugated to CRM197 (Pn14PS-CRM197; Wyeth Research, Pearl River, NY, USA, 2.5 μg of carbohydrate), free $OVA_{323-339}$ peptide (2.5 μg), and $OVA_{323-339}$ peptide conjugated to CRM197 protein ($OVA_{323-339}$ peptide-CRM197, 50 μg). The $OVA_{323-339}$ peptide-CRM197 was constructed by coupling of the $OVA_{323-339}$ peptide to CRM197 protein as described previously [xxxiv]. All control antigens were injected into mice in combination with the adjuvants mentioned above (**Table S1**). All booster immunizations were given without adjuvant and were performed on weeks 5 and 10. Blood samples were taken before and after the booster and the sera were stored at -20 °C.

Measurement of type-specific antibodies and phagocytosis titer

The enzyme-linked immunosorbent assay (ELISA) was performed to measure the antibodies to native Pn14PS, to the synthetic branched tetrasaccharide structure Gal-Glc-(Gal-)GlcNAc-Gal (one repeating unit of Pn14PS with extra one galactose residue), and to ovalbumin, as described previously [xxxiv].

The opsonophagocytosis assay was performed by using human polymorphonuclear leukocytes (PMN cells) isolated from peripheral blood of healthy donors, as previously described [xxxiv, [xli]]. Details of the protocol are provided in the **Supplementary Material**.

In-vitro spleen cells stimulation

Mouse spleens (n=2) were isolated three weeks after the second booster immunization. Spleen cells suspensions (10^7 cells/mL) were stimulated with $OVA_{323-339}$ peptide (10 μg) in Roswell Park Memorial Institute (RPMI) 1640 tissue culture medium supplemented with 10% fetal calf serum and gentamycin. The cells were cultured at 37 °C, in 100% relative

humidity, and with 5% CO_2 in air. Finally, the supernatants were collected at 72 h after initiation of the cultures, and stored at -70 °C until use. Six different cytokines were selected to screen the supernatants: IL-2 (171-G5003M), TNF-α (171-G5023M), and IFN-γ (171-G5017M) as Th1 cytokines; IL-4 (171-G5005M) and IL-5 (171-G5006) as Th2 cytokines; and IL-17 as Th17 marker (171-G50013M). We used a luminex-multiplex cytokine assay, following the manufacturer's instructions (Bio-Rad, Hercules, CA, USA). The lower limits of detection were 0.31 pg/mL (IL-2), 0.71 pg/mL (IL-4), 0.24 pg/mL (IL-5), 0.20 pg/mL (IL-17), 0.48 pg/mL (IFN-γ), and 5.2 pg/mL (TNF-α).

Other methods

General information about chemicals and techniques, and details of the synthesis of branched tetrasaccharide conjugate **1**, the preparation and characterization of hybrid gold nanoparticles GNP-1-4, detection of type-specific antibody by ELISA and phagocytosis titers can be found in the **Supplementary Material.**

Results

Preparation and characterization of hybrid gold GNPs

Hybrid gold glyconanoparticles (GNP1-4) used in this study were prepared by *in situ* reduction of a Au(III) salt in the presence of mixtures of thiol-armed conjugates **1**, **2**, and **3**, as gold binds thiols with a high affinity [[xlii]]. Conjugates **1**, **2**, and **3** are constituted by the antigenic synthetic branched tetrasaccharide β-D-Gal*p*-(1→4)-β-D-Glc*p*-(1→6)-[β-D-Gal*p*-(1→4)-]β-D-Glc*p*NAc-(1→), D-glucose, and the $OVA_{323-339}$ peptide, respectively (**Figure 1**). The conjugates were used in excess with respect to the Au(III) salt in order to assure full coverage of the nascent gold nanoclusters and to ensure that their molar ratios in solution are maintained on the nanoparticles surface. The one-step method which has been used allows in fact the incorporation of the conjugates in different and defined proportions on the same gold nanoparticles [xix, xxviii]. GNP-1 and GNP-4 were prepared from mixtures of **1**, **2**, and **3** in 45:50:5 and 20:70:10 molar ratios, respectively. The preparation GNP-1 was also repeated using a different batch of tetrasaccharide conjugate **1**. The resulting nanoparticles (GNP-1b) showed the same physicochemical properties, indicating that the methodology is reproducible, and elicited similar immune response (see below). GNP-2 contained tetrasaccharide conjugate **1** and glucose conjugate **2** in 50:50 ratio was prepared to study the immune response to the tetrasaccharide in the absence of the immunodominant OVA peptide conjugate **3**. GNP-3 contained ~10% of OVA peptide **3** and ~90% of glucose conjugate **2** served as the control system. The presence of conjugates on the GNPs was assessed qualitatively by comparing the ^{1}H NMR spectra of the initial mixtures and the formed GNPs (**Figures S3-S6**). The GNPs were monodisperse and showed exceptionally small gold core diameters, ranging from 1.7 to 1.9 nm (assuming a spherical shape), as demonstrated by TEM analysis (**Figure S9**). The lack of a gold surface plasmon band at approximately 520 nm in the UV/Vis spectra (**Figure S10**) confirmed the small core size of the GNPs. All of the prepared GNPs were water-soluble and stable for months in solution. Moreover, they survived freeze-drying processes and could be re-dispersed in water without losing their physicochemical properties and integrity. Average molecular formulae and weights of the GNPs were estimated according to the literature [xl], and are given in **Table 1**.

The immunogenicity of hybrid gold GNPs

Specific IgG antibodies against the synthetic branched tetrasaccharide, the native Pn14PS, and the $OVA_{323-339}$ peptide were then determined in the sera of these mice using ELISA. The antibody response to the tetrasaccharide was determined on a glycoconjugate constructed from the branched tetrasacchaide and bovine serum albumin (BSA) protein. Sera obtained from mice immunized with GNP-1 (Tetra:Glc:OVA = 45:50:5) recognized the branched tetrasaccharide structure (**Figure 2A**). The IgG antibodies induced by GNP-1 also bound to native Pn14PS (**Figure 2B**), but the titer was one $\log_{10}$ lower than the response to the positive control antigen Pn14PS-CRM197. Immunization with GNP-2 (Tetra:Glc = 50:50) or with GNP-3 (Glc:OVA = 90:10), did not elicit any specific IgG antibodies against Pn14PS (**Figure 2B**). When GNP-2 + GNP-3 were admixed a marginal response was obtained. Immunization with GNP-4 (Tetra:Glc:OVA = 20:70:10) elicited an even lower level of specific IgG antibodies against Pn14PS than GNP-1, bearing twice as much tetrasaccharide (**Figure 2B, and Supplementary Table S1**). It can thus be concluded that the presence of the T cell epitope $OVA_{323-339}$ peptide in the GNP is a prerequisite for the induction of an antibody response to the tetrasaccharide.

Specific IgG antibodies to ovalbumin were detected after immunization with the $OVA_{323-339}$ peptide, which contains a T cell epitope of this protein, and $OVA_{323-339}$ peptide-CRM_{197} conjugate, in contrast to the GNP preparations which elicited negligible levels of IgG antibodies against ovalbumin (**Figure 2C**). Similar results (data not shown) were obtained by ELISAs using plates coated with the $OVA_{323-339}$ peptide conjugated to BSA. Overall, these data indicate that immunization with $OVA_{323-339}$-containing GNPs (GNP-1, GNP-3, and GNP-4) did not induce antibodies against the complete OVA protein or against this specific peptide (**Figure 2C**).

Phagocytic capacity of sera obtained from the GNPs immunization

An opsonophagocytosis assay which serves as a correlate of protection for candidate vaccines was used to test the functionality of the anti-saccharide antibodies. To that end, the activity of sera from mice immunized with different GNPs was tested in a phagocytosis assay using *S. pneumoniae* type 14 bacteria and human polymorphonuclear cells. Sera obtained from mice immunized with GNP-1 were able to opsonise *S. pneumoniae* type 14 bacteria, although in a lower fashion than sera from mice immunized with Pn14PS-CRM197. The other GNPs, including GNP-4 and the mixture of GNP-2+GNP-3, were not capable of inducing *S. pneumoniae* type 14-opsonizing antibodies (**Figure 2D**).

Cytokine levels after spleen cell stimulation

To investigate whether $OVA_{323-339}$ peptide-containing GNPs can actually lead to T-lymphocyte activation, spleen cells from mice treated with GNP-1, GNP-2, GNP-3, and a mixture of GNP-2+GNP-3 were (re)stimulated *in vitro* with the $OVA_{323-339}$ peptide. Spleen cells of mice previously immunized with $OVA_{323-339}$ peptide-containing GNPs (GNP-1, GNP-3, or the combination GNP-2+GNP-3) did respond to *in vitro* restimulation by producing interleukin-2 (IL-2), IL-4, IL-17, and interferon γ (IFNγ) (**Figure 3**). Induction of IL-5 occurred only in the cells from mice immunized with GNP-1, which correlates with the production of specific IgG antibodies to Pn14PS *in vivo* (**Figure 2** and **Figure 3C**). *In vitro* stimulation with the complete ovalbumin protein led to a lower but otherwise similar cytokine-production profile (data not shown). Overall, the data indicate that immunization with either GNP-1, GNP-3, or the combination GNP-2+GNP-3 always resulted in the activation of T cells, but that specific antibody production to the branched tetrasaccharide structure or native Pn14PS only occurred, if both the tetrasaccharide and $OVA_{323-339}$ peptide (GNP-1) were presented on the same gold glyconanoparticle.

Discussion

Metal-based glyconanoparticles (GNPs) are biofunctional nanomaterials that combine the unique physical, chemical and optical properties of the metallic nucleus with the characteristics of the carbohydrate coating [xxix, xxx]. In the present study, we propose gold nanoclusters as a versatile platform to incorporate varying density of the synthetic branched tetrasaccharide β-D-Gal*p*-(1→4)-β-D-Glc*p*-(1→6)-[β-D-Gal*p*-(1→4)-]β-D-Glc*p*NAc-(1→), related to *S. pneumoniae* type 14 polysaccharide (Pn14PS), $OVA_{323-339}$ peptide, and glucose. The short glucose conjugate **2** was used as an inner component to assist water dispersibility and biocompatibility and to allow the tetrasaccharide fragment moiety, armed with a long amphiphilic linker, to protrude above the organic shell of GNPs. The aliphatic part of the linkers allows good self assembled monolayers packaging and confers rigidity to the inner organic shell to protect the gold core, while the external polyether moiety, due to its flexibility upon solvation in water, assists water solubility, and prevents non-specific adsorption of proteins [xxviii, [xliii]].

We found that GNPs coated with the tetrasaccharide and $OVA_{323-339}$ peptide induce specific IgG antibodies that recognize the branched tetrasaccharide homologue β-D-Gal*p*-(1→4)-β-D-Glc*p*-(1→6)-[β-D-Gal*p*-(1→4)-]β-D-Glc*p*NAc-(1→3)-β-D-Gal-(1→) [xxxiv] and the native polysaccharide of Pn14PS. The synthetic tetrasaccharide epitope does not lose its biofunctionality after conjugation to the gold nanoplatform.

The different molar ratio of tetrasaccharide conjugate **1**, glucose conjugate **2,** and $OVA_{323-339}$ peptide conjugate **3** in the GNPs has a key effect on the immunogenic response. The GNP-4 with a molar ratio Tetra:Glc:OVA = 20:70:10 induced a very low titer of anti-Pn14PS IgG antibodies compared to the GNP-1 which has a molar ratio Tetra:Glc:OVA = 45:50:5. These experimental data indicate that epitope density on gold surface is of crucial importance to obtain significant levels of IgG antibodies. The ligand density and the nature of spacers used to separate a selected ligand from the gold cluster are important factors for proper receptor targeting of GNPs, as demonstrated with different types of lactose-coated gold GNPs in aggregation experiments with *Ricinus communis* agglutinin [[xliv]] or in enzymatic studies with *Escherichia coli* β-galactosidase [[xlv]], and with (oligo)mannose-coated GNPs in cellular models of inhibition of HIV-1 trans-infection of T cells [[xlvi]] or in 2G12-mediated neutralization of HIV-1 infection of TZM-bl cells [[xlvii]]. It is worth mentioning that a different batch of GNP-1 (named GNP-1b) was also used in mice immunization (**Figure S11**). While the primary immunizations were always performed with 6 μg of these nanoparticles, the

booster dosage of GNP-1b was augmented five fold (30 μg) with respect to GNP-1 (6 μg). Following this, an increase in the level of specific antibodies induced by GNP-1b against Pn14PS was observed.

Another finding is that the presence of the T cell stimulating peptide $OVA_{323-339}$ in the hybrid GNPs was crucial for the induction of specific carbohydrate-directed IgG antibodies. In this study, we found that GNPs which do not contain $OVA_{323-339}$ peptide (GNP-2) are not able to elicit either anti-tetrasaccharide antibodies (**Figure 2B**) or anti-Pn14PS IgG antibodies (**Figure 2C**). The presence of the peptide was essential to evoke anti-saccharide antibodies, but it did not lead to anti-peptide antibodies and thereby avoids the risk of epitope suppression. [ix] The activation of memory T cells was demonstrated by the cytokines profiles after *in vitro* $OVA_{323-339}$ peptide-mediated (re)stimulation of the spleen cells from immunised mice. The induction of IL-2 (**Figure 3A**) is significant because it is the major growth factor for T cells, including regulatory T cells [xlviii]. It is important to note that spleen cells derived from mice immunized with GNPs containing the $OVA_{323-339}$ peptide produced cytokine IL-4, when stimulated by $OVA_{323-339}$ peptide. This indicates a Th2 response to the peptide. Those T cells provide help in the B cell response (antibody formation) to the saccharide moiety on GNP-1. Induction of IL-5 occurred only in those cells from animals previously immunized with GNPs which contain tetrasaccharide and peptide (GNP-1, **Figure 3C**) and correlates with the production of specific anti-Pn14PS IgG antibodies *in vivo*. In fact, IL-5 produced by Th2 cells acts as a B cell differentiation factor by stimulating activated B cells to secrete antibodies [xlix]. These results are in line with other immunization studies in which the same synthetic tetrasaccharide was conjugated to the CRM197 [xxxiv]. In human vaccination trials with the pneumococcal conjugate vaccine an enhanced IL-5 secretion was observed in response to the carrier protein [l]. While cytokines IL-4 and IL-5 are well known Th2 markers, TNFα (regulatory cytokine), IFNγ (Th1 marker), and IL-17 (Th17 marker and regulatory cytokine) were studied because they play a key role in influencing the migration and pathogenic behaviour during inflammatory diseases [li]. Especially, IL-17 has recently attracted much attention because of its role in protection against invasive pneumococcal infections [lii, liii].

The presentation of both the antigenic carbohydrate and the T-helper peptide on the same gold nanoplatform seems to be crucial for eliciting a significant antibody response, even though the T-helper peptide and the B-cell epitope are not directly covalent linked. This observation is substantiated by the fact that the cocktail of GNP-2 (lacking $OVA_{323-339}$) and

GNP-3 (lacking tetrasaccharide) elicited much lower level of specific IgG antibodies against Pn14PS than GNP-1 that simultaneously present both $OVA_{323-339}$ and tetrasaccharide.

In phagocytosis assays, only the antibodies in sera of mice immunised with GNP-1 were able to render *S. pneumoniae* type 14 bacteria critically susceptible to the action of human polymorphonuclear leukocytes (**Figure 2D**). Although the phagocytic titer was lower than the one obtained with Pn14PS-CRM197, this result indicates that GNP-1 is a promising *S. pneumoniae* type 14 vaccine candidate. No opsonophagocytosis of the bacteria was promoted by the sera from mice immunised with the other GNPs, including the cocktail of GNP-2 and GNP-3.

Conclusions & Future perspective

Hybrid gold nanoparticles coated with a synthetic branched tetrasaccharide antigen, $OVA_{323-339}$ peptide, and glucose are capable of inducing IgG antibodies against native polysaccharide of *S. pneumoniae* type 14. The molar ratio between tetrasaccharide, glucose and peptide in the hybrid gold nanoparticles turned out to be critical for optimal immunogenicity: Gold nanoparticles containing 45% of tetrasaccharide, 5% of peptide, and glucoconjugate as inner component were able to trigger specific anti-Pn14PS antibodies. Three main factors emerged for the induction of a robust carbohydrate-directed immune response with GNPs: (i) the density of the antigenic tetrasaccharide on the gold nanoplatform; (ii) the presence of the T cell-stimulating peptide $OVA_{323-339}$ on the GNP; and (iii) the simultaneous presence of a combination of both T-helper and B cell epitopes on the same GNP.

Although further optimization of vaccine efficacy is necessary, this study presents the first example of a fully synthetic carbohydrate vaccine based on gold nanoclusters that is able to induce specific IgG antibodies that react with native capsular polysaccharide of *S. pneumoniae*. The current results demonstrate the usefulness of gold nanoparticles as a versatile platform for the development of a great diversity of synthetic carbohydrate-based vaccines.

Colloidal gold have been used in humans since the 1950s, [liv] but many concerns regarding the translation to clinic have still to be carefully addressed. Retention in organs (especially liver) and nanotoxicity [lv] are the main concerns against systemic administration of metallic nanoparticles. Risk-benefit analysis may suggest that nanotechnology-based tools could be admitted for one-off or limited administration such as primary immunization / boosters for vaccination, diagnostics and thermal cancer treatments [lvi].

The opportunity of easily producing stable conjugate vaccines bearing arrays of carbohydrate antigens and simultaneously targeting various bacterial structures arranged on a single gold nanoparticle open new perspectives in the vaccine field and thus may promote gold nanoparticles to the frontline for tailor-made polyvalent carbohydrate vaccine candidates.

Executive summary

- Specific IgG antibodies against *Streptococcus pneumoniae* type 14 capsular polysaccharide (Pn14PS) were induced by small (~2 nm) gold nanoparticles coated with a conjugate of the branched tetrasaccharide β-D-Gal*p*-(1→4)-β-D-Glc*p*-(1→6)-[β-D-Gal*p*-(1→4)-]β-D-Glc*p*NAc-(1→), which corresponds to a single repeating unit of Pn14PS, a conjugate of the $OVA_{323-339}$ peptide, and a conjugate of D-glucose, after intracutaneous administration to BALB/c mice.
- The co-presence of the T cell-stimulating $OVA_{323-339}$ peptide and the tetrasaccharide antigen on the gold nanoparticles was a prerequisite for the induction of the anti-Pn14PS IgG antibodies.
- The molar ratio between tetrasaccharide, $OVA_{323-339}$, and glucose on the gold nanoparticles was critical for optimal immunogenicity.
- The $OVA_{323-339}$ (T cell epitope) on the nanoparticle does not lead to antibodies against the peptide and this avoids the risk of epitope suppression.
- *In vitro* stimulation with the $OVA_{323-339}$ peptide of spleen cells from immunised mice revealed cytokines levels (especially IL-5) which confirmed that GNPs led to helper Th cells activation.
- The antibodies in sera of mice immunised with GNP-1 (tetrasaccharide: Glc : $OVA_{323-339}$ = 45 : 50 : 5) were able to coat heat-inactivated FITC-labelled *S. Pneumoniae* type 14 and make the bacteria critically susceptible to the action of human polymorphonuclear leukocytes (opsonophagocytosis) as demonstrated by a phagocytosis assay.
- This is the first example of a fully synthetic carbohydrate vaccine candidate based on gold nanoparticles capable of evoking specific antibodies against *S. pneumoniae* type 14.

Financial & competing interests disclosure

This research was supported by the European Union (grant GlycoGold, MRTN-CT-2004-005645), the Spanish Ministry of Science and Innovation, MICINN (grant CTQ2008-04638), and the Department of Industry of the Basque Country (grant ETORTEK2009). The authors have no other relevant affiliations or financial involvement with any organization or entity with a financial interest in or financial conflict with the subject matter or materials discussed in the manuscript apart from those disclosed.

Writing assistance was utilised in the production of this manuscript.

Ethical conduct of research

All immunization studies were approved by the Ethics Committee on Animal Experiments of Utrecht University, Utrecht, The Netherlands.

Paper - Supplementary Material

Title: Gold nanoparticles as carriers for a synthetic *Streptococcus pneumoniae* type 14 conjugate vaccine

Authors names & affiliations: Dodi Safari[1], Marco Marradi[2,3], Fabrizio Chiodo[2], Huberta A. Th. Dekker[1], Yulong Shan[4], Roberto Adamo[5], Stefan Oscarson[6], Ger T. Rijkers[7], Martina Lahmann[4], Johannis P. Kamerling[5], Soledad Penadés[2,3]*, Harm Snippe[1]*

[1]Department of Medical Microbiology, University Medical Center Utrecht, Utrecht, The Netherlands; [2]Laboratory of GlycoNanotechnology, Biofunctional Nanomaterials Unit, CIC biomaGUNE and [3]Networking Research Centre on Bioengineering, Biomaterials and Nanomedicine (CIBER-BBN), San Sebastián, Spain; [4]School of Chemistry, Bangor University, Bangor, United Kingdom; [5]Bijvoet Center, Department of Bio-Organic Chemistry, Utrecht University, Utrecht, The Netherlands; [6]Center for Synthesis and Chemical Biology, University College Dublin, Belfield, Dublin 4, Ireland; [7]Department of Medical Microbiology and Immunology, St. Antonius Hospital, Nieuwegein, The Netherlands

*Corresponding authors:

Harm Snippe
Department of Medical Microbiology
University Medical Center Utrecht
Heidelberglaan 100, 3584 CX Utrecht, The Netherlands
Tel: +31 (0) 887553890; Fax: +31 (0) 302541770
Email: h.snippe@umcutrecht.nl

Soledad Penadés
Laboratory of GlycoNanotechnology,
Biofunctional Nanomaterials Unit
CIC biomaGUNE / CIBER-BBN
Paseo Miramón 182, 20009 San Sebastián, Spain
Tel: +34 943 00 53 07; Fax: +34 943 00 53 01
E-mail: spenades@cicbiomagune.es

General information

All chemicals were purchased as reagent grade from Sigma-Aldrich and used without further purification, unless otherwise stated. Dichloromethane (DCM) was distilled from calcium hydride before use. Dry methanol was kept over molecular sieves (3 Å). Purified water was obtained from a Simplicity Ultrapure Water System (Millipore). Nanopure water (18.2 MΩ-cm) was obtained by a Thermo Scientific Barnstead NANOpure DIamond Water System. Thin layer chromatography (TLC) was performed on 0.25 mm pre-coated silica gel glass plates or aluminium backed sheets (Merck silica gel 60 F_{254}) with detection by UV-light (254 nm) and/or heating at over 200 °C after staining either with 10 % sulfuric acid (aqueous solution) or *p*-anisaldehyde solution (*p*-anisaldehyde [25 mL], H_2SO_4 [25 mL], EtOH [450 mL], and CH_3COOH [1 mL]). Organic solvents were removed by rotary evaporation under reduced pressure at approximately 40 °C (water bath). Silica gel (0.041 – 0.063 mm, Amicon and 0.063-0.200 mm, Merck) was used for flash column chromatography (FCC). Polyethylene (PE) columns equipped with PE frits (20 μm pore-size) were used for flash chromatography. Size-exclusion column chromatography was performed on Sephadex LH-20 (GE Healthcare) or Bio-Gel P-2 (BioRad, polyacrylamide, fine) at a flow rate recommended by the manufacturer. To remove small particles (e.g. Pd/C), a PE column was equipped with a filter sandwich made by stacking PE frits (pore size: 20 μm, 10 μm, and 5 μm) on-top of each other. NMR spectra were recorded at 500 MHz (Bruker) (^{1}H) or 125 MHz (^{13}C) at 25 °C. If not otherwise stated, chemical shifts (δ) are given in ppm relative to the residual solvent signal. NMR spectra of both GNPs and mixtures of thiol-armed compounds **1**, **2** and **3** used in different ratios to prepare GNPs were recorded by setting the delay time (d1) at 15 s. Infrared spectra (IR) were recorded from 4000 to 400 cm^{-1} with a Nicolet 6700 FT-IR spectrometer (Thermo Spectra-Tech); solids were pressed into KBr pellets. Optical rotations were determined with a Perkin-Elmer 341 polarimeter. UV/Vis spectra were measured with a

Beckman Coulter DU 800 spectrophotometer. Mass spectrometric data were obtained from a Waters LCT Premier XE instrument with a standard ESI source by direct injection. The instrument was operated with a capillary voltage of 1.0 kV and a cone voltage of 200 V. Cone and desolvation gas flow were set to 50 and 500 L/h, respectively; source and desolvation temperatures were 100 °C. High-resolution mass (HR-MS) was determined using glycocholic acid (Sigma) as an internal standard (2 $M+Na^+$, m/z = 953.6058). The masses for compound **5** and **6** were recorded on a Bruker Daltonics MicrOTOF (ESI). MALDI-Tof spectra were recorded on a Bruker Reflex IV using 2',4',6'-trihydroxy-acetophenone monohydrate (THAP) as matrix. For transmission electron microscopy (TEM) examinations, a single drop (10 μL) of the aqueous solution (*ca.* 0.1 mg/mL in milliQ water) of the GNPs was placed onto a copper grid coated with a carbon film (Electron Microscopy Sciences). The grid was left to dry in air for several hours at room temperature. TEM analyses were carried out in a Philips JEOL JEM-2100F microscope working at 200 kV.

Glucose conjugate **2** was prepared according to the literature [lviiS]. The $OVA_{323-339}$-peptide **3,** consisting of ISQAVHAAHAEINEAGR with an additional glycine and mercaptopropionic acid (MPA) linker at the *N*-terminus, was obtained from GenScript Corp (Piscataway , NJ , USA) and a single batch was used throughout the study. These conjugates, together with tetrasaccharide conjugate **1**, are depicted in Figure S1 and their ^1H NMR spectra are reported in Figure S2.

Synthesis of branched tetrasaccharide conjugate 1 (Scheme S1)

Following a reported protocol, the known protected thioethyl tetrasaccharide **4** was treated with 3-azidopropanol in the presence of NIS/AgOTf as a promoter system, leading to the corresponding 3-azidopropyl glycoside (90% yield) [lviiiS]. Concomitant removal of the benzoyl groups and conversion of the phthalimido group into the *N*-acetylamido group provided tetrasaccharide **5** (74% yield over three steps). Subsequent cleavage of the bromoisopropylidene acetal with 90% CF_3COOH (96% yield) and reduction of the azido group under Pd-catalysed hydrogenation conditions resulted in β-D-Gal*p*-(1→4)-β-D-Glc*p*-(1→6)-[β-D-Gal*p*-(1→4)-]β-D-Glc*p*NAc-(1→$(CH_2)_3NH_2$ **6** (89% yield) as hydrochloric acid salt. The coupling of aminopropyl tetrasaccharide **6** with the isothiocyanate linker **7** in a water/isopropanol/acetonitrile mixture and triethylamine was performed following a described procedure [lviiS] to afford thioacetyl-protected neoglycoconjugate **8** (71% yield). After deprotection neoglycoconjugate **1** was obtained as a mixture of disulfide and thiol (~2.5:1, 81% yield), which could be used for the preparation of the GNPs under reductive conditions.

3-Azidopropyl 3,4-O-(1-bromomethylethylidene)-β-D-galactopyranosyl-(1→4)-β-D-glucopyranosyl)-(1→6)-[β-D-glucopyranosyl-(1→4)]-2-acetamido-2-deoxy-β-D-glucopyranoside (**5**). Compound **4** (150 mg, 82 μmol) was dissolved in dry DCM (2 mL), and then molecular sieves (4 Å, 200 mg), azidopropanol (30 μL, 0.32 mmol) and *N*-iodosuccinimide (30 mg, 0.13 mmol) were added. The reaction mixture was stirred at room temperature for 15 min. After that, the mixture was cooled down to 0 °C in an ice bath, and a catalytic amount of AgOTf was added. The reaction was monitored by TLC (toluene/ EtOAc 6:1), while stirring of the reaction mixture continued for 1 h at room temperature. After

complete conversion, the mixture was concentrated and purified by flash column chromatography (toluene → toluene/EtOAc, 15:1→10:1→7:1→5:1) to give 3-azidopropyl [2,6-di-*O*-benzoyl-3,4-*O*-(1-bromomethylethylidene)-β-D-galactopyranosyl]-(1→4)-(2,3,6-tri-*O*-benzoyl-β-D-glucopyranosyl)-(1→6)-[(2,3,4,6-tetra-*O*-benzoyl-β-D-glucopyranosyl)-(1→4)]-2-deoxy-2-phthalimido-β-D-glucopyranoside as diastereomeric mixture (138 mg, 71 μmol, 90 %). MALDI-Tof for $C_{101}H_{89}BrN_4O_{31}$: Calcd. 1933.4767 $[M + H]^+$, 1955.4586 $[M + Na]^+$. Found 1933.5150 $[M + H]^+ \pm 20$ ppm, 1955.5625 $[M + Na]^+ \pm 25$ ppm. NMR data were in agreement with the previously reported ones [lviiiS].

This material (138 mg, 71 μmol) was dissolved in dry ethanol (5 mL), and after addition of ethylenediamine (500 μL, 7.4 mmol) the reaction mixture was stirred at 60 °C overnight. After complete consumption of the starting material (TLC: 6:1, DCM/MeOH), the mixture was concentrated and the residue co-evaporated 2 times with toluene. Then dry methanol (5 mL) and acetic anhydride (250 μL) was added to the residue, and the resulting mixture was stirred for 1 hour at room temperature, concentrated, co-evaporated with toluene, and again dissolved in dry methanol (10 mL). Then NaOMe (approx. 1 M solution in MeOH, 10 drops) was added, and the reaction mixture was stirred at room temperature overnight. The progress of the reaction was monitored by MALDI-Tof. After complete conversion, the mixture was neutralized using H^+-ion-exchange resin (Dowex-50WX-8). The resin was filtered off the reaction solution, and the filtrate was concentrated before the residue applied onto a column. Flash chromatography (DCM/MeOH 15:1 → 10:1 → 8:1 → 6:1 → 3:1 → 1:1→ methanol) gave compound **5** as diastereomeric mixture (48 mg, 53 μmol, 74 %).

HR-MS for $C_{32}H_{53}BrN_4O_{21}$: Calcd. 931.2278 $[M + Na]^+$. Found 931.1931 $[M + Na]^+ \pm 37$ ppm; ^{13}C NMR (CD_3OD) δ 173.6 ($NC(O)CH_3$), 110.1 ($C(CH_3)(CH_2Br)$), 104.9, 104.6, 104.2, 103.1 (C-1^{I-IV}), 81.8, 81.5, 81.0, 80.5, 77.0, 76.5, 76.5, 76.0, 75.9, 75.5, 75.4, 74.9, 74.4, 74.1, 72.8, 70.5, 68.7, 67.5, 62.6, 62.5, 62.0, 56.8 (C-2^{I-IV}-6^{I-IV}, $OCH_2CH_2CH_2N_3$), 37.0

($C(CH_3)(CH_2Br)$), 30.2 ($OCH_2CH_2CH_2N_3$), 25.0, 23.1 ($C(CH_3)(CH_2Br)$) and ($NC(O)CH_3$). ($OCH_2CH_2CH_2N_3$) undetected (under CD_3OD signals).

3-Aminopropyl β-D-galactopyranosyl-(1→4)-β-D-glucopyranosyl-(1→6)-[β-D-glucopyranosyl-(1→4)]-2-acetamido-2-deoxy-β-D-glucopyranoside·HCl salt. Compound **5** (48 mg, 53 μmol) was dissolved in 90% trifluoroacetic acid (1.8 mL). The reaction mixture was stirred at room temperature for 3 hours and the progress of the reaction monitored by TLC (DCM/MeOH, 6:1) and MALDI-Tof. After complete consumption of the starting material, the mixture was co-evaporated with toluene (2 x 5 mL). Purification by size-exclusion chromatography (Bio-Gel P-2 column, 1% *n*-BuOH in purified water) provided 3-azidopropyl β-D-galactopyranosyl-(1→4)-β-D-glucopyranosyl)-(1→6)-[β-D-glucopyranosyl-(1→4)]-2-acetamido-2-deoxy-β-D-glucopyranoside (40 mg, 51 μmol, 96%).

^1H NMR (D_2O) δ 4.49-4.42 (m, 3H, 3xH-1); 4.36 (d, 1H, J = 7.8 Hz, H-1); 4.20 (d, 1H, J = 9.8 Hz); 3.94-3.82 (m, 5H); 3.81-3.54 (m, 15H), 3.54-3.49 (m, 1H); 3.49-3.42 (m, 1H); 3.33-3.24 (m, 2H), 1.96 (s, 3H, NAc); 1.79-1.72 (m, 2H, $OCH_2CH_2CH_2N_3$). ^{13}C NMR (D_2O) δ 174.5 ($NC(O)CH_3$), 103.0, 102.8, 102.4, 101.2 ($C\text{-}1^{I\text{-}IV}$), 78.4, 77.9, 75.4, 75.3, 74.7, 74.3, 73.5, 72.7, 72.5, 72.3, 71.0, 68.6, 67.4, 67.3, 61.1, 61.0, 60.1, 55.1 ($C\text{-}2^{I\text{-}IV}$-$6^{I\text{-}IV}$, $OCH_2CH_2CH_2N_3$), 47.8 ($OCH_2CH_2CH_2N_3$), 28.1 ($OCH_2CH_2CH_2N_3$), and 22.2 ($NC(O)CH_3$). HR-MS for $C_{29}H_{50}N_4O_{21}$: Calcd. 813.2860 $[M + Na]^+$. Found 813.2754 $[M + Na]^+$ ± 13 ppm.

This material (40 mg, 51 μmol) was dissolved in water/MeOH (1:1, v/v) and 2 M HCl (1 equiv., 30 μL), and a catalytic amount Pd/C was added. The reaction mixture was stirred under a hydrogen atmosphere at room temperature. When complete conversion had taken place, as indicated by MALDI-Tof, the catalyst was removed by filtration over a filter sandwich. The solvents were then removed by evaporation. The residue was dissolved in water (2 mL), and freeze-dried to obtain compound **6** (36 mg, 45 μmol, 89%).

^1H NMR (D_2O) δ 4.41-4.33 (m, 3H, 3xH-1); 4.29 (d, 1H, J = 7.8 Hz, H-1); 4.14 (d, 1H, J = 9.0 Hz); 3.88-3.77 (m, 3H); 3.76 (sb, 2H); 3.72-3.47 (m, 15H), 3.47-3.42 (m, 1H); 3.41-3.35

(m, 2H); 3.25-3.18 (m, 1H), 2.92 (t, 2H, J = 6.8 Hz, $OCH_2CH_2CH_2NH_2$), 1.88 (s, 3H, NAc); 1.78 (dt, 2H, J = 13.0 Hz, $OCH_2CH_2CH_2NH_2$). ^{13}C NMR (D_2O) δ 174.7 ($NC(O)CH_3$), 103.0, 102.8, 102.4, 101.3 (C-1^{I-IV}), 78.4, 77.7, 75.4, 75.3, 74.7, 74.3, 73.4, 72.7, 72.5, 72.1, 71.0, 68.6, 68.1, 61.0, 61.0, 55.1 (C-2^{I-IV}-6^{I-IV}, $OCH_2CH_2CH_2NH_2$), 37.7 ($OCH_2CH_2CH_2NH_2$), 26.6 ($OCH_2CH_2CH_2NH_2$), and 22.1 ($NC(O)CH_3$). HR-MS for $C_{29}H_{52}N_2O_{21}$: Calcd. 787.2955 $[M + Na]^+$. Found 787.3105 $[M + Na]^+$ ± 19 ppm.

S-Acetylated tetrasaccharide conjugate **8**. A solution of isothiocyanate linker **7** [lviiS] (12.1 mg, 26.1 μmol, 1.8 equiv.) in H_2O-^{i}PrOH-CH_3CN (1:1:1, v/v/v, 0.6 mL) was added to a solution of 3-aminopropyl tetrasaccharide **6** (11.62 mg, 14.5 μmol, 1 equiv.) in H_2O-^{i}PrOH-CH_3CN (1:1:1, v/v/v, 1.8 mL) and the pH was set to basic by addition of triethylamine (18 μL, 130 μmol, 9 equiv.). The mixture was stirred at room temperature for 17 h and then evaporated. The crude material was kept in high vacuum to remove the residual triethylamine and then triturated with Et_2O (4 x 2 mL) in order to get rid of the excess of the linker. The insoluble solid was purified by Sephadex LH-20 chromatography (column: diameter = 2 cm; height = 45 cm) using as eluent MeOH/H_2O = 9/1 to afford the *S*-protected tetrasaccharide conjugate **8** as a white solid after lyophilization (12.6 mg, 10.3 μmol, 71%).

^1H NMR (D_2O) δ 4.61-4.52 (m, 3H, 3xH-1); 4.48 (br d, 1H, J = 7.6 Hz, H-1); 4.31 (d, 1H, J = 10.2 Hz); 4.03-3.60 (m, 40H); 3.57 (m, 2H, 2xH-2); 3.50 (br t, 2H, J = 6.0 Hz, $OCH_2CH_2CH_2$); 3.41 (br t, 1H, J = 7.6 Hz, H-2); 2.88 (t, 2H, J = 7.1 Hz, CH_2SAc); 2.35 (s, 3H, SAc), 2.07 and 2.06 (s, 3H, NAc); 1.91-1.82 (m, 2H, $OCH_2CH_2CH_2N$); 1.65-1.53 (m, 4H, CH_2CH_2SAc and $OCH_2CH_2CH_2$); 1.44-1.26 (m, 14H, $(CH_2)_7$). ^{13}C NMR (D_2O) δ 102.9 (d, 2C, C-1); 102.4 (d, 1C, C-1); 101.1 (d, 1C, C-1); 78.4; 77.8; 75.3; 74.7; 74.2; 73.4; 72.7; 72.6 (d, 1C, C-2); 72.5; 72.3; 71.0 (t, 1C, $OCH_2CH_2CH_2$); 70.9 (d, 2C, 2xC-2); 70.3; 70.0; 69.8; 69.7; 68.6; 67.3; 67.2 (d, 1C); 61.0; 60.9; 60.2; 43.7 (br t; CH_2NH); 30.2 (q, 1C,

SC(O)CH_3); 29.7-29.0 and 25.8 (t, 9C, $(CH_2)_9$); 28.8 (t, 1C, CH_2SAc); 28.3 (t, 1C, $OCH_2CH_2CH_2N$); 22.2 (q, 1C, NC(O)CH_3); *C*=S and C=O undetected. IR (KBr): $\tilde{\nu}$ 3424 (broad), 2925, 2850, 1745, 1655, 1374, 1232, 1068 cm^{-1}. HR-MS for $C_{51}H_{93}N_3O_{26}S_2$: Calcd. 1250.5381 $[M+Na]^+$, 1228.5561 $[M+H]^+$. Found 1250.5468 $[M + Na]^+ \pm 6.9$ ppm, 1228.5591 $[M + H]^+ \pm 2.4$ ppm. $[\alpha]^{29}_D = -8.1$ (c = 0.4; H_2O).

Branched tetrasaccharide conjugate **1**. Sodium methoxide (0.5 mg, 9.2 μmol, 1 equiv.) was added to a solution of compound **8** (11.28 mg, 9.2 μmol, 1 equiv.) in MeOH (5 mL). The mixture was stirred at room temperature for 4 hours and then evaporated. The crude material was concentrated and purified by Sephadex LH-20 chromatography (column: diameter = 2 cm; height = 45 cm) using as eluent MeOH/ H_2O = 9/1 to afford the tetrasaccharide conjugate **1** (~2.5:1 mixture of disulfide and thiol) as a white solid after lyophilisation (8.8 mg, 7.4 μmol (considered as thiol), 81%).

^{1}H NMR (D_2O) δ 4.60-4.52 (m, 3H, 3xH-1); 4.48 (br d, 1H, H-1, *J* = 7.3 Hz); 4.30 (br d, 1H, *J* = 9.9 Hz); 4.03-3.59 (m, 40H); 3.57 (m, 2H, 2xH-2); 3.53-3.46 (m, 2H, $OCH_2CH_2CH_2$); 3.42 (br t, 1H, *J* = 7.6 Hz, H-2); 2.76-2.68 (br signal, ~1.4H, CH_2SS); 2.57-2.51 (br signal, ~0.6H, CH_2SH); 2.07 and 2.05 (s, 3H, NAc) 1.90-1.82 (m, 2H, $OCH_2CH_2CH_2N$); 1.77-1.68 (m, 1.5H, CH_2CH_2SS); 1.65-1.55 (m, 2.5H, CH_2CH_2SH and $OCH_2CH_2CH_2$); 1.50-1.22 (m, 14H, $(CH_2)_7$). ^{13}C NMR (D_2O) δ 103.0 (d, 1C, C-1); 102.8 (d, 2C, C-1); 101.2 (d, 1C, C-1); 78.6; 77.8; 75.3; 74.7; 74.2; 72.5 (d, 1C, C-2); 72.3; 71.1 (t, 1C, $OCH_2CH_2CH_2$); 71.0; 70.9 (d, 2C, 2xC-2); 70.0; 68.4; 67.3 (d, 1C); 67.2; 61.0; 60.1; 43.7 (br t; CH_2NH); 38.8 (t, ~0.7C, CH_2SS); 24.4 (t, ~0.3C, CH_2SH); 29.1 (t, 2C, CH_2CH_2S and $OCH_2CH_2CH_2$); 29.7-28.8 and 25.9 (t, 9C, $(CH_2)_9$); 28.2 (t, 1C, $OCH_2CH_2CH_2N$); 22.3 (q, 1C, NC(O)CH_3); *C*=S and *C*=O undetected. IR (KBr): $\tilde{\nu}$ 3369 (broad), 2925, 2854, 1654, 1564, 1381, 1075, 1047. HR-MS for $C_{49}H_{91}N_3O_{25}S_2$: Calcd. 1208.5275 $[M+Na]^+$. Found 1208.5261 $[M+Na]^+ \pm 1.2$ ppm.

Preparation and characterization of hybrid gold nanoparticles

GNP-1 (Tetra:Glc:OVA = 45:50:5). Two different batches (GNP-1 and GNP-1b) were prepared. OVA peptide conjugate **3** (0.34 mg, 0.18 μmol) (Figure S1 and Figure 1) was dissolved in CF_3COOD (50 μL) and dried under air stream until formation of an oil. Tetrasaccharide conjugate **1** (1.89 mg, 1.6 μmol) and glucose conjugate **2** (0.5 mg, 1.8 μmol) were then added and the mixture was dissolved in CD_3OD-D_2O (1:1, v/v, 600 μL). ^{1}H NMR analysis of the mixture showed a **1**:**2**:**3** ratio of ~9:10:1 (Figure S3). After evaporation of the solvent, MeOH was added up to a 0.012 M concentration of organic material, and the pH was adjusted to 1 by addition of CF_3COOH. An aqueous solution of $HAuCl_4$ (28.3 μL, 0.025 M) was then added, followed by an aqueous $NaBH_4$ solution (15 μL, 1 M) under rapid shaking. The black suspension was shaken for 2 h, and the supernatant was separated by decantation. The black solid was washed with EtOH (4 x 1 mL) and MeOH (3 x 1 mL), dissolved in Nanopure water (0.5 mL) and purified by centrifugal filtering (AMICON MWCO 10.000, 50 min, 10.000 rpm). The residue in the AMICON filter was dissolved in 0.5 mL of Nanopure water and lyophilized to afford 0.7 mg of GNP-1.

UV/Vis (H_2O, 0.1 mg/mL): surface plasmon band not observed. TEM: average gold diameter 1.8 ± 0.5 nm (Figure S9). Average molecular formula estimated based on the size of the cluster obtained from the TEM micrographs: $Au_{201}(C_{49}H_{90}N_3O_{25}S_2)_{32}(C_{11}H_{21}O_6S)_{35}(C_{79}H_{126}N_{27}O_{27}S)_4$ (MW 95 KDa). ^{1}H NMR (500 MHz, D_2O) and IR (KBr): Figure S3 and Figure S8.

GNP-2 (Tetra:Glc = 50:50). Tetrasaccharide conjugate **1** (4.6 mg, 3.9 μmol) and glucose conjugate **2** (1.1 mg, 3.9 μmol) were dissolved in D_2O (656 μL). ^{1}H NMR analysis of the mixture showed a ~1:1 ratio of **1** and **2** (Figure S4). After evaporation of the solvent,

MeOH was added up to a 0.012 M concentration of organic material. Next, an aqueous solution of $HAuCl_4$ (62.8 μL, 0.025 M) was added, followed by an aqueous $NaBH_4$ solution (33 μL, 1 M) under rapid shaking. The black suspension was shaken for 2 h, and then the supernatant was separated by decantation. The black solid was washed with EtOH (4 x 1 mL) and MeOH (3 x 1 mL), dissolved in Nanopure water (0.5 mL) and purified by centrifugal filtering (AMICON MWCO 10.000, 50 min, 10.000 rpm). The residue in the AMICON filter was dissolved in 0.5 mL of Nanopure water and lyophilized to afford 0.86 mg of GNP-2. UV/Vis (H_2O, 0.1 mg/mL): surface plasmon band not observed. TEM: average gold diameter 1.9 ± 0.3 nm (Figure S9). Average molecular formula: $Au_{225}(C_{49}H_{90}N_3O_{25}S_2)_{36}(C_{11}H_{21}O_6S)_{35}$ (97 KDa). ^1H NMR (500 MHz, D_2O): Figure S4.

GNP-3 (Glc:OVA = 90:10). OVA peptide derivative **3** (1.68 mg, 0.87 μmol) was dissolved in CF_3COOD (100 μL) and dried under air stream until formation of an oil. Glucose conjugate **2** (2.2 mg, 7.8 μmol) was then added and the mixture was dissolved in CD_3OD-D_2O (1:1) (600 μL). ^1H NMR analysis of the mixture showed a compound **2**:**3** ratio of ~9:1 (Figure S5). After evaporation of the solvent, MeOH was added up to a 0.012 M concentration of organic material. An aqueous solution of $HAuCl_4$ (70 μL, 0.025 M) was added, followed by an aqueous $NaBH_4$ solution (37 μL, 1 M) under rapid shaking. The black suspension was shaken for 2 h, and then the supernatant was separated by decantation. The black solid was washed with EtOH (4 x 1 mL) and MeOH (3 x 1 mL), dissolved in Nanopure water (3 mL) and purified by dialysis (Slide-A-Lyzer Dialysis cassette, Pierce, 10.000 MWCO) against 3 L of distilled water, recharging with fresh distilled water every 3–4 h over the course of 72 h. The solution in the membrane was then lyophilized to regain 0.60 mg of GNP-3.

UV/Vis (H_2O, 0.1 mg/mL): surface plasmon band not observed. TEM: average gold diameter 1.9 ± 0.5 nm (Figure S9). Average molecular formula: $Au_{225}(C_{11}H_{21}O_6S)_{64}(C_{79}H_{126}N_{27}O_{27}S)_7$ (76 KDa). ^1H NMR (500 MHz, D_2O) and IR (KBr): Figure S5 and Figure S7.

GNP-4 (Tetra:Glc:OVA = 20:70:10). OVA peptide derivative **3** (0.38 mg, 0.20 μmol) was dissolved in CF_3COOD (50 μL) and dried under air stream until formation of an oil. Tetrasaccharide conjugate **1** (0.48 mg, 0.40 μmol) and glucose conjugate **3** (0.395 mg, 1.4 μmol) were added to the oil, and the mixture was dissolved in CD_3OD (600 μL). ^1H NMR analysis of the mixture showed a compound **1**:**2**:**3** ratio of ~2:7:1 (Figure S6). After evaporation of the solvent, MeOH was added up to a 0.012 M concentration of organic material, and the pH was adjusted to 1 by addition of CF_3COOH. An aqueous solution of $HAuCl_4$ (16 μL, 0.025 M) was added, followed by an aqueous $NaBH_4$ solution (9 μL, 1 M) under rapid shaking. The black suspension was shaken for 2 h, and then the supernatant was separated by decantation. The black solid was washed with EtOH (4 x 1 mL) and MeOH (3 x 1 mL), dissolved in Nanopure water (0.5 mL) and purified by centrifugal filtering (AMICON MWCO 10.000, 50 min., 10.000 rpm). The residue in the AMICON filter was dissolved in 0.5 mL of water and lyophilized to afford 0.8 mg of GNP-4.

UV/Vis (H_2O, 0.1 mg/mL): surface plasmon band not observed. TEM: average gold diameter 1.7 ± 0.7 nm (Figure S9). Average molecular formula: $Au_{201}(C_{49}H_{90}N_3O_{25}S_2)_{14}(C_{11}H_{21}O_6S)_{50}$-$(C_{79}H_{126}N_{27}O_{27}S)_7$ (84 KDa). ^1H NMR (500 MHz, D_2O): Figure S6.

Detection of type-specific antibodies by ELISA

The enzyme-linked immunosorbent assay (ELISA) was performed to measure the antibodies to native Pn14PS, to the synthetic branched tetrasaccharide structure Gal-Glc-(Gal-)GlcNAc-Gal (one repeating unit of Pn14PS with extra one galactose residue), and to ovalbumin, as described previously [[lix]]. Briefly, serially diluted sera were incubated for 1 h at 37 °C in flat-bottom plates (Corning, Inc., Corning, NY), coated with native Pn14PS (0.3 μg/mL), Gal-Glc-(Gal-)GlcNAc-Gal conjugated to bovine serum albumin (BSA) (1 μg/mL), or ovalbumin protein (1 μg/mL). After coating the plates were blocked with 3% gelatin, then washed, and horseradish peroxidase-conjugated goat anti-mouse IgG (Nordic Immunology Laboratories, Tilburg, The Netherlands) was added and incubated for 1 h at 37 °C. Then, a mixture of 3,3',5,5'-tetramethylbenzidine (Sigma Chemical Co., St. Louis, MO) and H_2O_2 (Sigma Chemical Co.) was added to visualize the amount of bound peroxidase. The reaction was stopped by the addition of 0.5 M H_2SO_4. Optical density (OD) values were obtained with a micro-titer plate spectrophotometer at 450 nm (Bio-Rad, model 3550 UV; Bio-Rad Laboratories, Hercules, CA). Antibody titers were expressed as the $\log_{10}$ of the dilution giving twice the OD obtained for control mice (immunized with saline) with a cut-off value of 0.2.

Measurement of phagocytosis titer

The opsonophagocytosis assay was performed by using human polymorphonuclear leukocytes (PMN cells) isolated from peripheral blood of healthy donors, as previously described [lix, [lx]]. Twofold dilutions of heat-inactivated pooled sera in Hank's balanced salt solution-1% BSA were mixed with 2% complement (guinea-pig serum) in round-bottom plates (Greiner Bio-One, Frickenhausen, Germany). The assay was performed by mixing 20 μL of PMN cells (3×10^6 cells/mL) and 20 μL of heat-killed fluorescein isothiocyanate (FITC)-labeled *S. pneumoniae* type 14 (ATTC 634; 3×10^7 cells/mL), followed by incubation at 37 °C under vigorous shaking at 900 rpm for 50 min. The mixtures were then fixed with cold 2% paraformaldehyde and analyzed in a flow cytometer (FACS Calibur; Becton Dickinson, Mountain View, CA). The percentage of FITC-positive PMN cells was used as a measure of the phagocytic activity and corrected by using the values found in the mixtures without sera. The phagocytosis titers are expressed as the $\log_{10}$ of the serum dilution during phagocytosis that resulted in 25% of the PMN cells being positive for FITC.

Illustrations and Tables

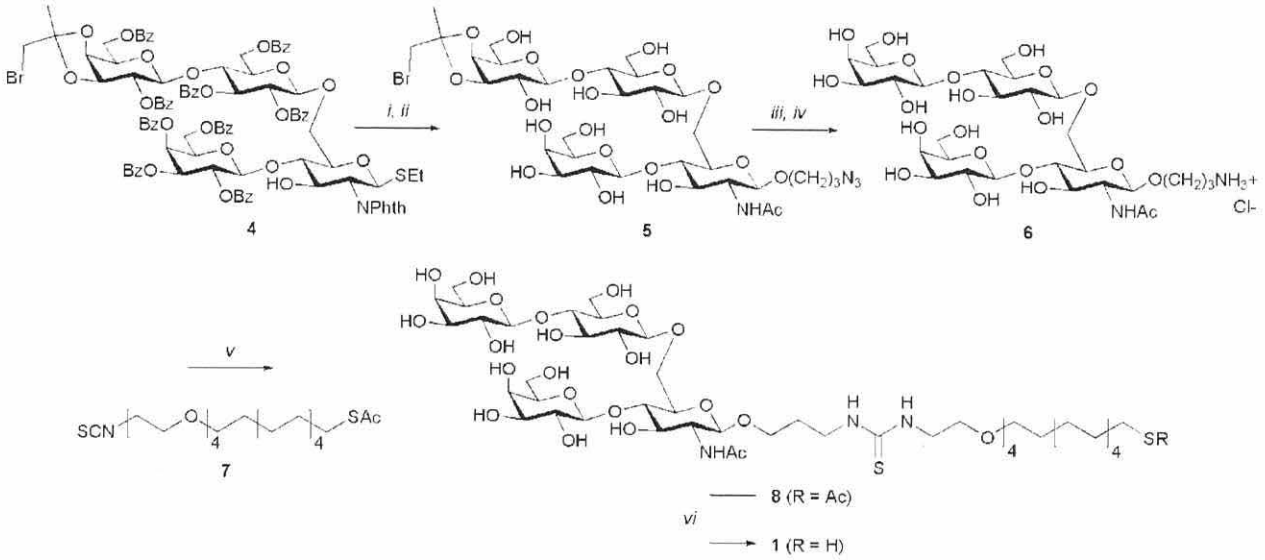

Scheme S1. Synthesis of tetrasaccharide conjugate **1**. Reagents and conditions: *i)* 3-azidopropanol, NIS/AgOTf (cat.), DCM, 90%; *ii)* 1. ethylenediamine, EtOH; 2. Ac_2O, MeOH; 3. NaOMe, MeOH; (74 % over three steps); *iii)* 90% TFA, 96%; *iv)* H_2, Pd/C, MeOH/H_2O (1:1, v/v), 89%; *v)* NEt_3, H_2O/^{i}PrOH/CH_3CN, (1:1:1, v/v/v), 17 h, 25 °C, 71%; *vi)* MeONa/MeOH, 4 h, 25 °C, 81%. For clarity reasons, tetrasaccharide conjugate **1** is depicted as thiol.

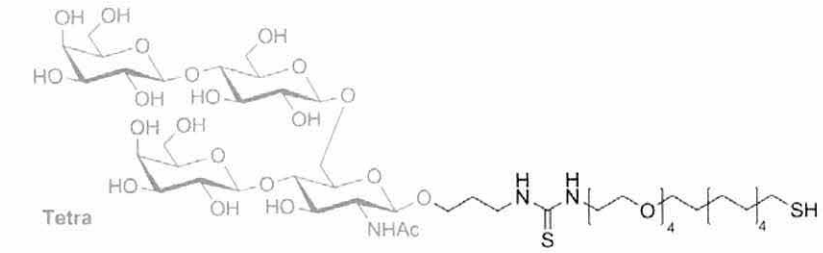

Gal(β1-4)Glc(β1-6)[Gal(β1-4)]GlcNAc(β1-O)$(CH_2)_3$NH(CS)NH-TEG-C_{11}-SH

1

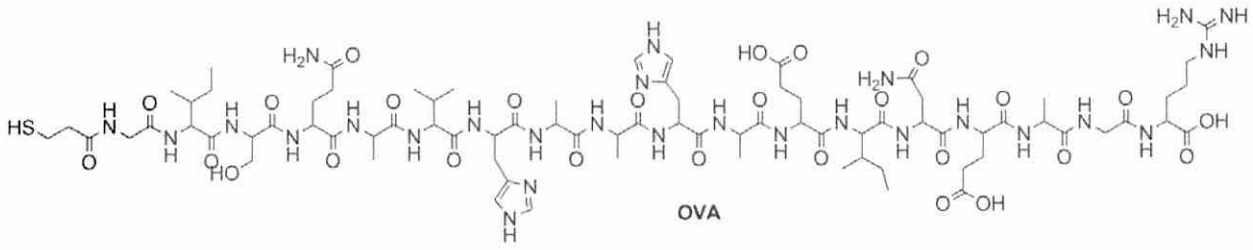

HS$(CH_2)_2$C(O)GISQAVHAAHAEINEAGR ({MPA}GlyOVA$_{323-339}$)

3

Figure S1. Conjugates used for the preparation of GNPs. Tetrasaccharide (Tetra) β-D-Gal*p*-(1→4)-β-D-Glc*p*-(1→6)-[β-D-Gal*p*-(1→4)-]β-D-Glc*p*NAc (Gal-Glc-(Gal-)GlcNAc) conjugate **1**, D-glucose (Glc) conjugate **2**, and $OVA_{323-339}$ peptide (OVA) conjugate **3**. For clarity reasons, all conjugates are depicted as thiols.

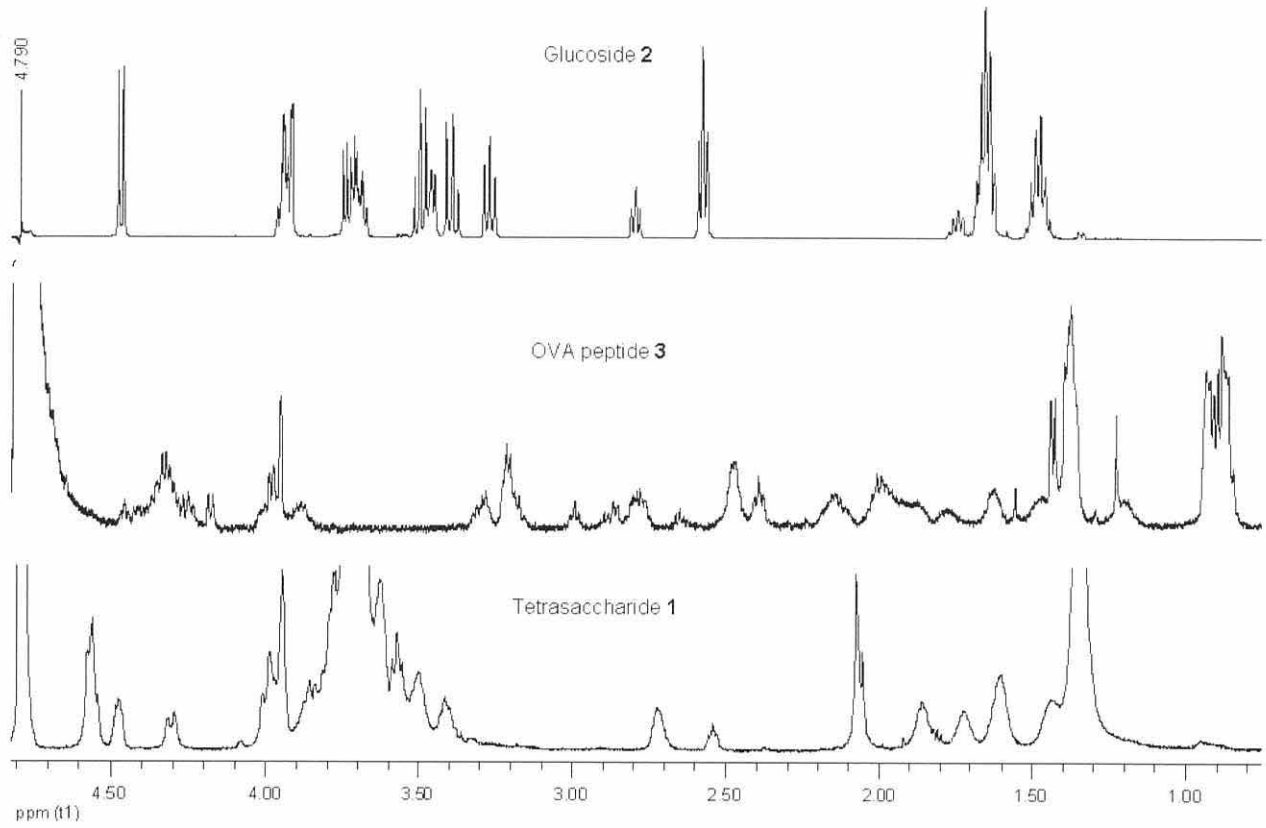

Figure S2. ^{1}H NMR spectra of conjugates **1**, **2**, and **3**. From top to bottom: ^{1}H NMR (500 MHz, D_2O) of D-glucose conjugate **2** (water suppression), $OVA_{323-339}$ peptide derivative **3** (His signals out of scale), and tetrasaccharide conjugate **1**.

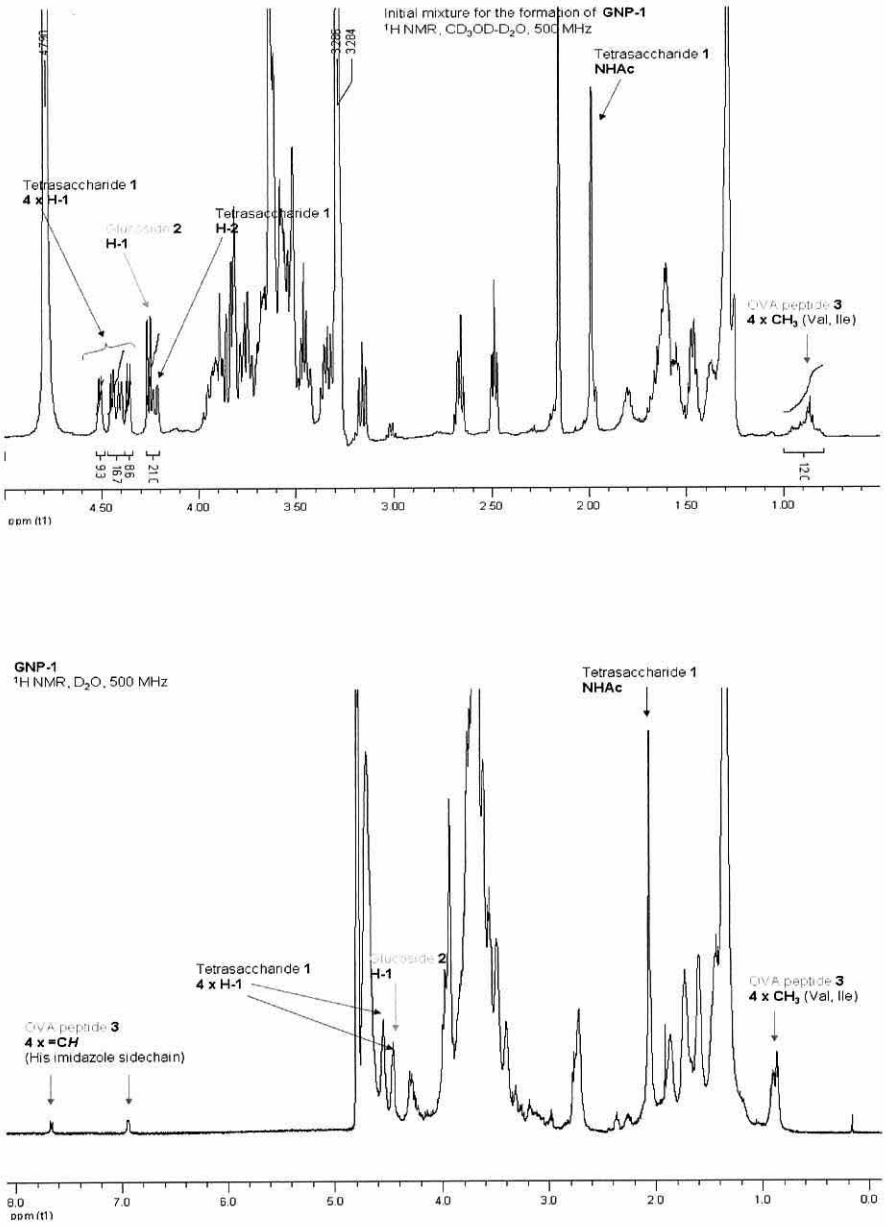

Figure S3. *Top panel*: ^{1}H NMR (500 MHz, CD_3OD:D_2O = 1:1) of the mixture used to prepare GNP-1. Integration of selected signals shows that the ratio between tetrasaccharide **1**, glucose conjugate **2**, and OVA peptide conjugate **3** is about 9:10:1. *Bottom panel*: ^{1}H NMR (500 MHz, D_2O, water suppression) of GNP-1. The selected signals show the presence of all three components (tetrasaccharide **1**, glucose conjugate **2**, and OVA peptide derivative **3**) in the same nanoparticle.

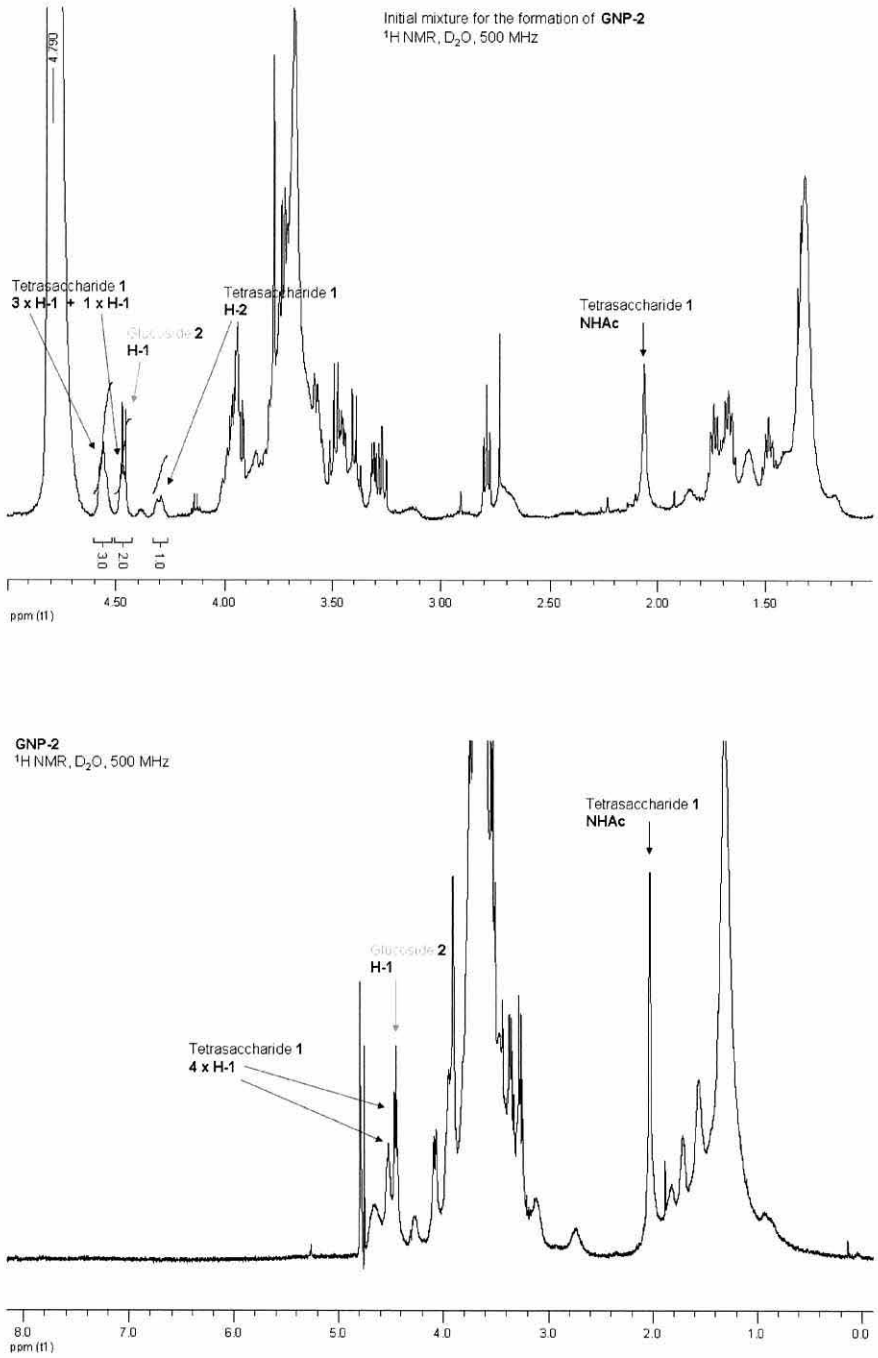

Figure S4. *Top panel*: ^{1}H NMR (500 MHz, D_2O) of the mixture used to prepare GNP-2. Integration of selected signals shows that the ratio between tetrasaccharide **1** and glucose conjugate **2** is about 1:1. *Bottom panel*: ^{1}H NMR (500 MHz, D_2O, water suppression) of GNP-2. The selected signals show the presence of both tetrasaccharide **1** and glucose conjugate **2** in the same nanoparticle.

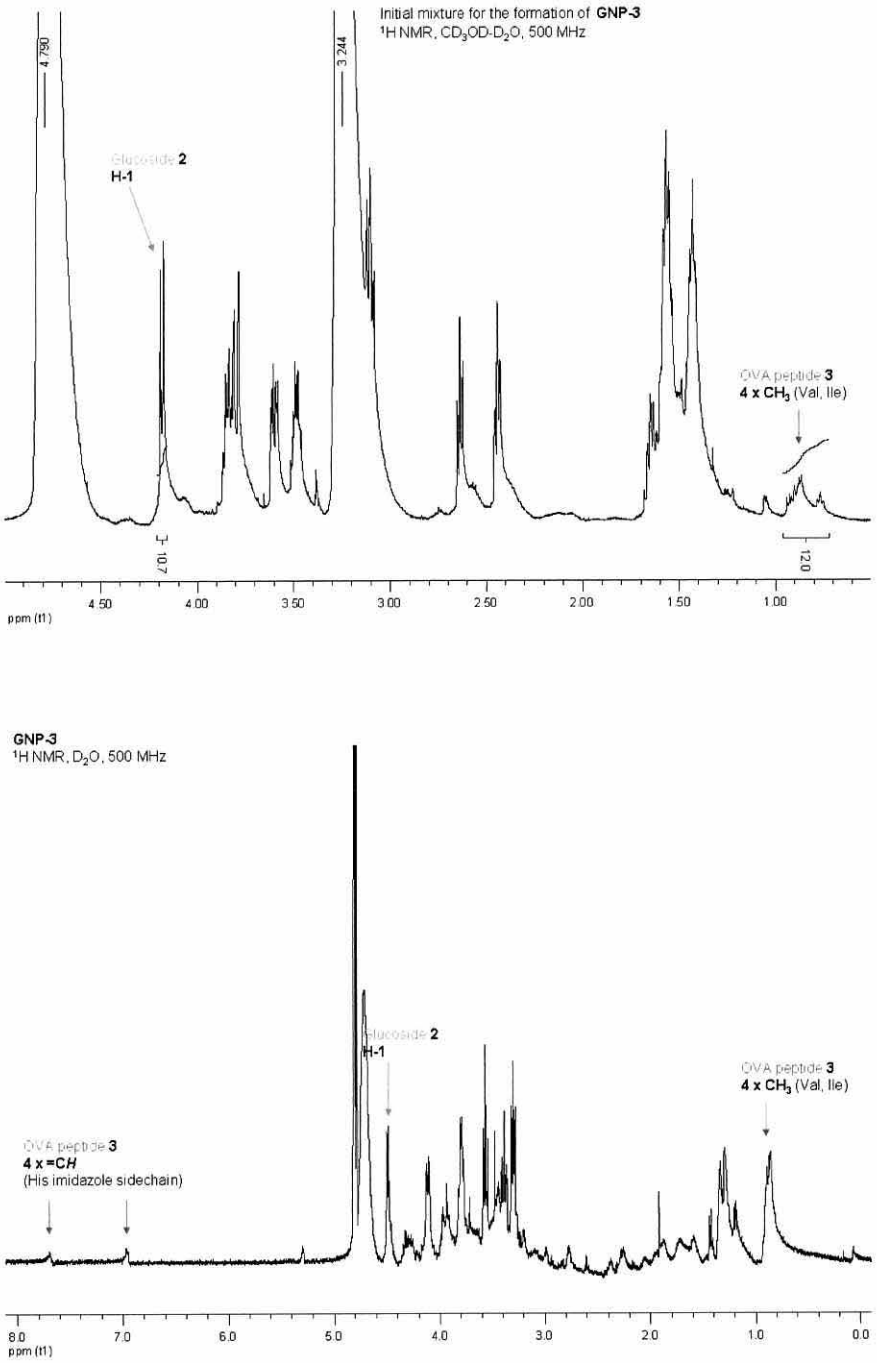

Figure S5. *Top panel*: ^{1}H NMR (500 MHz, CD_3OD:D_2O = 1:1) of the mixture used to prepare GNP-3**.** Integration of selected signals shows that the ratio between glucose conjugate **2** and OVA peptide derivative **3** is about 9:1. *Bottom panel*: ^{1}H NMR (500 MHz, D_2O, water suppression) of GNP-3. The selected signals show the presence of both glucose conjugate **2** and OVA peptide derivative **3** in the same nanoparticle.

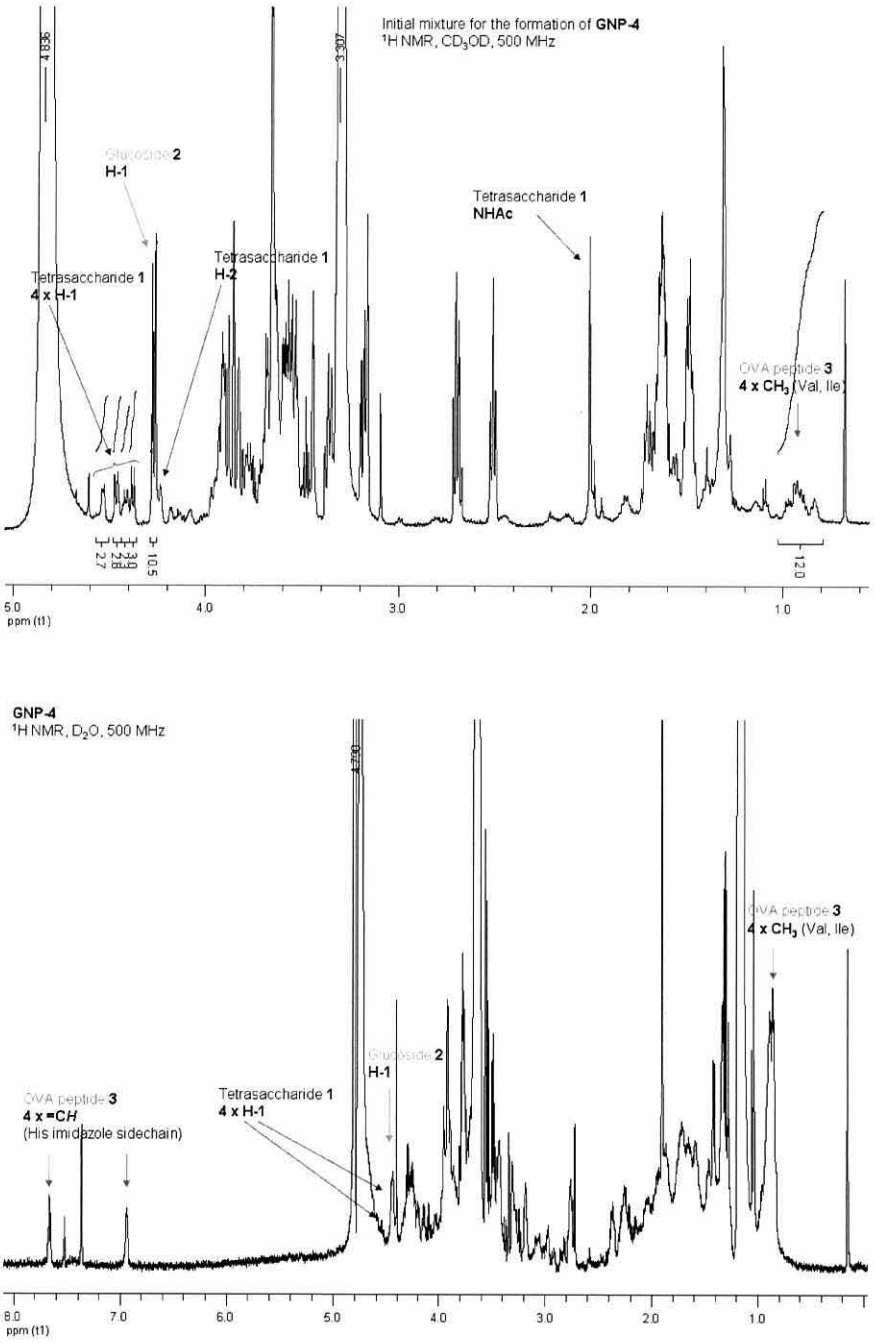

Figure S6. *Top panel*: ^{1}H NMR (500 MHz, CD_3OD) of the mixture used to prepare GNP-4. Integration of selected signals shows that the ratio between tetrasaccharide **1**, glucose conjugate **2**, and OVA peptide derivative **3** is about 2:7:1. *Bottom panel*: ^{1}H NMR (500 MHz, D_2O, water suppression) of GNP-4. The selected signals show the presence of all three components (tetrasaccharide **1**, glucose conjugate **2**, and OVA peptide derivative **3**) in the same nanoparticle.

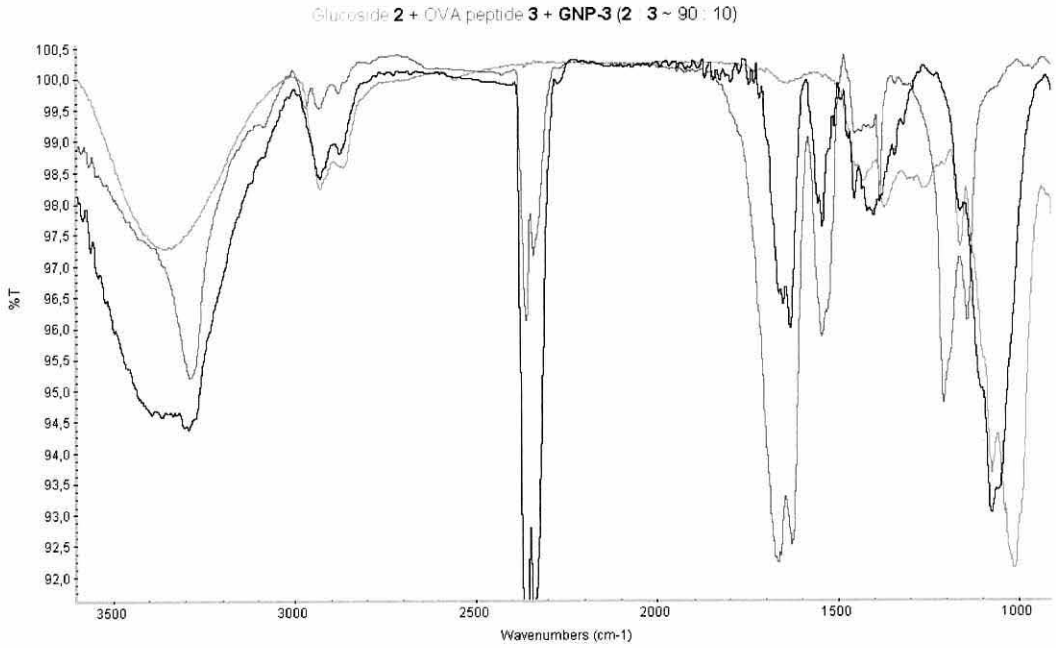

Figure S7. Infrared spectra of gold glyconanoparticle GNP-3. Infrared (IR) spectra of GNP-3 (black) and its free components glucoside **2** (red) and OVA peptide conjugate **3** (blue), obtained after pressing each compound into KBr pellets. The bands around 1650 cm^{-1} which are present in the spectrum of GNP-3, and absent in the glucoside **2**, indicate the incorporation of the OVA peptide conjugate **3** into GNP-3.

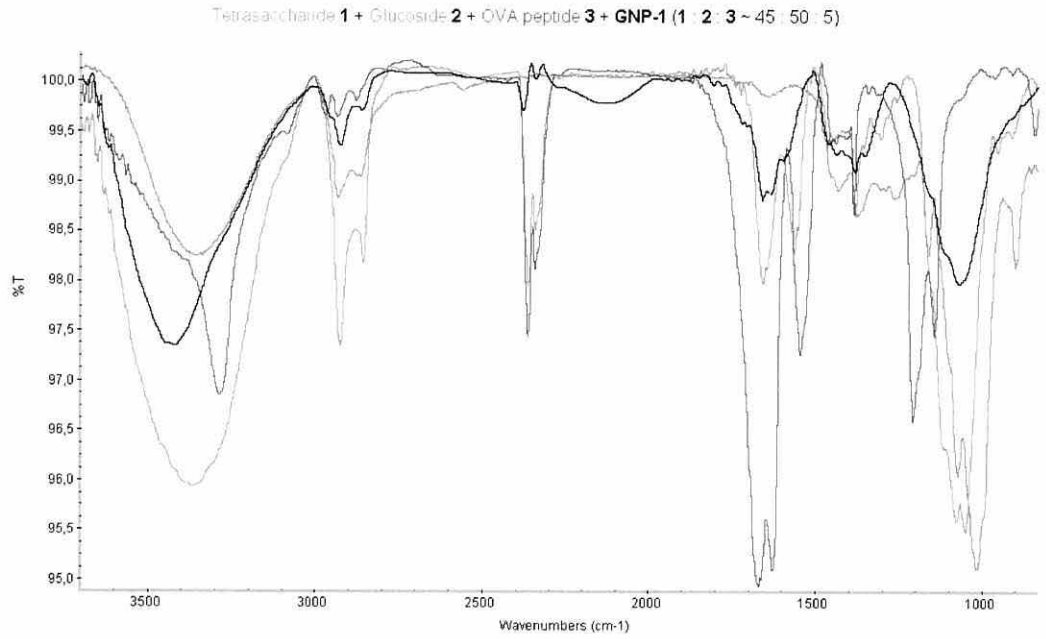

Figure S8. Infrared spectra of gold glyconanoparticle GNP-1. Infrared (IR) spectra of GNP-1 (black) and its free components tetrasaccharide **1** (magenta), glucoside **2** (red) and OVA peptide conjugate **3** (blue), obtained after pressing each compound into KBr pellets.

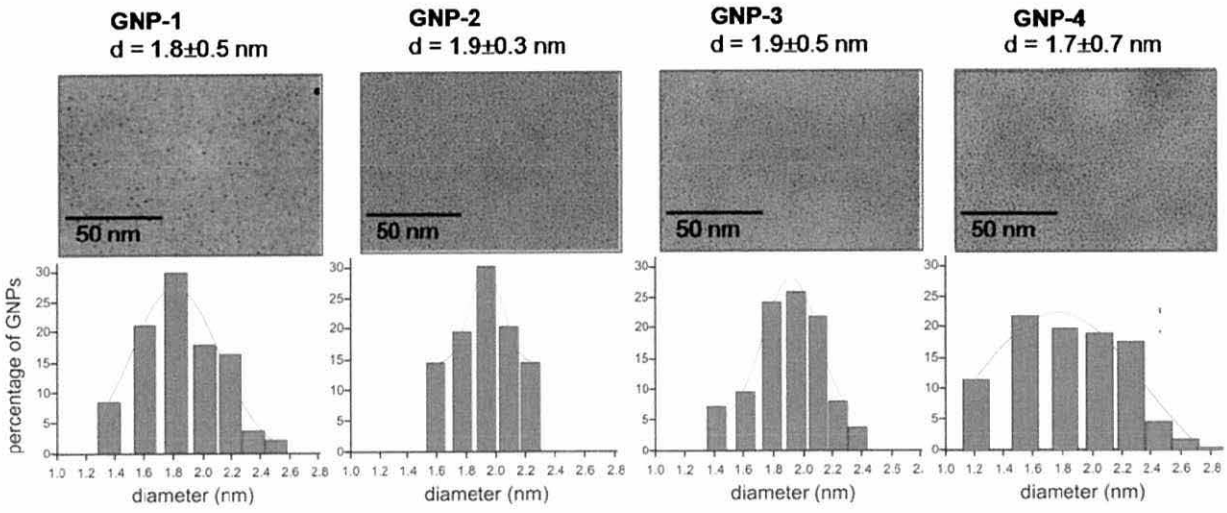

Figure S9. TEM micrographs and histograms of size distribution of gold GNPs.

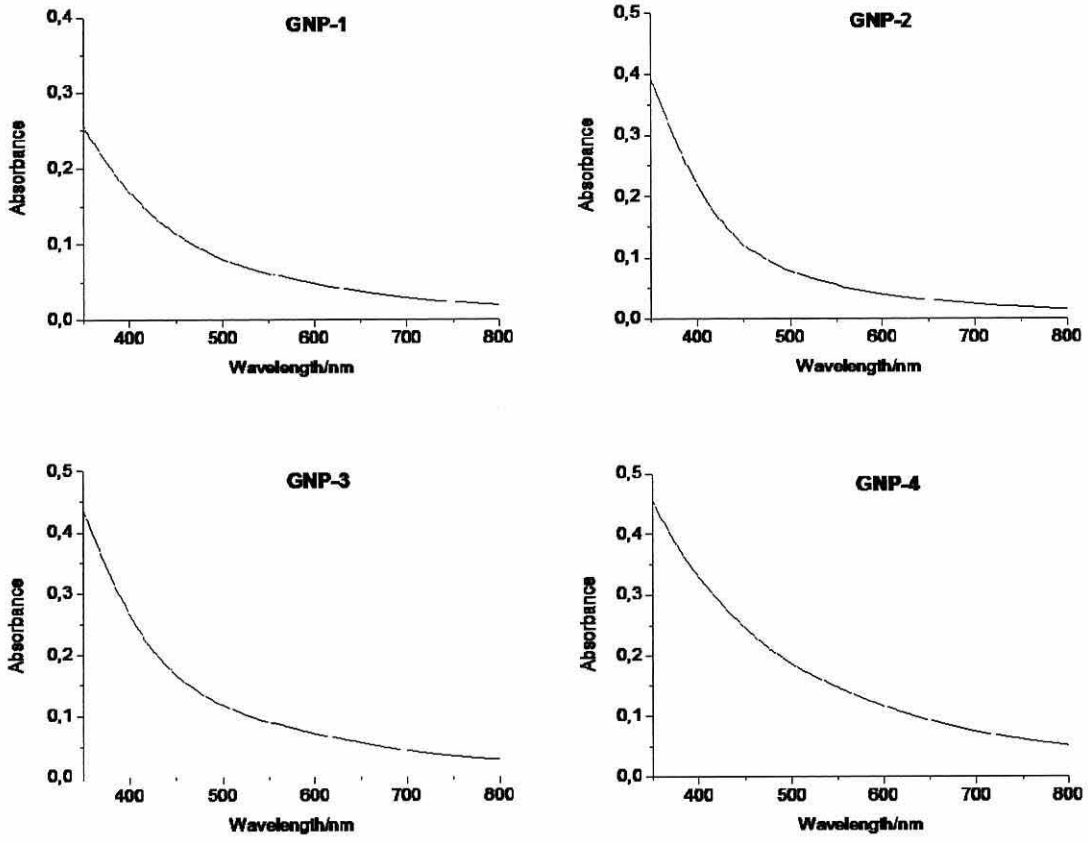

Figure S10. UV-visible adsorption spectra of gold GNPs at 0.1 mg/mL.

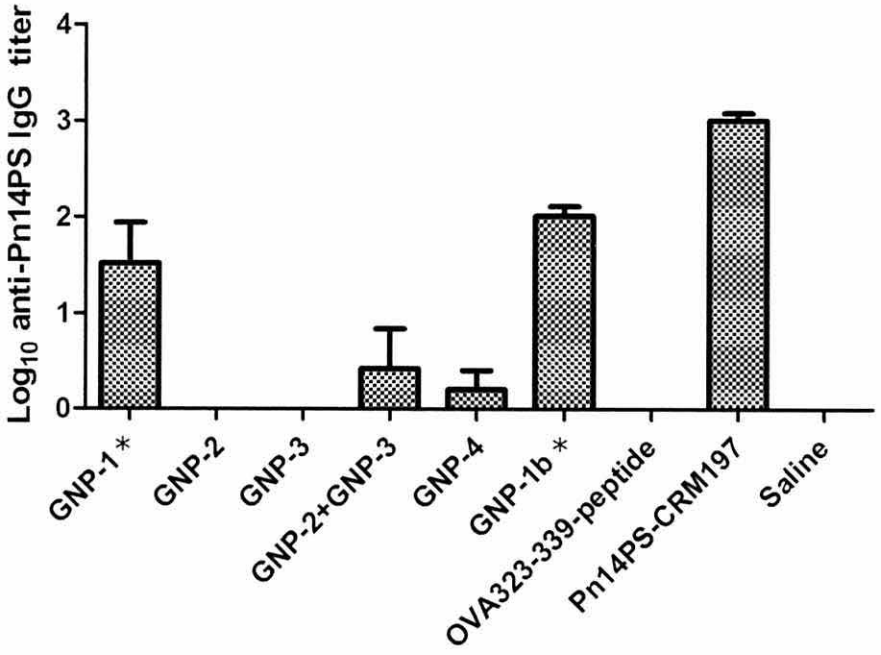

Figure S11. Specific anti-*S. pneumoniae* type 14 polysaccharide (Pn14PS) IgG antibodies determined by ELISA. Mice were immunized intracutaneously with GNPs co-administered with a mixture of MPL (Monophosphoryl lipid A) and Quil-A adjuvants. Sera were collected two weeks after the second booster injection without adjuvants. For more details, see Table S1. ELISA was performed using Pn14PS as coating material. The level of antibodies is expressed as the $\log_{10}$ of the dilution giving twice the OD obtained for control mice (immunized with saline). Pn14PS-CRM_{197} and saline buffer immunization served as positive and negative control respectively.

* GNP-1 and GNP-1b (same nanoparticle, different batches) induced significant immune responses: The higher titer of antibodies elicited by GNP-1b is reasonable as a higher dosage of GNP-1b (30 μg) in the boosters' administration was used with respect to GNP-1.

Table S1. Mouse immunization studies

Compound	Number of mice	Primary immunization		Approximately quantity of GNPs components[a]		Booster (no adjuvant)
		Adjuvant	Compound (μg)	Tetrasaccharide (μg)	$OVA_{323-339}$-peptide (μg)	Compound (μg)
GNP-1	5	MPL+Quil-A	6	2.4±0.2	0.48±0.08	6
GNP-2	4	MPL+Quil-A	6	2.6±0.2	-	6
GNP-3	4	MPL+Quil-A	6	-	1.1±0.2	6
GNP-2 + GNP-3	5	MPL+Quil-A	6+6	2.6±0.2	1.1±0.2	6+6
GNP-4	5	MPL+Quil-A	12	2.4±0.4	1.9±0.2	30
GNP-1b	5	MPL+Quil-A	6	2.4±0.2	0.48±0.08	30
Pn14PS-CRM_{197}	5	MPL+Quil-A	0.5[b]	-	-	2.5[b]
$OVA_{323-339}$-peptide	5	MPL+Quil-A	2.5	-	-	12.5
$OVA_{323-339}$-peptide-CRM_{197}	5	MPL+Quil-A	50[c]	-	-	50[c]
Saline	5	No	-	-	-	No

[a] Based on molar ratio of ligands of GNPs (Table 1)

[b] Dose of Pn14PS-CRM_{197} is based on carbohydrate part

[c] Dose of $OVA_{323-339}$-peptide-CRM_{197} immunization is based on the complete conjugate

Bibliography

[i]. Astronomo RD, Burton DR: Carbohydrate vaccines: Developing sweet solutions to sticky situations? *Nat. Rev. Drug Discov.* 9, 308–324 (2010).

[ii]. Kalka-Moll WM, Tzianabos AO, Bryant PW, Niemayer M, Ploegh HL, Kasper DL: Zwitterionic polysaccharides stimulate T cells by MHL class II-dependent interactions. *J. Immunol.* 169, 6149–6153 (2002).

[iii]. Avci FY, Kasper DL: How Bacterial Carbohydrates Influence the Adaptive Immune System. *Annu. Rev. Immunol.* 28, 107–130 (2010).

[iv]. Pena Icart L, Fernández-Santana V, Veloso RC *et al.*: Protective immunity of pneumococcal glycoconjugates. In: *Carbohydrate-Based Vaccines (Volume 989).* René Roy (Ed.), ACS Symposium Series, American Chemical Society, Washington, DC, USA, 1–19 (2008).

[v]. Schofield L, Hewitt MC, Evans K, Siomos MA, Seeberger PH: Synthetic GPI as a candidate anti-toxic vaccine in a model of malaria. *Nature* 418, 785–789 (2002).

[vi]. Slovin SF, Ragupathi G, Adluri S *et al.*: Carbohydrate vaccines in cancer: Immunogenicity of a fully synthetic globo H hexasaccharide conjugate in man. *Proc. Natl. Acad. Sci. USA* 96, 5710–5715 (1999).

[vii]. Whitney CG, Farley MM, Hadler J *et al.*: Decline in invasive pneumococcal disease after the introduction of protein-polysaccharide conjugate vaccine. *New Engl. J. Med.* 348, 1737–1746 (2003).

[viii]. Verez-Bencomo V, Fernández-Santana V, Hardy E *et al.*: A synthetic conjugate polysaccharide vaccine against *Haemophilus influenzae* type b. *Science* 305, 522–525 (2004).

[ix]. Schutze MP, Leclerc C, Jolivet M, Audibert F, Chedid L: Carrier-induced epitopic suppression, a major issue for future synthetic vaccines. *J. Immunol.* 135, 2319–2322 (1985).

[x]. Stallforth P, Lepenies B, Adibekian A, Seeberger PH: Carbohydrates: a frontier in medicinal chemistry. *J. Med. Chem.* 52, 5561–5577 (2009).

[xi]. Keding SJ, Danishefsky S: Synthetic Carbohydrate-based Vaccines. In: *Carbohydrate-Based Drug Discovery.* Chi-Huey Wong (Ed.), Wiley-VCH Verlag, 381–406 (2003)

[xii]. Ingale S, Wolfert MA, Gaekwad J, Buskas T, Boons GJ: Robust immune responses elicited by a fully synthetic three-component vaccine. *Nat. Chem. Biol.* 3, 663–667 (2007).

[xiii]. Hassane FS, Phalipon A, Tanguy M *et al.*: Rational design and immunogenicity of liposome-based diepitope constructs: Application to synthetic oligosaccharides mimicking the *Shigella flexneri* 2a O-antigen. *Vaccine* 27, 5419–5426 (2009).

[xiv]. Wang SK, Liang PH, Astronomo RD, Hsu TL, *et al.*: Targeting the carbohydrates on HIV-1: Interaction of oligomannose dendrons with human monoclonal antibody 2G12 and DC-SIGN. *Proc. Natl. Acad. Sci. USA* 105, 3690–3695 (2008).

[xv]. Joyce JG, Krauss IJ, Song HC *et al.*: An oligosaccharide-based HIV-1 2G12 mimotope vaccine induces carbohydrate-specific antibodies that fail to neutralize HIV-1 virions. *Proc. Natl. Acad. Sci. USA* 105, 15684–15689. (2008).

[xvi]. Song EH, Osanya AO, Petersen CA, Pohl NL: Synthesis of multivalent tuberculosis and Leishmania-associated capping carbohydrates reveals structure-dependent responses allowing immune evasion. *J. Am. Chem. Soc.* 132, 11428–11430 (2010).

[xvii]. Fahmy TM, Demento SL, Caplan MJ, Mellman I, Saltzman WM: Design opportunities for actively targeted nanoparticle vaccines. *Nanomedicine* 3, 343–355 (2008).

[xviii]. Sarkar S, Lombardo SA, Herner DN, Talan RS, Wall KA, Sucheck SJ: Synthesis of single-molecules L-rhamnose-containing three-component vaccine and evaluation of antigenicity in the presence of anti-L-rhamnose antibodies. *J. Am. Chem. Soc.* 132, 17236–17246 (2010).

[xix]. Ojeda R, de Paz JL, Barrientos AG, Martín-Lomas M, Penadés S: Preparation of multifunctional glyconanoparticles as a platform for potential carbohydrate-based anticancer vaccines. *Carbohydr. Res.* 342, 448–459 (2007).

[xx]. Krishnamachari Y, Geary SM, Lemke CD, Salem AK: Nanoparticle delivery systems in cancer vaccines. *Pharm. Res.* 28, 215–236 (2011).

[xxi]. Yang NS, Burkholder J, Roberts B, Martinell B, McCabe D: *In vivo* and *in vitro* gene transfer to mammalian somatic cells by particle bombardment. *Proc. Natl. Acad. Sci. USA* 87, 9568–9572 (1990).

[xxii]. Roya MJ, Wua MS, Barra LJ *et al.*: Induction of antigen-specific CD8+ T cells, T helper cells, and protective levels of antibody in humans by particle-mediated administration of a hepatitis B virus DNA vaccine. *Vaccine* 19, 764–778 (2001).

[xxiii]. Drape RJ, Macklin MD, Barr LJ, Jones S, Haynes JR, Dean HJ: Epidermal DNA vaccine for influenza is immunogenic in humans. *Vaccine* 24, 4475–4481 (2006).

[xxiv]. Castillo PM, Herrera JL, Fernandez-Montesinos R *et al.*: Tiopronin monolayer-protected silver nanoparticles modulate IL-6 secretion mediated by Toll-like receptor ligands. *Nanomedicine* 3, 627–635 (2008).

[xxv]. Bastús NG, Sánchez-Tilló E, Pujals S *et al.*: Peptides conjugated to gold nanoparticles induce macrophage activation. *Mol. Immunol.* 46, 743–748 (2009).

[xxvi]. Snippe H, Jansen WTM, Kamerling JP: Immunology of experimental synthetic carbohydrate-protein conjugate vaccines against *Streptococcus pneumoniae* serotypes. In:

Carbohydrate-Based Vaccines (Volume 989). René Roy (Ed.), ACS Symposium Series, American Chemical Society, Washington, DC, USA, 85–104 (2008).

[xxvii]. Barrientos AG, de la Fuente JM, Rojas TC, Fernandez A, Penadés S: Gold glyconanoparticles: Synthetic polyvalent ligands mimicking glycocalyx-like surfaces as tools for glycobiological studies. *Chem. Eur. J.* 9, 1909–1921 (2003).

[xxviii]. Martínez-Ávila O, Hijazi K, Marradi M *et al.*: Gold *manno*-glyconanoparticles: Multivalent systems to block HIV-1 gp120 binding to the lectin DC-SIGN. *Chem. Eur. J.* 15, 9874–9888. (2009).

[xxix]. Marradi M, Martín-Lomas M, Penadés S: Glyconanoparticles: polyvalent tools to study carbohydrate-based interactions. *Adv. Carbohydr. Chem. Biochem.* 64, 211–290 (2010).

[xxx]. García I, Marradi M, Penadés S: Glyconanoparticles: Multifunctional nanomaterials for biomedical applications. *Nanomedicine* 5, 777–792 (2010).

[xxxi]. Rijkers GT, van Mens SP, van Velzen-Blad H: What do the next 100 years hold for pneumococcal vaccination? *Expert Rev. Vaccines* 9, 1241-1244 (2010).

[xxxii]. Veenhoven R, Bogaert D, Uiterwaal C *et al.*: Effect of conjugate pneumococcal vaccine followed by polysaccharide pneumococcal vaccine on recurrent acute otitis media: a randomised study. *Lancet* 361, 2189–2195 (2003).

[xxxiii]. Mawas F, Niggemann J, Jones C, Corbel MJ, Kamerling JP, Vliegenthart JF: Immunogenicity in a mouse model of a conjugate vaccine made with a synthetic single repeating unit of type 14 pneumococcal polysaccharide coupled to CRM197. *Infect. Immun.* 70, 5107–5114 (2002).

[xxxiv]. Safari D, Dekker HA, Joosten JA *et al.*: Identification of the smallest structure capable of evoking opsonophagocytic antibodies against *Streptococcus pneumoniae* type 14. *Infect. Immun.* 76, 4615–4623 (2008).

[xxxv]. Buus S, Colon S, Smith C, Freed JH, Miles C, Grey HM: Interaction between a "processed" ovalbumin peptide and Ia molecules. *Proc. Natl. Acad. Sci. USA* 83, 3968–3971 (1986).

[xxxvi]. Renz H, Bradley K, Larsen GL, McCall C, Gelfand EW: Comparison of the allergenicity of ovalbumin and ovalbumin peptide 323-339. Differential expansion of V beta-expressing T cell populations. *J. Immunol.* 151, 7206–7213 (1993).

[xxxvii]. Svetic A, Finkelman FD, Jian YC *et al.*: Cytokine gene expression after *in vivo* primary immunization with goat antibody to mouse IgD antibody. *J. Immunol.* 147, 2391–2397 (1991).

[xxxviii]. Svetic A, Jian YC, Lu P, Finkelman FD, Gause WC: Brucella abortus induces a novel cytokine gene expression pattern characterized by elevated IL-10 and IFN-gamma in CD4+ T cells. *Int. Immunol.* 5, 877–883 (1993).

[xxxix]. Sundgren A, Lahmann M, Oscarson S: Block synthesis of *Streptococcus pneumoniae* type 14 capsular polysaccharide structures. *J. Carbohydr. Chem.* 24, 379–391 (2005)

[xl]. Hostetler MJ, Wingate JE, Zhong C-J *et al.*: Alkanethiolate gold cluster molecules with core diameters from 1.5 to 5.2 nm: Core and monolayer properties as a function of core size. *Langmuir* 14, 17–30 (1998).

[xli]. Jansen WT, Gootjes J, Zelle M *et al.*: Use of highly encapsulated *Streptococcus pneumoniae* strains in a flow-cytometric assay for assessment of the phagocytic capacity of serotype-specific antibodies. *Clin. Diagn. Lab. Immunol.* 5, 703–710 (1998).

[xlii]. Love JC, Estroff LA, Kriebel JK, Nuzzo RG, Whitesides GM: Self-assembled monolayers of thiolates on metals as a form of nanotechnology. *Chem. Rev.* 105, 1103–1169 (2005).

[xliii]. Mrksich M, Whitesides GM: Using self-assembled monolayers to understand the interactions of man-made surfaces with proteins and cells. *Annu. Rev. Biophys. Biomol. Struct.* 25, 55–78 (1996).

[xliv]. Otsuka H, Akiyama Y, Nagasaki Y, Kataoka K: Quantitative and reversible lectin-induced association of gold nanoparticles modified with α-lactosyl-ω-mercapto-poly(ethylene glycol). *J. Am. Chem. Soc.* 123, 8226–8230 (2001).

[xlv]. Barrientos AG, de la Fuente JM, Jiménez M *et al.*: Modulating glycosidase degradation and lectin recognition of gold glyconanoparticles. *Carbohydr. Res.* 344, 1474–1478 (2009).

[xlvi]. Martínez-Ávila O, Bedoya LM, Marradi M, Clavel C, Alcami J, Penadés S: Multivalent manno-glyconanoparticles inhibit DC-SIGN-mediated HIV-1 trans-infection of human T cells. *ChemBioChem* 10, 1806–1809 (2009).

[xlvii]. Marradi M, Di Gianvincenzo P, Enríquez-Navas PM *et al.*: Gold nanoparticles coated with oligomannosides of HIV-1 glycoprotein gp120 mimic the carbohydrate epitope of antibody 2G12. *J. Mol. Biol.* (2011), doi:10.1016/j.jmb.2011.03.042.

[xlviii]. Smith KA: Interleukin-2: Inception, Impact, and Implications. *Science* 240, 1169–1176 (1988).

[xlix]. Randall TD, Lund FE, Brewer JW, Aldridge C, Wall R, Corley RB. Interleukin-5 (IL-5) and IL-6 define two molecularly distinct pathways of B-cell differentiation. *Mol. Cell. Biol.* 13, 3929–3936 (1993).

[l]. Wuorimaa T, Käyhty H, Eskola J, Bloigu A, Leroy O, Surcel HM: Activation of cell-mediated immunity following immunization with pneumococcal conjugate or polysaccharide vaccine. *Scand. J. Immunol.* 53, 422–428 (2001).

[li]. Cox CA, Shi G, Yin H et al.: Both Th1 and Th17 are immunopathogenic but differ in other key biological activities. J. Immunol. 180, 7417–7422 (2008).

[lii]. Lu Y, Gross J, Bogaert D et al.: Interleukin IL-17A mediates acquired immunity to pneumococcal colonization. *PLoS Pathog.* 4, e1000159 (2008).

[liii]. Zhang Z, Clarke TB, Weiser JN: Cellular effectors mediating Th17-dependent clearance of pneumococcal colonization in mice. *J. Clin. Invest.* 119, 1899–1909 (2009).

[liv]. Baker WS Jr.: Carcinoma of the uterine cervix: Interstitial radioactive colloidal gold therapy of the lateral pelvic nodes. *Calif. Med.* 92, 25–30 (1960).

[lv]. Hall JB, Dobrovolskaia MA, Patri AK, McNeil SE: Characterization of nanoparticles for therapeutics. *Nanomedicine* 2, 789–803 (2007).

[lvi]. Kennedy LC, Bickford LR, Lewinski NA et al.: New era for cancer treatment: Gold-nanoparticle-mediated thermal therapies. *Small* 7, 169–183 (2011).

[lvii] S. Martínez-Ávila O, Hijazi K, Marradi M *et al.*: Gold *manno*-glyconanoparticles: Multivalent systems to block HIV-1 gp120 binding to the lectin DC-SIGN. *Chem. Eur. J.* 15, 9874–9888. (2009).

[lviii]S. Sundgren A, Lahmann M, Oscarson S: Block synthesis of *Streptococcus pneumoniae* type 14 capsular polysaccharide structures. *J. Carbohydr. Chem.* 24, 379–391 (2005).

[lix]S. Safari D, Dekker HA, Joosten JA *et al.*: Identification of the smallest structure capable of evoking opsonophagocytic antibodies against *Streptococcus pneumoniae* type 14. *Infect.Immun.* 76, 4615–4623 (2008).

[lx] S. Jansen WT, Gootjes J, Zelle M *et al.*: Use of highly encapsulated *Streptococcus pneumoniae* strains in a flow-cytometric assay for assessment of the phagocytic capacity of serotype-specific antibodies. *Clin. Diagn. Lab. Immunol.* 5, 703-710 (1998).